Early tectono-sedimentary history of a Neogene extensional basin in east-central Nevada
by Cheryl Lynn Brown

A thesis submitted in partial fulfillment of the requirements for the degree of Master of Science in Earth Sciences
Montana State University

Abstract:
The Neogene Horse Camp Formation of east-central Nevada is a thick, well-exposed extensional basin-fill sequence composed of conglomerate, sandstone, mudrock, and limestone. The lowest member of this formation, Member 1, was examined to develop a tectono-sedimentary model for the initial phases of an extensional basin evolution. Nine stratigraphic sections were measured. Sixteen lithofacies and five lithofacies assemblages were described. Spatial and temporal distribution of these lithofacies assemblages provide the basis for determining the paleogeography and depositional environments that characterized the area while Member 1 was being deposited.

Fifty-three samples of volcaniclasdc sandstone analysis were collected for petrographic analysis. Clast counts were completed in order to determine conglomerate compositions. Conglomerate and sandstone compostion provide infomation about the provenance of Member 1. The paleogeography of the area was determined by calculating the paleoflow and paleoslope directions from measured trough axes in sandstone and folds at the base of megabreccias.

Member 1 is composed of two distict petrofacies which record a temporal change in sediment source areas. The lower portion is composed of sediment deposited on the medial to distal portions of a large radius alluvial fan derived from a western source terrain composed of volcanic rocks. The upper portion is composed of sediment deposited on large alluvial fans shed from a hangingwall block to the north and small alluvial fans deposited off of a football block to the south. Both source terrains were composed of Oligocene volcanic rocks and Paleozoic sedimentary rocks. Mudrock was deposited in a lacustrine setting between these alluvial fans.

EARLY TECTONO-SEDIMENTARY HISTORY OF A NEOGENE EXTENSIONAL BASIN IN EAST-CENTRAL NEVADA

by

Cheryl Lynn Brown

A thesis submitted in partial fulfillment
of the requirements for the degree

of

Master of Science

in

Earth Sciences

MONTANA STATE UNIVERSITY
Bozeman, Montana

May 1993

APPROVAL

of a thesis submitted by

Cheryl Lynn Brown

This thesis has been read by each member of the thesis committee and has been found to be satisfactory regarding content, English usage, format, citations, bibliographic style, and consistency, and is ready for submission to the College of Graduate Studies.

March 9, 1993
Date

James Schmitt
Chairperson, Graduate Committee

Approved for the Major Department

March 9, 1993
Date

Head, Major Department

Approved for the College of Graduate Studies

3/10/93
Date

R L Brown
Graduate Dean

STATEMENT OF PERMISSION TO USE

In presenting this thesis in partial fulfillment of the requirements for a master's degree at Montana State University, I agree that the Library shall make it available to borrowers under the rules of the Library.

If I have indicated my intention to copyright this thesis by including a copyright notice page, copying is allowable only for scholarly purposes, consistent with "fair use" as prescribed in the U.S. Copyright Law. Requests for permission for extended quotation from or reproduction of this thesis in whole or in parts may be granted only by the copyright holder.

Signature ________________

Date 3/1/93

ACKNOWLEDGEMENTS

I would like to thank my friends and family, especially my parents Tom and Jacquie Brown, for providing all of the moral and financial assistance necessary. I am grateful for the support and encouragement that I received from Dr. James G. Schmitt who suggested this project and provided the funding and expertise necessary in guiding me through it. I would like to express my appreciation to Drs. Joseph Ashley, Stephen Custer, and Joan Fryxell for serving as members on my thesis committee. I would also like to thank Galin and Barbara Manzonie for the hospitality that they extended to me by allowing me to stay at their ranch while doing my field work.

I am grateful for the research grants provided to me by the Geological Society of America, American Association of Petroleum Geologists, and Marathon Oil Company. Other financial assistance that I received during this time included the E.D. McKee Research Grant from the Rocky Mountain Section of the Society of Economic Paleontologists and Mineralogists and D.L. Smith Award from the Department of Earth Sciences and Mrs. D.L.Smith. I would like to thank Christopher J. Potter (U.S.G.S. Denver, CO) for his interest in this project and providing me with drafting support.

TABLE OF CONTENTS

LIST OF TABLES

LIST OF FIGURES

LIST OF PLATES

ABSTRACT

The Neogene Horse Camp Formation of east-central Nevada is a thick, well-exposed extensional basin-fill sequence composed of conglomerate, sandstone, mudrock, and limestone. The lowest member of this formation, Member 1, was examined to develop a tectono-sedimentary model for the initial phases of an extensional basin evolution. Nine stratigraphic sections were measured. Sixteen lithofacies and five lithofacies assemblages were described. Spatial and temporal distribution of these lithofacies assemblages provide the basis for determining the paleogeography and depositional environments that characterized the area while Member 1 was being deposited.

Fifty-three samples of volcaniclastic sandstone analysis were collected for petrographic analysis. Clast counts were completed in order to determine conglomerate compositions. Conglomerate and sandstone compostion provide infomation about the provenance of Member 1. The paleogeography of the area was determined by calculating the paleoflow and paleoslope directions from measured trough axes in sandstone and folds at the base of megabreccias.

Member 1 is composed of two distict petrofacies which record a temporal change in sediment source areas. The lower portion is composed of sediment deposited on the medial to distal portions of a large radius alluvial fan derived from a western source terrain composed of volcanic rocks. The upper portion is composed of sediment deposited on large alluvial fans shed from a hangingwall block to the north and small alluvial fans deposited off of a footwall block to the south. Both source terrains were composed of Oligocene volcanic rocks and Paleozoic sedimentary rocks. Mudrock was deposited in a lacustrine setting between these alluvial fans.

INTRODUCTION

Patterns of sedimentation in extensional basins are fundamentally related to local normal fault geometry and kinematics. The spatial and temporal geometry of the basin and its surrounding orogen must be analyzed in order to understand the evolution of extensional basins. This study represents the initial phase of an ongoing research project of James G. Schmitt and others focused on the tectono-sedimentary development of the Neogene Horse Camp basin of east-central Nevada and its surrounding extensional orogen: the northern Grant, Horse, and southern White Pine Ranges (Figures 1 and 2). This area was selected for study because of the presence of an unusually thick (3000 meter), well-exposed, Neogene basin-fill sequence of conglomerate, sandstone, mudrock, and limestone called the Horse Camp Formation. Seismic data reveal that many Oligocene to Recent basin-fill sequences in the northern Basin and Range province reach thicknesses of 2000-3000 meters beneath modern valleys (Effimoff and Pinezich, 1981, 1986; Anderson and others, 1983; Gans and others, 1989). However, continuing late Cenozoic extension and basin subsidence cause exposures of basin-fill to be relatively uncommon. Therefore, field-based studies of extensional basin-fill sedimentology and stratigraphy are inhibited and the tectono-sedimentary history of extensional orogenic systems is obscured. From this perspective, the Neogene Horse Camp Formation provides an unusual opportunity to examine the development of a synextensional basin.

A detailed analysis of the sedimentology and stratigraphy of the basal member (Member 1) is described and related to local structures in order to develop a tectono-sedimentary model for the initial phases of development of the Horse Camp depositional

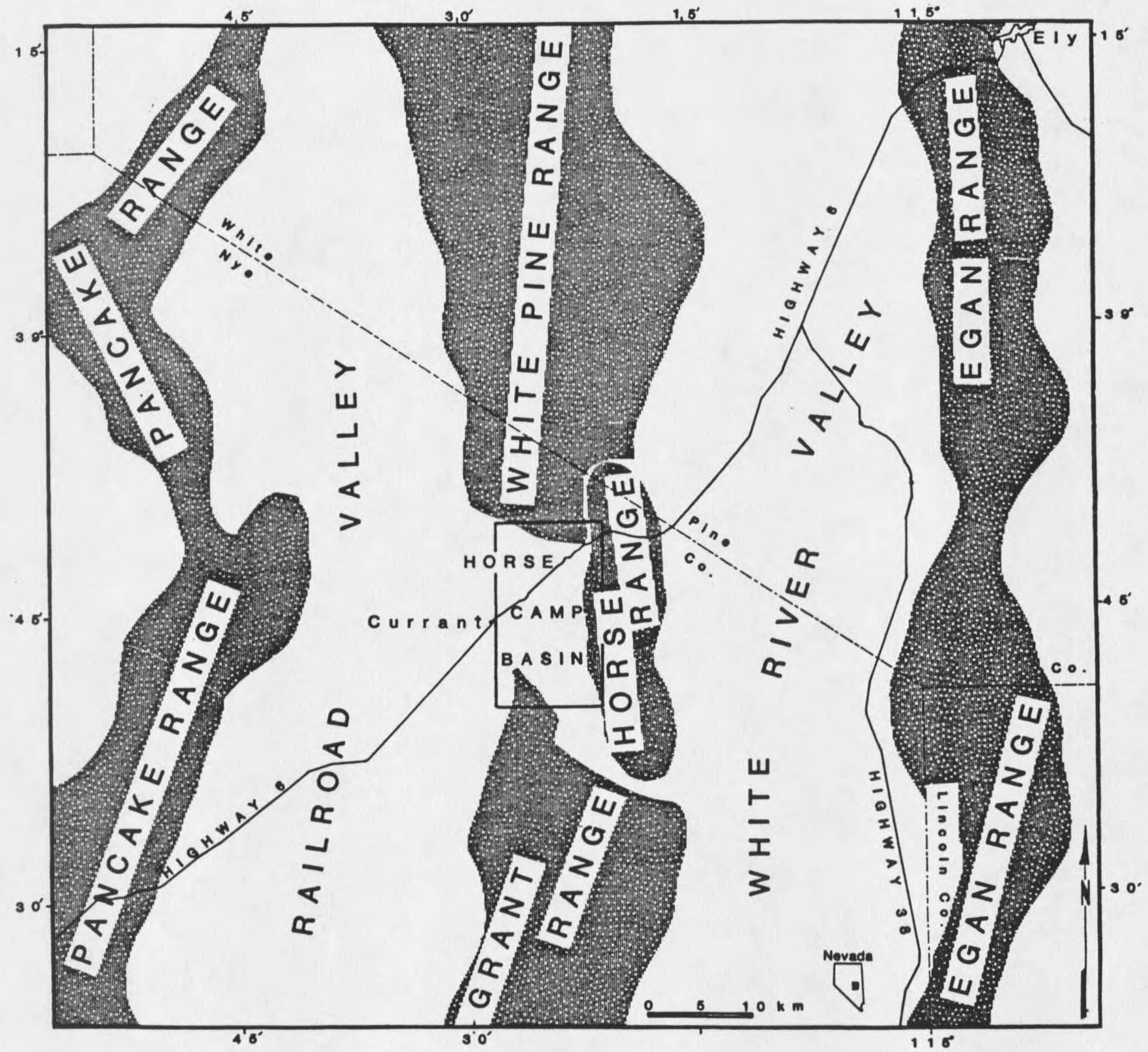

Figure 1. Location of Horse Camp basin study area relative to pertinent geographical features in the region. Stippled areas are mountain ranges. Outlined area is shown in more detail in Figure 2

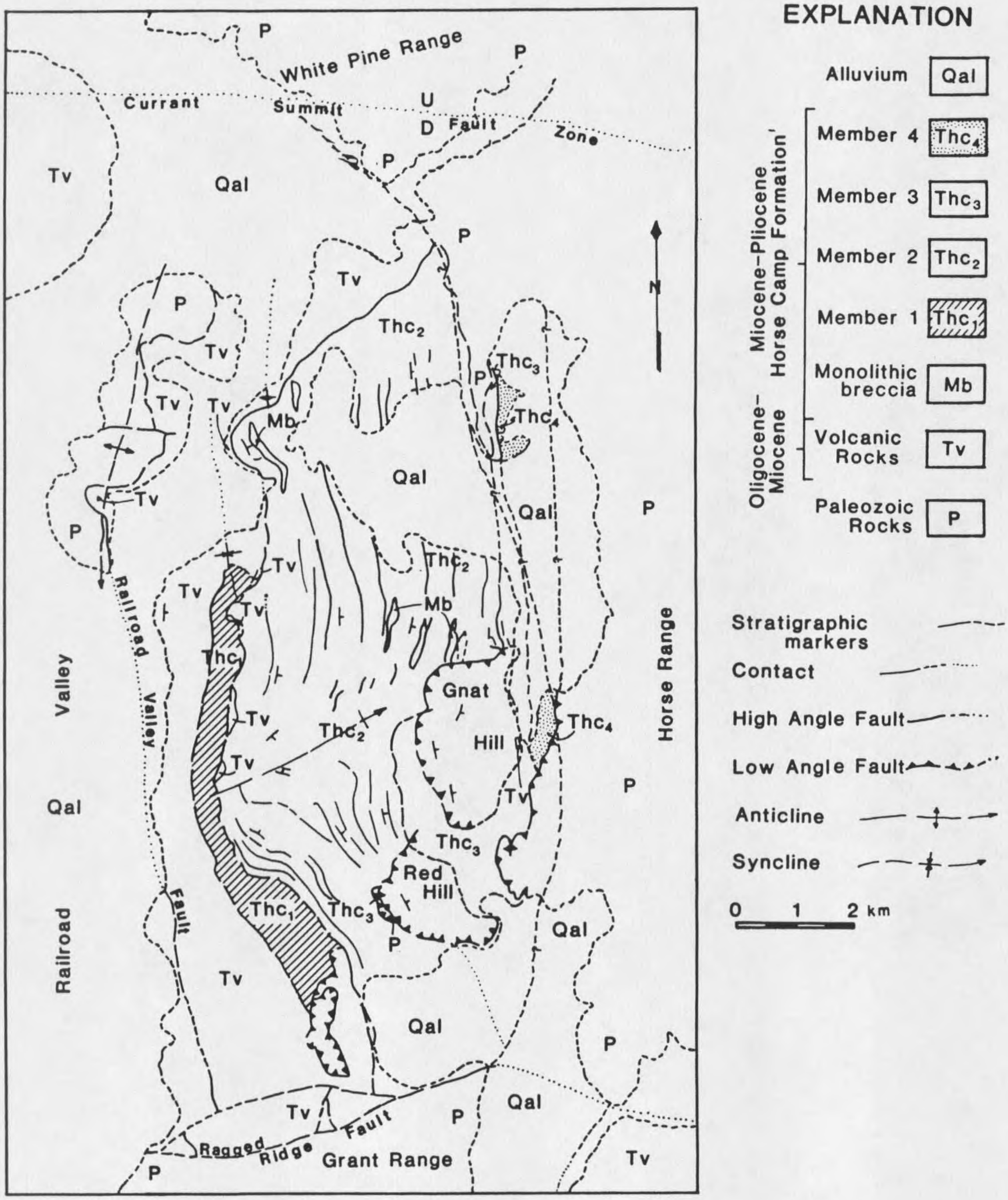

Figure 2. Generalized geologic map of the Horse Camp basin and surrounding area. Modified from Moores (1968).

basin(s). The results of this research are compared to various sedimentary and structural models of extensional basins which are described below.

Sedimentary Models of Extensional Basins

Integration of sedimentology and structural geology have advanced our understanding of relations between development of extensional sedimentary basins and mechanics and style of continental lithospheric extension (e.g. Sclater and Celerier, 1987; Schlische and Olsen, 1990). Numerous models describing the development of extensional sedimentary basins have been developed in the last 15 years. The earliest models describe these basins as relatively simple grabens bounded by high-angle normal faults (Stewart, 1978; Illies, 1981). Because of the structural symmetry of this type of basin, sediment dispersal patterns are also symmetrical with coarser sediment deposited nearest to the adjacent highlands and finer sediment near the center of the basin (Reading, 1982). However, detailed analyses of sedimentology and stratigraphy of actual extensional basins indicate that these types of models are over simplified (Bally and Snelson, 1980).

Advancements in structural geology and geophysics have led to the identification of half grabens that develop in response to block rotation on listric normal faults which sole at depth into low-angle detachments or crustal shear zones (e.g. Wernicke and Burchfiel, 1982; Jackson and others, 1982; Jackson and McKenzie, 1983; Gibbs, 1984; and Rosendahl and others, 1986). Gibbs (1984) has identified several structural complexities of listric normal fault systems including hanging wall folds, transfer structures which act as accommodation zones between areas which have undergone different amounts of extension, and intrabasinal antithetic and synthetic normal faulting. The asymmetry of basins bounded by listric normal faults within continental rift systems is not consistently unidirectional (Bally, 1982; Gibbs, 1983) and segments with opposing structural polarity have been recognized (Bosworth, 1985; Rosendahl and others, 1986; Faulds and others, 1992).

The asymmetry of listric normal fault-bounded basins has a strong influence on sediment dispersal patterns in the basin fill. Tectono-sedimentary models for internally and axially drained basins developed by Leeder and Gawthorpe (1987) take these effects into account. Internally drained basins such as Death Valley of southern California have small, steep gradient alluvial fans adjacent to the tectonically active footwall. Large, low-gradient fans and bajadas on the opposite side of the basin extend from the hanging wall block and prograde towards the more active side thereby restricting the location of playas and saltflats close to the steeper, smaller fans. In externally drained half grabens such as the Aegean area of Greece, Rhine Graben of Germany, Rio Grande Rift of Texas and New Mexico, and Madison Valley of southwest Montana, axial drainage systems occupy a narrow belt close to the active basin bounding fault. Fluvial systems draining the active footwall block have steep gradients whereas those draining the tilted hanging wall block have lower gradients. Both the internal and external drainage models provide much insight into the characteristics of drainage systems in half grabens; however, neither takes into consideration the effects of synthetic and antithetic faulting, transverse structural elements, erosion of hanging wall rollover anticlines, or segmentation of major basin bounding faults.

Recent studies suggesting that the East African Rift Zone is dominated by listric normal faulting and half graben basins (Reid and Frostick, 1986; Cohen and others, 1986; Tircelin, 1986; Williamson and Savage, 1986; Frostick and Reid, 1987) lend credence to the internally and externally drained tectono-sedimentary basin models of Leeder and Gawthorpe (1987). These studies suggest that sediment eroded from the zone of hanging wall rollover is transported towards the active basin bounding fault and into an axial drainage system. Similar evidence has been found for sediment transport from the eroded hanging wall towards the tectonically active side of the basin by axial drainage from the Miocene Espanola basin of New Mexico (Cavazza, 1989). Mack and Seager (1990) suggest that axial fluvial facies are restricted to a narrow belt along the locus of maximum subsidence in the Pliocene - Pleistocene Palomas and Mesilla half graben subbasins of the Rio Grande Rift while, in contrast, axial fluvial facies occupy almost the entire width of the symmetrical Hatch - Rincon graben. Blair (1987) reports that the position of axial drainage relative to regions of active faulting changes as a function of rates of basin subsidence in the Jurassic - Cretaceous Todos Santos half grabens of Mexico. With increased rates of subsidence lacustrine and axial fluvial drainage systems migrate towards the active basin-bounding fault. Axial drainages and lacustrine systems are then displaced away from the fault by progradation of alluvial fans into the basin from the fault-bounded margins during periods of decreased subsidence. In their study of the Oligocene - early Miocene Soledad basin of California, Hendrix and Ingersoll (1987) use detailed lithofacies analysis to demonstrate that an asymmetrical distribution of alluvial facies was indicative of deposition in several tectonically active half graben subbasins.

Structural Models of Extensional Basins

Improved understanding of mechanisms of lithospheric extension have resulted in the need to advance tectono-sedimentary models of extensional basins. Within the last ten years researchers have recognized the importance of two structural features in extensional terranes: isostatic uplift within the extensional footwall due to tectonic denudation (Spencer, 1984; Wernicke, 1985; Barr, 1987; Wernicke and Axen, 1988; Lister and Davis, 1989; Bartley and others, 1990) and the role of transverse structures in effecting local changes in extension (Gibbs, 1984, 1987, 1990; Faulds and others, 1990, 1992).

During periods of extension along major normal faults the lithosphere is thinned resulting in isostatic uplift of the extensional footwall due to tectonic denudation. Uplift of the footwall results in the arching of the normal fault trace and generation of a shallow-dipping detachment. Buck (1988), Hamilton (1988), and Wernicke and Axen (1988) recognize that the hinge separating the shallow dipping portion of the fault from the more steeply dipping segment "rolls" through the footwall as it migrates with the trailing edge of the hanging wall. As slabs spall off the trailing edge of the hanging wall, this migration results in the sequential stranding of fault blocks and basins that are separated by low-angle detachment faults.

Although, it is generally agreed that this "rolling hinge" model fits many known extensional scenarios, disagreement exists concerning the attitude of the master fault during extension. Wernicke (1981), Spencer (1984), and Davis and Lister (1988) suggest that as the footwall is uplifted, displacement is actively accommodated by the low-angle master fault. Indeed, initiation and continued motion is documented along the low-angle Chemeheuvi detachment of southeastern California (which presently dips less than 15°) by Miller and John (1988). However, absence of earthquakes along modern low-angle faults (Jackson and McKenzie, 1983; Jackson, 1987) and limitations imposed by rock mechanic considerations (Buck, 1988; Hamilton, 1988; Wernicke and Axen, 1988) indicate that the master faults are active when they are in a high-angle position through the seismogenic zone and subsequently tilted passively to low angles by footwall uplift. The tilting of the master fault by migration of isostatic uplift causes abandonment of fault bounded blocks separated by half-graben basins.

Faults oriented at high angles to the strike of major normal fault systems, termed transverse structures or transfer zones, play a significant role in extensional tectonics. The transverse orientation of these fault systems may exert significant influence on patterns of sediment dispersal and distribution of depositional environments in extensional basins. Unfortunately, the development of transverse structures is not well understood. Transverse zones may be reactivated structures which act as regional barriers to propagating normal faults (Bartley and others, 1992). Gibbs (1984) recognizes transverse fault systems as accommodation zones between areas of opposing structural polarity or differing amounts and rates of extension . Because these structures potentially have a strike-slip component, any transpression would produce contractional structures and any transtension would produce extensional structures within the normal fault hanging wall and hence, basin-fill sequence (Gibbs, 1984, 1987, 1990). However, Faulds and others (1990) suggest that any strike-slip displacement is rare and instead, scissor-like torsional offset on a transverse fault is more common. In any event, transverse structures may be the longest lived fault element in any extensional setting because activity along these faults must continue as displacement is transferred along strike to younger normal faults. The transverse orientation and long-lived nature of a transfer zone can potentially enhance the complexities of any extensional basin-fill sequence associated with it. This is particularly true of such parameters as sediment dispersal patterns and facies distributions.

Integration of Sedimentologic and Structural Models

Complexities in the geometry, provenance, and sedimentology of basin-fill sequences arise when considering the role played by the rolling hinge model in extensional settings. Isostatic footwall uplift results in the development and abandonment of numerous fault-bounded basins. These basins evolve into a complex series of subbasins separated by tilted fault-bounded blocks with internal or integrated drainage. Temporal changes in the drainage patterns occur as the basin complex evolves with continued footwall uplift (Mack and Seager, 1990). As low-angle fault blocks are stranded, subsidence rates decrease. This eventually can cause a drainage direction reversal (Buck, 1988; Hamilton, 1988; Miller and John, 1988; Wernicke and Axen, 1988). As the hinge zone migrates, basin-fill is topographically inverted and intrabasinal unconformities develop as the older strata are cannibalized (Miller and John, 1988). Eventually, the complex of half-graben basins becomes integrated into a single sedimentary basin behind the area of active uplift and fault blocks are buried in their own erosional detritus (Lister and Davis, 1989). Stewart and Diamond (1990) interpret isostatic footwall uplift and erosion during detachment faulting as the cause of basin dismemberment of the Miocene Esmeralda basin of western Nevada. Isostatic uplift of the Chemeheuvi Mountains metamorphic core complex in California resulted in erosional removal of the hanging wall fault block as well as basin-fill sequences (Miller and John, 1988).

The influence of transverse structures on extensional basin-fill sequences has not been well defined. Nielson and Beratan (1990) and Beratan (1991) recognize the importance of an extensional transfer fault on sedimentation patterns and facies in the Whipple Mountains detachment system of California. Kinematic coupling of the Saddle Island detachment with the transverse Las Vegas Valley shear zone has strongly influenced the evolution of the geometry, provenance, and sedimentology of Miocene extensional basins in the Lake Mead region of southern Nevada (Duebendorfer and Wallin, 1991). Gibbs (1990) recognizes that similar kinematic coupling at a smaller scale characterizes many transfer fault zones.

As extensional basins evolve they are controlled by complexly interrelated structural elements. To understand both basin and orogen evolution, field-based analyses of basin-fill sequences must be completed to determine the significance of isostatic extensional footwall uplift and transfer structures on the history of basin infilling.

Objectives of Study

In order to determine the relations between extensional tectonism and patterns of sediment dispersal during early phases of development of the Horse Camp basin complex, a detailed analysis of the stratigraphy, sedimentology, provenance, and structure of Member 1 of the Neogene Horse Camp Formation was undertaken. This investigation addresses three questions:

1) What depositional environments characterized the Horse Camp basin complex during its early history?

Studies of both the spatial distribution and temporal changes in depositional environments during early phases of Horse Camp basin evolution provide a better understanding of Neogene paleogeography and help delineate areas of active uplift and subsidence. Changes in the style of extension during basin evolution are recorded by changes in composition and distribution of sediment deposited in alluvial fan, sandflat, and lacustrine environments that characterize Member 1 (Anderson and others, 1983; Effimoff and Pinezich, 1986; Alexander and Leeder, 1987). In general, understanding the spatial and temporal relations between mapped lithofacies distributions and consideration of regional fault trends facilitates synthesis of basin evolution (Leeder and Gawthorpe, 1987). Therefore, mapping of lithofacies and their relations to possible faults which may have controlled lithofacies distribution is given special attention.

2) What is the provenance of the lower Horse Camp Formation deposits?

Although Moores (1968) suggests possible source areas for Horse Camp deposits, detailed provenance investigation has not been completed until now. This study uses conglomerate clast composition trends (Graham and others, 1986), sandstone petrofacies (Stanley, 1976), sedimentary structures (DeCelles and others, 1983), and deformational structures at the base of megabreccia blocks to determine paleoslope and sediment source areas (Yarnold and Lombard, 1989). Knowledge of sediment provenance adds to the understanding of basin evolution by determining the composition, location, and duration of the adjacent highland uplifts.

3) Which tectono-sedimentary model best describes the earliest phase of basin development in the Horse Camp basin complex?

Existing geologic maps (Moores and others, 1968) and associated interpretive structural cross-sections of the Horse Camp basin and the surrounding area based on field studies (Moores, 1963; Scott, 1965; Lumsden, 1964; Fryxell, 1984, 1988; Bartley and Gleason, 1992) and available published seismic data (Vreeland and Berrong, 1979; Anderson and others, 1983; Effimoff and Pinezich, 1986) aid in determining basin geometry and sequence of faulting. Integrating these data with sedimentary facies distribution patterns and provenance information contributes toward development of a three-dimensional tectono-sedimentary model for the early phase of Horse Camp basin development (Leeder and Gawthorpe, 1987; Beratan and others, 1990). Comparisons are made of the Horse Camp conceptual model with existing tectono-sedimentary models developed for detachment fault basins (Frost, 1981; Spencer, 1984; Wernicke and Axen, 1988; Buck, 1988; Lister and Davis, 1989; Bartley and Fletcher, 1990; Li and others, 1990; Beratan and others, 1990; Nielson and Beratan, 1990; Perry and Schamel, 1990;

Dubendorfer and Wallin, 1991), listric normal fault basins (Rehrig and others, 1980; Vendeville and Cobbold, 1988), and planar/domino or half-graben fault basins (Leeder and Gawthorpe, 1987; Axen, 1988; Alexander and Leeder, 1990; Schlische and Olsen, 1990) in order to determine the applicability of these models to the Horse Camp basin area.

The Horse Camp basin complex is a particularily favorable setting to examine the influence of transverse structures and footwall uplift on sediment dispersal because of the presence of major transverse strutural elements and low-angle normal faults in the adjacent extensional orogen, as described below. As such, provenance, paleogeographic information, and the nature of intraformational unconformities are potentially useful to evaluating the importance of transverse structures and isostatic footwall uplift in controlling sedimentation during early phases of Horse Camp basin development.

GEOLOGIC SETTING

The Basin and Range province of western North America has a complex extensional deformational history. During Cenozoic time there were at least two episodes of differing extensional styles that partially overlap, both temporally and spatially (Zoback and others, 1981; Glazner and Bartley, 1984; Gans and others, 1989).

The first episode of lithospheric extension began as early as 39 - 38 Ma and was characterized by extensional faulting and caldera-centered ash-flow tuff eruptions. Extension during this time was characterized by low-angle detachment faulting and associated high-angle normal faulting in the hanging wall of the detachments (Coney, 1987). Faulting was generally not synvolcanic (Taylor and others, 1989; Best and Christiansen, 1991) as it either preceded or followed volcanism in different areas. In east-central Nevada, caldera-style volcanism was most prolific during the Oligocene to early Miocene. These eruptions collectively deposited one kilometer of ash-flow tuffs on folded and faulted Paleozoic rocks.

The second well-defined period of extension began as early as 27 - 17 Ma (depending on location) and was characterized by bimodal volcanism and low- and high-angle faulting (Wernicke and Burchfiel, 1982). This phase of extension may continue to be active today or may be temporally distinct from a later extensional phase that has created the modern Basin and Range physiography. In any case, seismic information suggests that different fault geometries generated during this period have controlled the evolution of different styles of extensional sedimentary basins. Anderson and others (1983) recognize three different relations between faults of different geometries and adjacent basins. Steeply dipping planar normal faults are associated with basins that resemble simple sags. Tilting of the hanging wall by listric normal faults result in the development of sedimentary prisms overlying bedrock ramps. Planar normal and sharply curving, shallow listric faults that sole into detachments produce assemblages of complexly deformed subbasins.

Because of the nature of rock exposures in extensional orogens, the timing and evolution of structures are typically better understood than is the associated basin-fill stratigraphy. Therefore, the relations between structural development of extensional fault systems and the depositional history of the basins are not clear. A field-based analysis of the sedimentology of basin-fill sequences can be a powerful tool in providing temporal and kinematic constraints important for determining the structural evolution of an extensional orogen (Duebendorfer and Wallin, 1991).

In east-central Nevada, exposures of Cenozoic basin-fill sequences are rare. Basin-fill sequences that have been investigated include the Oligocene to Recent strata of Pine Valley (Regnier, 1960; Gordon and Heller, 1993), the Oligocene Sacramento Pass Conglomerate in the Snake Range (Grier, 1983, 1984), the Miocene Humbolt Formation in the Ruby Mountain - East Humbolt Range area (Sharp, 1939; Snoke and Lush, 1984), and Quaternary sediments in White River Narrows at the south end of White River Valley (DiGuiseppi and Bartley, 1991).

The focus of this investigation is on the well exposed basin-fill strata of the Neogene Horse Camp Formation of east-central Nevada. The Horse Camp basin is located 80 kilometers southwest of Ely, Nevada at the intersection of the White Pine, Horse, and northern Grant ranges (Figure 1). This region is characterized by north-trending folds that involve Paleozoic and/or mid-Tertiary rocks cut by north-striking high- and low-angle normal faults (Moores and others, 1968). The Horse Camp basin and surrounding three mountain ranges constitute four structural domains: the White Pine Range, Horse Range, Grant Range, and Horse Camp Basin (Figure 2).

The White Pine Range is underlain by a north-trending, doubly-plunging anticline with Cambrian rocks exposed in the core. The anticline is dissected by a series of high- and low-angle faults that display up to 3.3 kilometers of stratigraphic throw (Moores and others, 1968). A high-angle normal fault with approximately 2 kilometers of dip offset bounds the west side of the range and lies along strike of the Railroad Valley fault to the south. The overall geometry of the White Pine Range suggests that it represents a region of major footwall uplift due to tectonic denudation via normal faulting.

The Horse Range is separated from the White Pine Range by the Currant Summit fault zone (Moores and others, 1968). This dominant east-west striking feature is interpreted as a left-lateral oblique slip fault accommodating the differential extension experienced by the White Pine and Horse ranges. The Horse Range is made up of two north-trending ridges of Paleozoic rocks separated by a fault-bounded valley underlain by east-dipping Oligocene volcanic rocks. The east ridge is the overturned limb of an anticline - syncline pair in upper Paleozoic rocks. The west ridge is composed of complexly folded, east-dipping Cambrian to Ordovician rocks which are autochthonous with respect to the east ridge (Moores and others, 1968).

At the southern termination of the west ridge of the Horse Range, Moores and others (1968) mapped five allochthonous blocks overlying lower Paleozoic rocks. These blocks were interpreted as low-angle normal fault klippen and gravity slide masses by Moores and others (1968) . The two blocks that lie north and west of the arcuate Ragged Ridge fault, a high-angle normal fault separating the Horse Camp basin from the Grant and Horse ranges (Figure 2), were interpreted as slide masses moving over an erosional surface and incorporated into the Horse Camp basin fill (Moores and others, 1968). Reconnaissance mapping of these two blocks suggests that the larger of the two blocks, Gnat Hill, composed of faulted Paleozoic rocks, is a tilted fault block. The other block, Red Hill, is a slide block composed of Oligocene volcanic rocks which overlies strata of Member 2 of the Horse Camp Formation.

The northern Grant Range is composed of Paleozoic and Tertiary rocks deformed by younger-over-older low-angle faults interpreted by Moores and others (1968) and Taylor (unpublished mapping) as late Cenozoic faults related to Basin and Range extension. Similar structures further south were previously interpreted as Mesozoic thrust faults by Cebull (1970) and Hyde and Hutter (1970). Both Mesozoic contractional and Cenozoic extensional structures were recognized through detailed remapping of portions of the Quinn Canyon Range (Murray, 1985; Bartley and others, 1988), the west side of the Grant Range from Little Meadow Creek to Grant Canyon (Fryxell, 1988, 1991, unpublished mapping), the east side of the Grant Range from the southern end to Schofield Canyon (Janecke, unpublished mapping; Fryxell, unpublished mapping; Gleason, 1988; Bartley and Gleason, 1992), and the central Grant Range (Lund and others, 1987, 1988; Camilleri, 1989, 1992).

The Horse Camp basin lies south of the White Pine Range, west of the Horse Range, and north of the Grant Range (Figure 1). In this area, Paleozoic strata are overlain by Oligocene volcanic rocks, the Neogene Horse Camp Formation, and Quaternary gravels(Figure 3). As mapped by Moores and others (1968), the Horse Camp basin is separated from the Horse and Grant Ranges by the arcuate trace of the Ragged Ridge fault and from the White Pine Range by the Currant Summit fault zone (Figure 2). They interpret the north-south segment of the Ragged Ridge fault to be a high-angle, down-to-the-west normal fault with as much as 10 kilometers of stratigraphic throw. Field relations indicate that the east-west segment of this fault has a left-lateral strike-slip component in addition to any rotational component. The Stone Cabin fault lies along strike and east of the Ragged Ridge fault. Together these east-west striking faults delineate a transverse zone that may represent a transfer fault system.

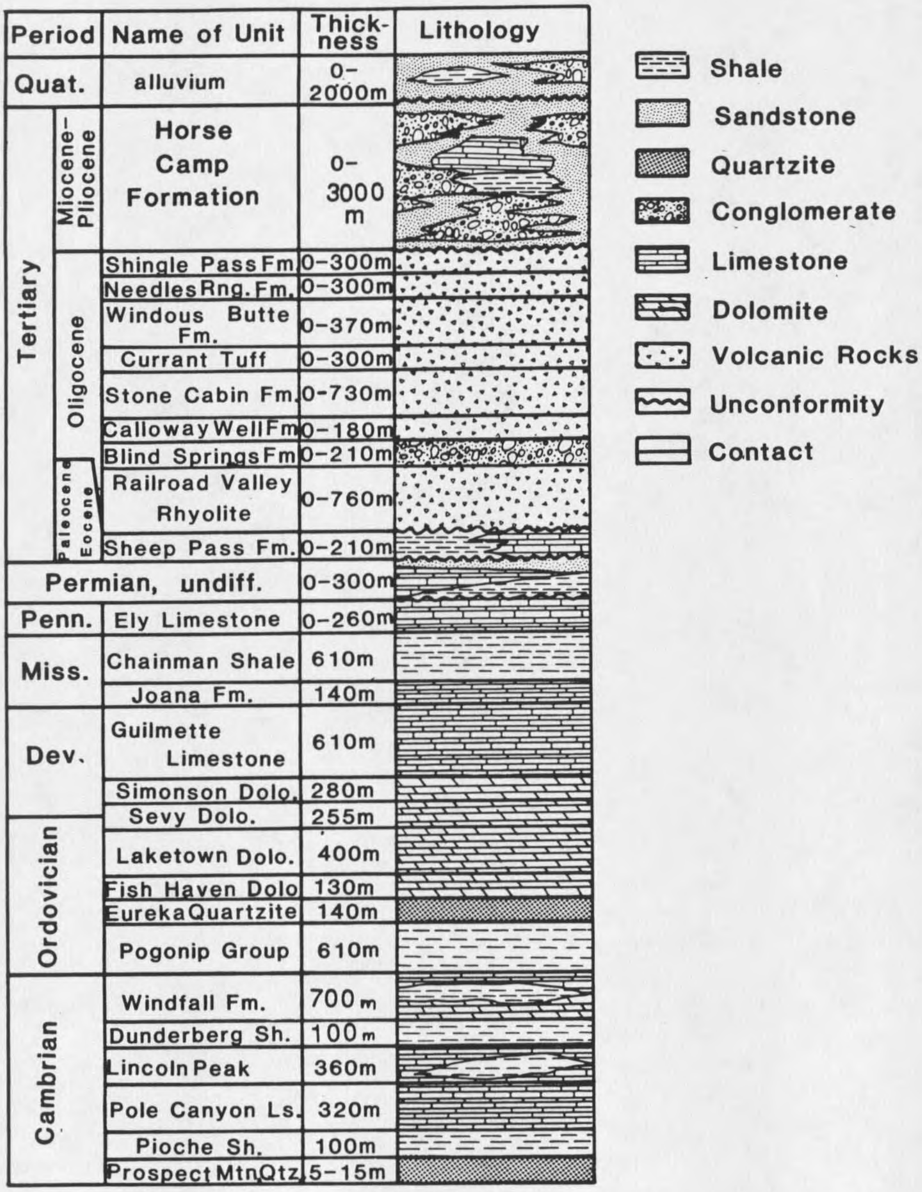

Figure 3. Stratigraphy of Paleozoic and Cenozoic rocks in the vicinity of the northern Grant, Horse and southern White Pine Ranges and Horse Camp basin. Modified from information in Moores (1968) and Fryxell (1988)

Although the mapping of Moores and others (1968) indicates that an angular unconformity separates the Oligocene volcanic section from older Paleozoic strata, they suggest that there was little deformation prior to Tertiary volcanism. However, this angular relationship is indicative of the presence of older deformational structures involving the Paleozoic section. Thrust faults and associated folds have been recognized in the Grant and Quinn Canyon Ranges to the south (Murray, 1985; Lund and others, 1987, 1988; Bartley and others, 1988; Fryxell, 1988, 1991, unpublished mapping; Janecke, unpublished mapping; Camilleri, 1989; Gleason, 1988; Bartley and Gleason, 1992) and in the Pancake Range to the west (Quinliven and others, 1974).

HORSE CAMP FORMATION

Moores (1968) divides the Horse Camp Formation into four stratigraphic units using lithologic differences and unit-bounding unconformities (Figure 4). Distribution of these units is delineated by the mapping of Moores and others (1968) (Figure 2). The lowest unit, Member 1 is a north striking sequence (Figure 5) composed of 300-600 meters of yellow, red, gray, and green volcaniclastic conglomerate, sandstone, siltstone, and megabreccia derived mostly from older Oligocene volcanic and Paleozoic miogeoclinal rocks (Moores, 1968). These strata unconformably overly the Oligocene Windous Butte, Needles Range, and Shingle Pass formations. The basal unconformity is angular and progressively truncates younger Oligocene rocks from north to south. The contact between the Oligocene rocks and Member 1 is characterized by a weathered zone on top of the older tilted volcanic bedrock (Figure 6) . This massive weathered zone typicallygrades into the beds of Member 1. Local faulting in the northern portion of the basin has omitted up to 350 meters of the lower portion of Member 1 (Plate 1). Moores (1968) suggests that the source area for Member 1 was to the west as indicated by sedimentary structures and information gathered from wells drilled in Railroad Valley (Smith, 1960). These well data show the Oligocene volcanic section to be missing where Miocene - Pliocene strata directly overlie Paleozoic carbonate rocks (Vreeland and Berrong, 1979; Foster, 1979).

The contact between Members 1 and 2 is slightly angular (Figure 7) and rocks of the two members are compositionally different. Member 1 dips 25° to 72° east and is dominated by rhyolitic and dacitic detritus; Member 2 dips about 60° east and is composed of conglomerate containing Oligocene rhyolite and dacite and Paleozoic carbonate clasts (Moores, 1968; Moores and others, 1968). Also, Moores (1968) identifies in Member 2

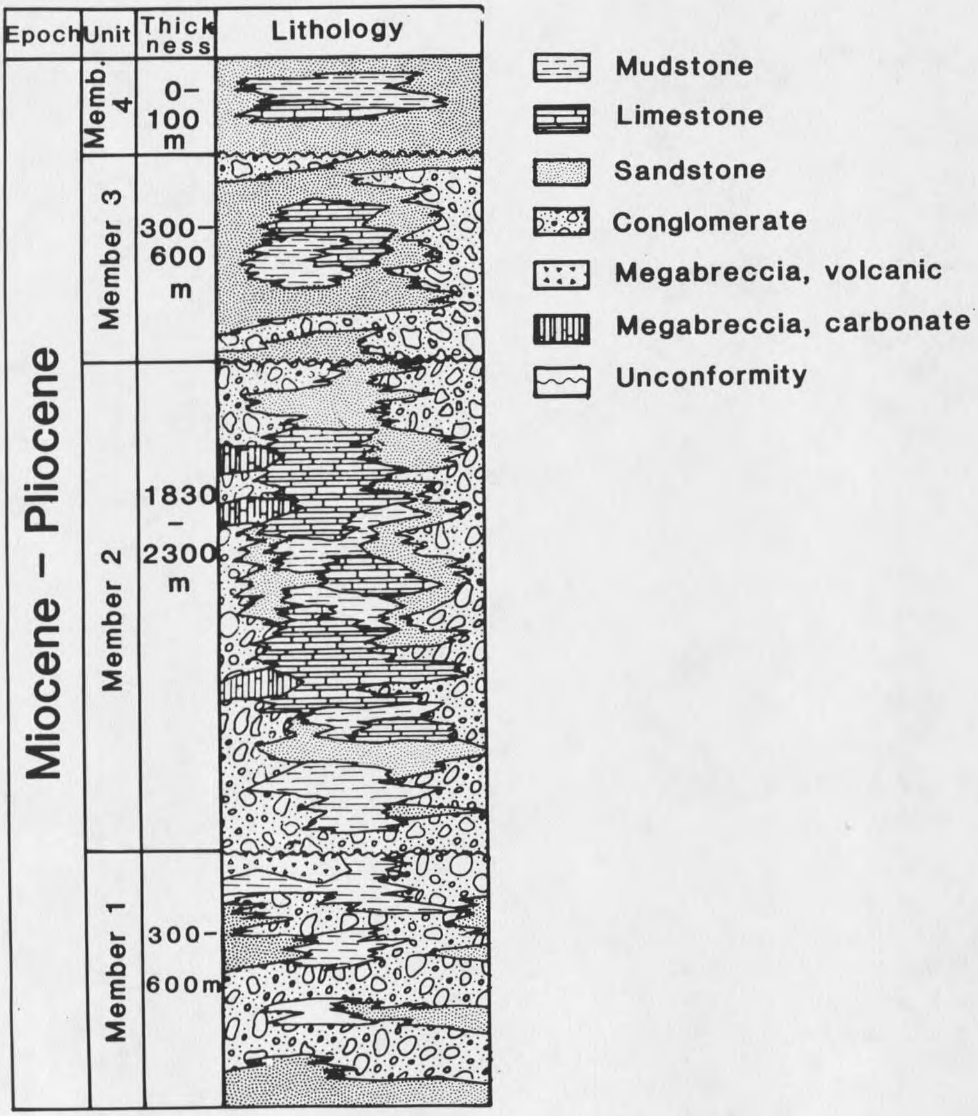

Figure 4. Generalized stratigraphic column for the Horse Camp Formation. Modified from Moores (1968).

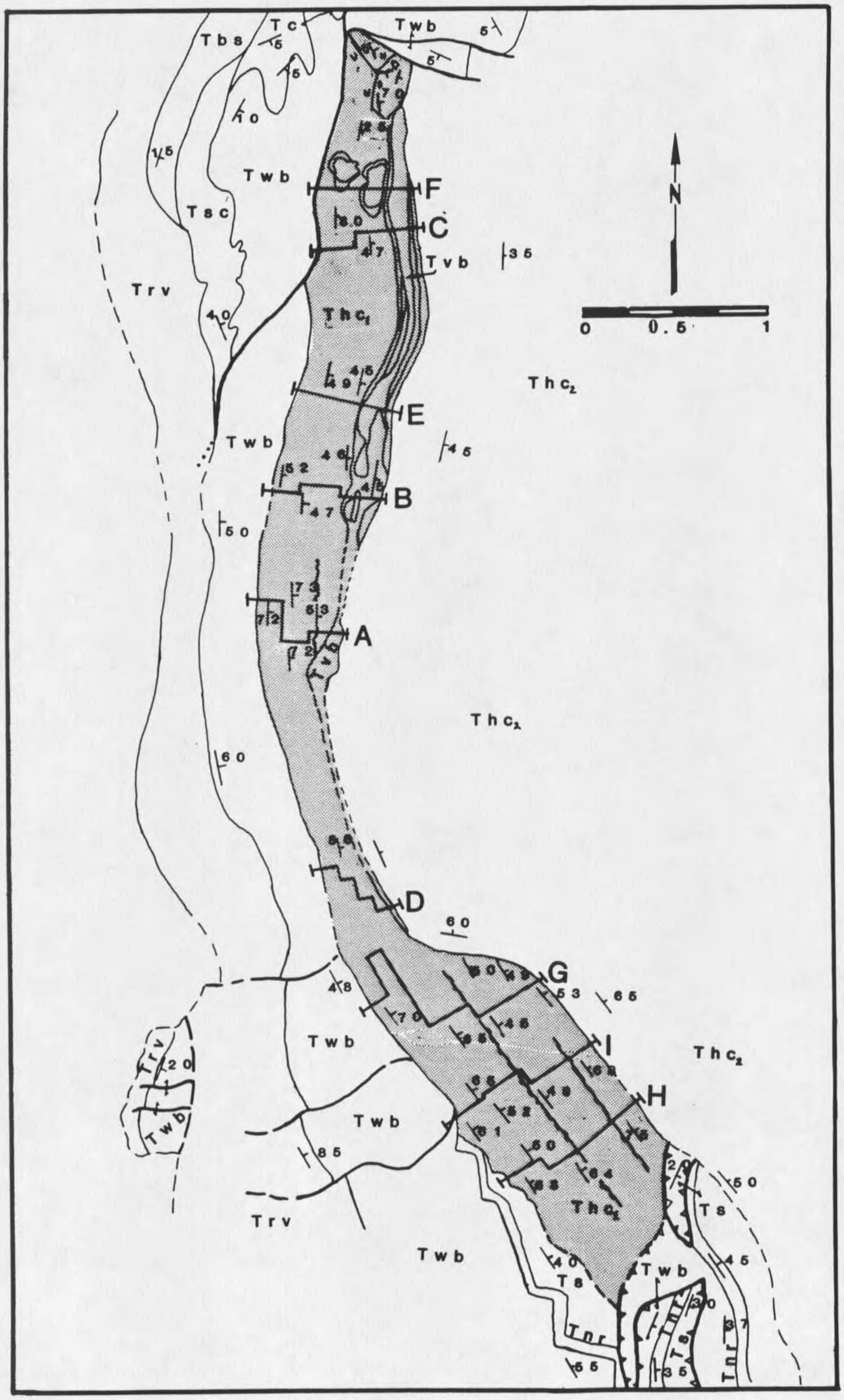

Figure 5. Geologic map of Member 1 of the Horse Camp Formation showing the location of measured sections A through I. Wavy lines denote locations of unconformities.

Figure 6. View toward north from near top of Section A showing the basal contact of Member 1 with underlying Windous Butte Formation. Arrows denote location of the basal contact.

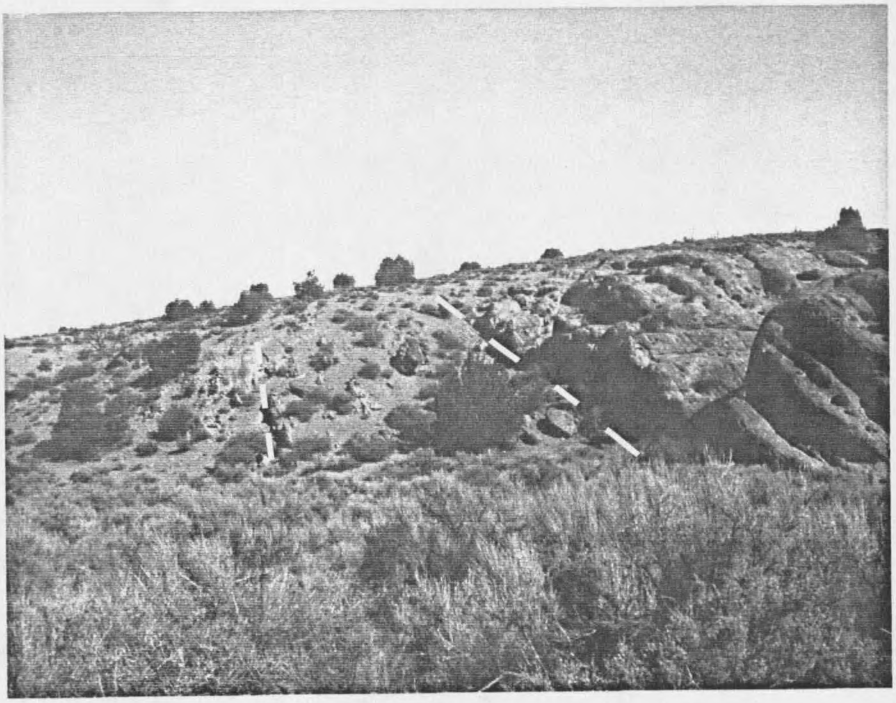

Figure 7. Angular contact between Member 1 on the left and Member 2 on the right along Big Wash. The white dashed lines denote the strike of bedding.

"muddy boulder breccias" containing Devonian dolomite and Ordovician sandstone clasts thought to be derived from the north. The "breccias" interfinger southward with a series of vitric ash and lacustrine deposits and volcaniclastic sandstone and conglomerate. Overlying the "muddy boulder breccias" are "monolithologic breccias" composed of Ordovician and Devonian quartzite and dolomite clasts in a carbonate matrix (Moores, 1968). These breccias are inferred by Moores (1968) to have source areas to the north and east.

Member 3 angularly overlies Member 2. Moores (1968) suggests that uplift, eastward tilting and erosion of Member 2 was followed by deposition of Member 3. Member 3 contains very coarse-grained, poorly-bedded, poorly-sorted conglomerate and muddy boulder breccias containing clasts from Paleozoic and Oligocene volcanic rocks as well as clasts from Members 1 and 2 of the Horse Camp Formation. (Moores, 1968; Moores and others, 1968). Moores (1968) interprets Gnat Hill as a sequence of brecciated and attenuated Paleozoic rocks, and Red Hill as an east dipping block of Tertiary volcanic rocks as "very large slide blocks" that were emplaced after Member 2 was tilted eastward.However, based on preliminary field observations and reconnaissance mapping, Gnat Hill may actually be a tilted fault block.

Member 4 is a sequence of poorly-indurated, carbonate-clast rich, fluvial mudstone, sandstone, and conglomerate that conformably overlies Member 3. It is lithologically similar to unnamed strata which crop out in topographic lows to the east in the Horse Range (Moores, 1968). The rocks of Member 4 of the Horse Camp Formation dip both eastward and westward whereas those in the Horse Range are horizontal. Member 4 strata cropping out in the Horse Camp Basin are composed of mudstone, sandstone, and conglomerate presumably derived from underlying Oligocene to early Miocene volcanic and sedimentary rocks and older Paleozoic strata (Moores, 1968; Moores and others, 1968).

The age of the Horse Camp Formation is not presently well known because vitric ash units within the formation have never been radiometrically dated. The Horse Camp

Formation overlies the 31 to 27 Ma (^{40}Ar / ^{39}Ar) Needles Range Formation, a rhyolitic tuff dated by Cook (1965) and Gans and others (1989), limiting the maximum age of the lower Horse Camp Formation to late Oligocene to early Miocene. A camel skull collected from near the top of Member 1 suggests a Barstovian age (16 to12 Ma) for this interval (T. Fouch, personal communication). Ostracods and gastropods found in Member 2 are of late Miocene to early Pliocene age (Van Houten, 1956; Moores, 1968).

To the south in the Grant Range, Taylor and others (1989) report a minimum biotite ^{40}Ar / ^{39}Ar age of 14.2 Ma from an air-fall tuff in the upper part of a conglomerate sequence that is lithologically similar to the Horse Camp Formation (Fryxell, 1984, 1988). This unnamed Miocene conglomerate crops out south of Horse Camp Basin on the north side of Little Meadow Creek in the central Grant Range. Fryxell (1988) uses this Miocene age to suggest that this conglomeratic sequence is older than the Horse Camp Formation but because the age of the Horse Camp Formation has not been well determined, its chronostratigraphic relationship with the unnamed conglomerate is not clear.

METHODS

Field Methods

Geological maps and structural interpretations of the Horse Camp area (Moores, 1963; Scott, 1965; Lumsden, 1964; Moores and others, 1968) were used as a foundation for more detailed mapping of Member 1 of the Horse Camp Formation on 1:24,000 aerial photographs and USGS Provisional topographic maps. Other existing geological maps were used to provide information on the structure of adjacent areas (Wire, 1959; Fryxell, 1988; Bartley and Gleason, 1992).

To determine depositional environments, strata of Member 1 of the Horse Camp Formation were measured and described in detail using the pace and compass method (Graham, 1988, p. 24-25). Nine stratigraphic sections were measured at locations where exposures were relatively complete and sample collection and lithofacies analysis were possible (Plate 2 and Figure 5). Data from the measured sections were combined with lateral profiles constructed from field sketches and photographs to contribute to large scale paleoenvironmental analysis stressing vertical and horizontal lithofacies associations (Miall, 1985). Lithofacies were delineated on the basis of grading, sedimentary structures, grain-size, and clast-to-matrix ratio (Table 1). Standard lithofacies classifications were used for mudstone and sandstone facies (Miall, 1977; Rust, 1978). Coarse-clastic lithofacies classifications were generally based on Miall (1977), Shultz (1984), and Waresback and Turbeville (1990). Modifications were necessary however because of the variety of the coarse clastic deposits represented. Megabreccia lithofacies were delineated using the nomenclature established by Yarnold and Lombard (1989) who recognized vertical and lateral trends within sedimentary breccia and megabreccia deposits.

Provenance of Member 1 of the Horse Camp Formation was determined by collection and analysis of compositional and directional information. Thirty-three clast counts were performed on pebble-cobble conglomerates to determine compositional trends and clast provenance. A minimum of 250 clasts were counted on a fixed grid which exceeded the mean observed clast size at locales of appropriate exposure. Because the composition of sedimentary rocks is controlled to some degree by grain size it was necessary to analyze the composition of sandstone Odom and others, 1976; Folk, 1980, p.49-59; Ingersoll and others, 1984; McManus, 1988, p. 63) as well as pebble, cobble and boulder conglomerates. Fifty-four representative sandstone units were sampled for thin-section petrographic analysis which is described in the laboratory methods section below.

Flow direction was estimated by direct measurement of trough axes in trough cross-stratified sandstones (Graham, 1988, p.31-33). Due to the scarcity of exposed trough cross-stratified sandstone units and overall lack of imbricated clasts (clasts were typically equidimensional), other means of determining paleoslope were necessary. The direction of scour development on the downflow side of cobble- and boulder-sized clasts was measured (Figure 8). These features are termed obstacle shadows or shadow structures (Karcz, 1968). Other evidence of paleoslope was recorded by measurement of the trend and plunge of vergent folds within deformed sediments underlying megabreccia sheets deposited during landslide events (Yarnold and Lombard, 1989). Textural trends in Member 1 megabreccias were compared with the proximal to distal trends recognized and modelled by Yarnold and Lombard (1989) in order to determine source area location for the megabreccias.

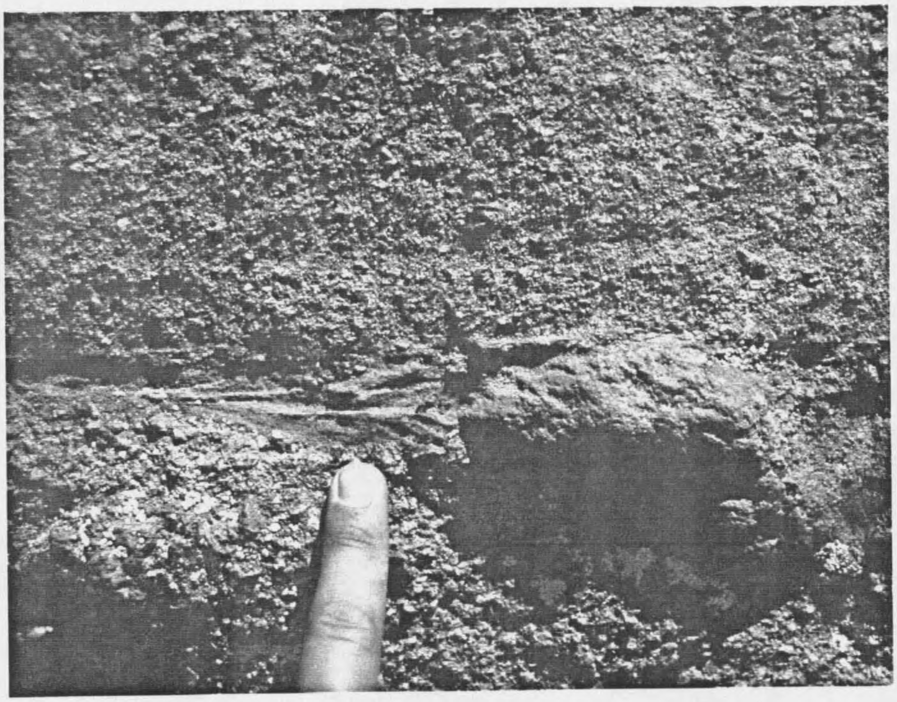

Figure 8. Well-developed shadow structure on downflow side of cobble clast.

Laboratory Methods

Thin sections of 54 sandstones of Member 1 of the Horse Camp Formation were examined using a petrographic microscope. Each thin-section was counted on a fixed-grid spacing for a minimum of 250 framework grains (points). Although only medium- to coarse-grained sandstones were used to facilitate point-counting, modal grain sizes were also visually estimated for each sample. Compositional data were plotted on QFL, Q_mFL_t, and $Q_pL_sL_v$ ternary diagrams to discern petrofacies and provenance (Dickinson and Suczec, 1979). The trend and plunge of trough axes and fold axes were plotted on an equal-angle stereo-net and rotated to correct for post-depositional tectonism (Graham, 1988, p.43). These data are discussed in a following section.

SEDIMENTOLOGY

Lithofacies

Fifteen lithofacies types are recognized in Member 1 utilizing differences in sedimentary structures, grading, grain size, and clast-to-matrix ratios (Table 1). Conglomerate lithofacies dominate Member 1 and comprise as much as 70% of measured sections. Sandstone and mudstone are less abundant. Lithofacies are discussed in order of abundance.

Clast-Supported Ungraded Conglomerate (Gcu)

Description: This facies consists of massive ungraded conglomerate that is clast-supported. It contains moderately to poorly sorted subangular to subrounded, blade and equidimensional shaped granule, pebble, cobble, and boulder (< 1.5 meters in diameter) sized clasts in a poorly sorted matrix of sandy mud to muddy sand. This facies is characterized by a lack of internal stratification and imbrication throughout. Individual units are most commonly tabular, 5 to 250 centimeters thick and extend as much as 250 meters laterally. Tabular units usually have sharp subplanar basal contacts (Figure 9). Occasionally, these units fill underlying topographic lows including broad, shallow, concave-up scours generally less than 2 meters deep and 15 meters wide (Figure 10). In these instances scour fill is typically entirely Gcu although interstratified horizontally bedded sandstone (Sh) is sometimes present. Upper bed contacts are typically erosional. Protruding clasts at unit tops are found in association with small (< 0.25 meters deep and

Table 1. Lithofacies code, description, and interpretation.

Code	Lithofacies	Sedimentary Structures	Interpretation
Gcu	Gravel, clast-supported, muddy to sandy mud matrix	Massive with some imbrication	Hyperconcentrated and psuedoplastic flow
Gcn	Gravel, clast-supported, muddy to sandy mud matrix	Normally graded	Hyperconcentrated, debris, and turbidity flow
Gci	Gravel, clast supported, muddy to sandy mud matrix	Inversely graded	Plastic and psuedoplastic debris flow
Gmu	Gravel, matrix-supported, muddy to sandy mud matrix	Massive	Viscous plastic debris flow and subaqueous gravity flow
Gmn	Gravel, matrix-supported, sandy mud matrix	Normally graded	Fluid debris flow and subaqueous gravity flow
Gmi	Gravel, matrix-supported, muddy to sandy mud matrix	Inversely graded	Viscous debris flow
Gh	Gravel, clast-supported, sandy to sandy-mud matrix	Horizontally stratified, imbricated	Sheetflow
Gt	Gravel, clast-supported,	Low-angle trough cross-bedded	Shallow stream flow

Table 1 (continued)

Code	Lithofacies	Sedimentary Structures	Interpretation
Sm	Sand, moderately to poorly-sorted	Massive	Hyperconcentrated, debris, and density modified grain flow
Sn	Sand, moderately to poorly-sorted	Normally-graded	Subaerial and subaqueous sediment gravity flows
Si	Sand, moderately to poorly-sorted	Inversely-graded	Debris flow
Sh/Sl	Sand, moderately to well sorted	Horizontally stratified Low-angle cross-stratified	Sheetflow and shallow stream flow
Sr	Sand, moderately to well sorted	Ripple cross-stratified	Sheetflow and shallow stream flow
St	Sand, moderately to well sorted	Trough cross-stratified	Shallow stream flow
Fl	Silt and clay	Thinly bedded to thinly laminated	Settling from suspension

Figure 9. Matrix-supported, ungraded, pebble to cobble conglomerate (Gmu) with overlying clast-supported, ungraded, cobble to boulder conglomerate (Gcu). Note subplanar contact. Notebook for scale.

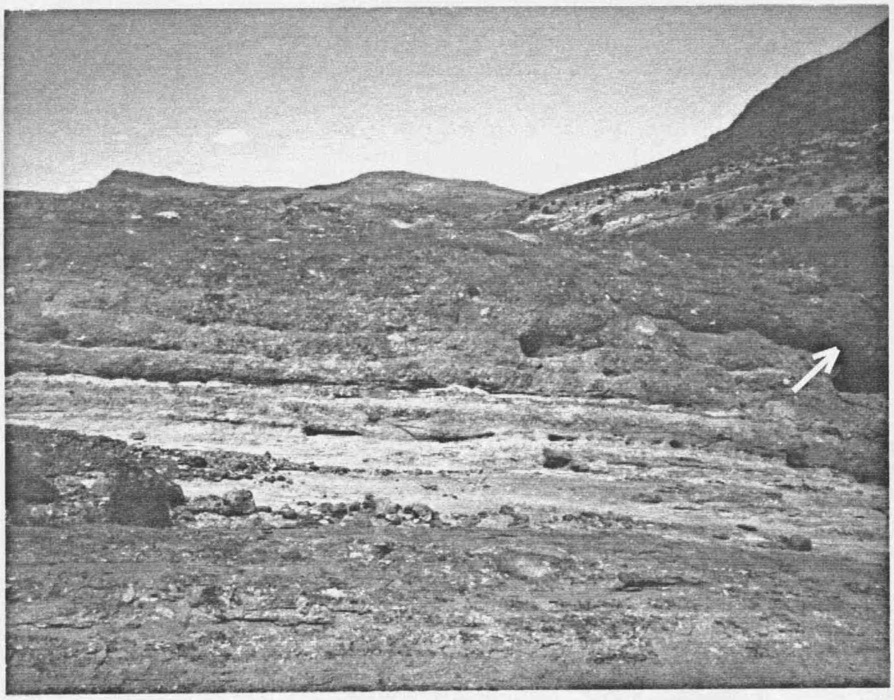

Figure 10. Interbedded, laterally continuous conglomerate and sandstone units. Arrow points to a 0.5 meters deep by 3 meters wide scour filled with conglomerate.

<0.5 meters wide) scour and fill sequences consisting of horizontally stratified (Sh), low-angle (Sl), and trough cross stratified (St) sandstone. Tabular clast-supported ungraded conglomerate units grade laterally into normal (Gcn) or inverse (Gci) graded, clast-supported conglomerate and clast-rich, matrix-supported, ungraded conglomerate (Gmu). These units are interstratified with all other lithofacies types and are frequently overlain by horizontally stratified sandstone and mudstone (Sh, Fl). In sequences where Gcu isinterbedded with mostly sandstone and mudstone, soft sediment deformation is common (Figure 11).

Interpretation : Clast-supported, massive, ungraded conglomerate (Gcu) was deposited by hyperconcentrated flow (Costa, 1988) and/or pseudoplastic debris flow processes (Shultz, 1984). Poorly sorted, clast-supported conglomerate units with poorly sorted muddy matrix and a lack of internal stratification are indicative of deposition by flows characterized by high sediment concentrations and relatively low yield strength. For hyperconcentrated flow, the primary mechanism of sediment-support is turbulence and clast interaction (Smith, 1986). In the case of pseudoplastic debris flow, matrix strength and grain dispersive pressure, and clast interaction support the sediment gravity flow (Shultz, 1984). The tabular geometry of these units suggests that hyperconcentrated and pseudoplastic debris flows deposited sediment on a surface that allowed for unconfined flow (Rodine and Johnson, 1976; Waresback and Turbeville, 1990). Interstratification with other lithofacies types and the common presence of horizontally stratified sandstone and mudstone overlying the deposits indicates that hyperconcentrated and debris flows were commonly followed by sheetflood events that reworked the deposit surfaces.

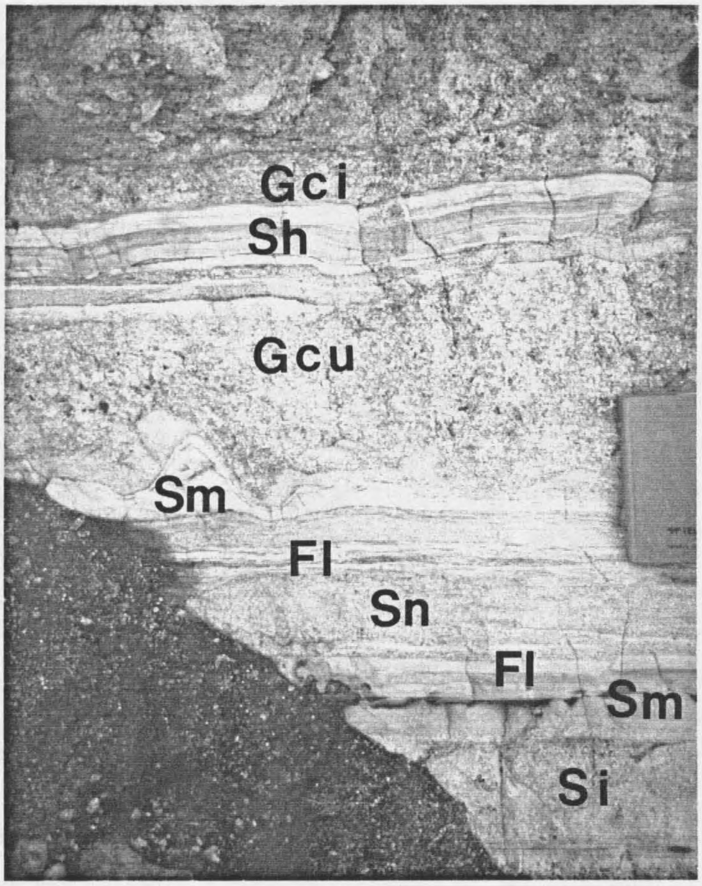

Figure 11. Interbedded sandstone and conglomerate units deposited in a distal alluvial fan environment. Note load structure in left-center of photo. Si - inversely graded sandstone; Sm - massive, ungraded sandstone; Fl - laminated mudstone; Sn - normally graded sandstone; Gcu - ungraded, clast-supported granule, pebble conglomerate; Sh - horizontally stratified sandstone; Gci - inversely graded clast supported granule to pebble conglomerate. Edge of fieldbook (15 cm) for scale.

Clast-Supported, Normally Graded Conglomerate (Gcn)

Description : This facies consists of clast-supported, massive normally graded conglomerate (Figure 12). The gravel framework is composed of very poorly sorted, angular to subrounded, blade to equant shaped, granule, pebble, cobble, and boulder (< 0.5 meters in diameter) sized clasts. Interstitial matrix is very poorly sorted and ranges from muddy sand to sandy mud and commonly supports coarse sand, granules, and pebbles. Internal stratification and imbrication are completely lacking in the units. Both coarse-tail and distribution grading are present in this facies. Depositional units are tabular, ranging in thickness from 5 to 100 centimeters and extending laterally as much as 200 meters. Deposits that fill shallow, broad scours that are generally less than 2 meters deep and up to 15 meters wide are typically massive but can be interstratified with horizontally bedded sandstone (Sh) (Figure 10). Both basal and upper contacts are abrupt and typically subplanar. Horizontally stratified (Sh) and low angle stratified (Sl)sandstone units capped by laminated mudrock (Fl) with desiccation cracks frequently overlie Gcn units. Clast-supported, normally graded conglomerate (Gcn) commonly grades laterally into matrix-supported, normally graded conglomerate (Gmn), and clast-supported, ungraded conglomerate (Gcu) (Figure 13). Units that possess coarse tail normal grading locally grade into clast- or matrix-supported, inversely-to-normally graded conglomerate. Units characterized by distribution grading are sometimes found associated with very thick (4 - 9 meters), laterally extensive sequences (10 - 45 meters) of laminated mudrock.

Interpretation : Clast-supported, normally graded conglomerates (Gcn) were deposited from either hyperconcentrated flood flow, debris flow, or turbidity flows. Those units with distribution grading were deposited by hyperconcentrated flows that were

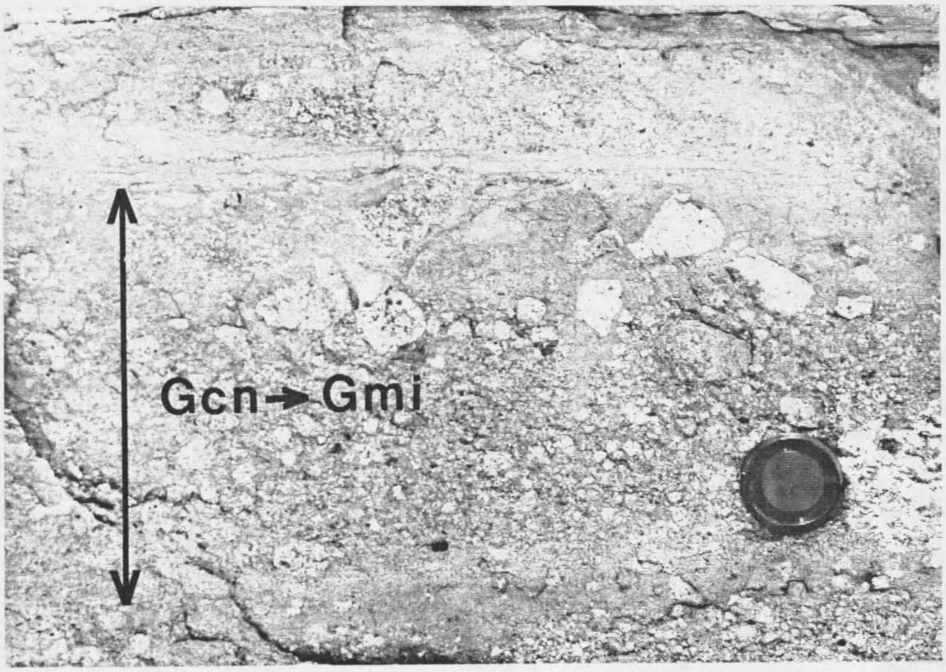

Figure 12. Lithofacies transition within a massive conglomerate. Transition from clast-supported normally graded pebble to cobble conglomerate (Gcn) near base of bed (lower arrows) to matrix-supported inversely graded pebble to cobble conglomerate (Gmi) at top of bed. Lens cap (5 cm) for scale.

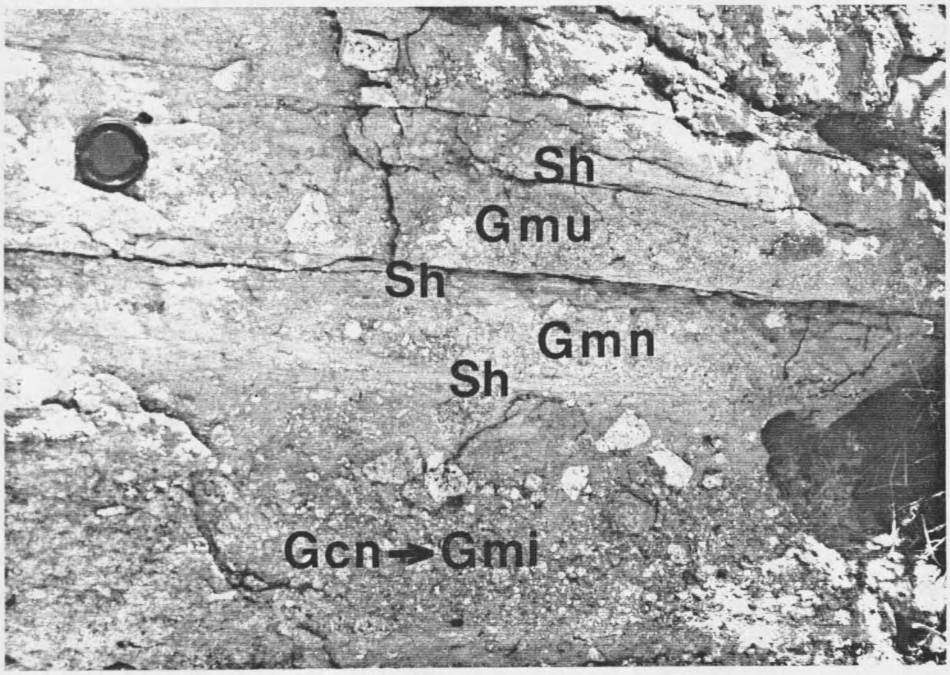

Figure 13. Interbedded conglomerate and sandstone units deposited in a medial alluvial fan setting. Gcn - clast-supported, normally graded pebble, cobble conglomerate; Gmi - matrix-supported, inversely graded pebble, cobble conglomerate; Sh - horizontally stratified sandstone; Gmn - matrix-supported normally grade granule, pebble conglomerate; Gmu - matrix-supported ungraded granule, pebble conglomerate. Lens cap (5 cm) for scale.

partially turbulent with some grain dispersive pressure that supported the sediment (Smith, 1986). Rapid grain-by-grain deposition produces units lacking in stratification with polymodal matrix. This type of deposition occurs when turbulence in the flows keep clasts in suspension much like in turbidity flows (Shultz, 1984; Smith, 1986). Clast-supported, coarse tail normally graded units were deposited by clast-rich pseudoplastic debris flows (Shultz, 1984) which are characterized as having relatively low yield strength and extreme reduction of the rigid-plug layer (Costa, 1984). The strength of the matrix alone is not enough to support clasts and dampened turbulence during periods of high flow velocity aid in supporting clasts. Turbulence decreases rapidly during flow deceleration allowing larger clasts to settle out of suspension thereby creating clast-supported, coarse-tail normally graded beds (Shultz, 1984; Smith, 1986). The presence of finer grained sandstone and mudstone units overlying these massive deposits suggests that flooding events were followed by shallow sheetflow events. Dessication cracks are suggestive of subaerial exposure.

Clast-supported, normally graded units associated with thick, extensive units of laminated mudrock are somewhat better sorted and contain less abundant clay-sized sediment. These deposits may have been deposited as turbidity currents in a shallow lacustrine system where clay can be forced out of the flow (Walker, 1978) and grain interaction improves clast sorting (Hampton, 1975; Naylor, 1980).

Clast-Supported, Inversely Graded Conglomerate (Gci)

Description : This facies is composed of clast-supported, inversely graded conglomerate (Gci). The framework consists of extremely poorly sorted, angular to subrounded, equidimensional to blade shaped, granule, pebble, cobble, and boulder (< 1.5 meters in diameter) sized clasts in a very poorly sorted sandy mud to muddy sand matrix.

Very coarse sand, granules, and pebbles are present in the interstices of the coarser conglomerates (Figure 14). This facies lacks imbrication and is void of internal stratification except near the base of some of the deposits. Beds are typically tabular, 10 to 200 centimeters thick, and extend laterally up to 150 meters. The basal contact is subplanar, sharp, and appears non-erosive (Figure 15). This facies is interbedded with all other types of lithofacies. Most commonly, it is overlain by horizontally laminated (Sh), low-angle cross stratified (Sl), and ripple cross-stratified sandstone (Sr) composed of finer grained material (silt, sand, and granule sized) derived from the surface of the conglomerate beds (Figure 16). Scour development is common adjacent to larger clasts protruding from the tops of the conglomerate beds. Clast-supported inversely graded conglomerates commonly grade into clast-supported ungraded (Gcu) and coarse-tail normally graded (inversely-to-normally graded) conglomerates (Gcn).

<u>Interpretation</u> : Clast-supported, inversely graded conglomerate units (Gci) were deposited by clast-rich plastic and pseudoplastic debris flows. These flows behave as density-modified grain flows (Lowe, 1976) where interstitial matrix enhances clast buoyancy and reduces normal stresses between clasts thereby allowing the flow to remain mobile for long distances (Rodine and Johnson, 1976). The primary sediment support mechanisms are grain dispersive pressure and cohesion during transport which result in inverse grading within the depositional units. Basal stratification and lack of evidence for erosion at the base suggests that flow was dominantly laminar (Fisher, 1971; Enos, 1977). Extremely poor sorting within the deposits (both matrix and framework portions) suggests that selective deposition did not occur during transport (Shultz, 1984). Rather, deposition en masse likely occurred, perhaps by freezing of a rigid plug.

Figure 14. Interbedded conglomerate and sandstone units deposited in a proximal alluvial fan setting. Gcu - ungraded, clast-supported pebble, cobble, and boulder conglomerate; Sm - massive, ungraded sandstone; Gci - inversely graded clast-supported pebble to cobble conglomerate. Fieldbook (15 cm long) for scale.

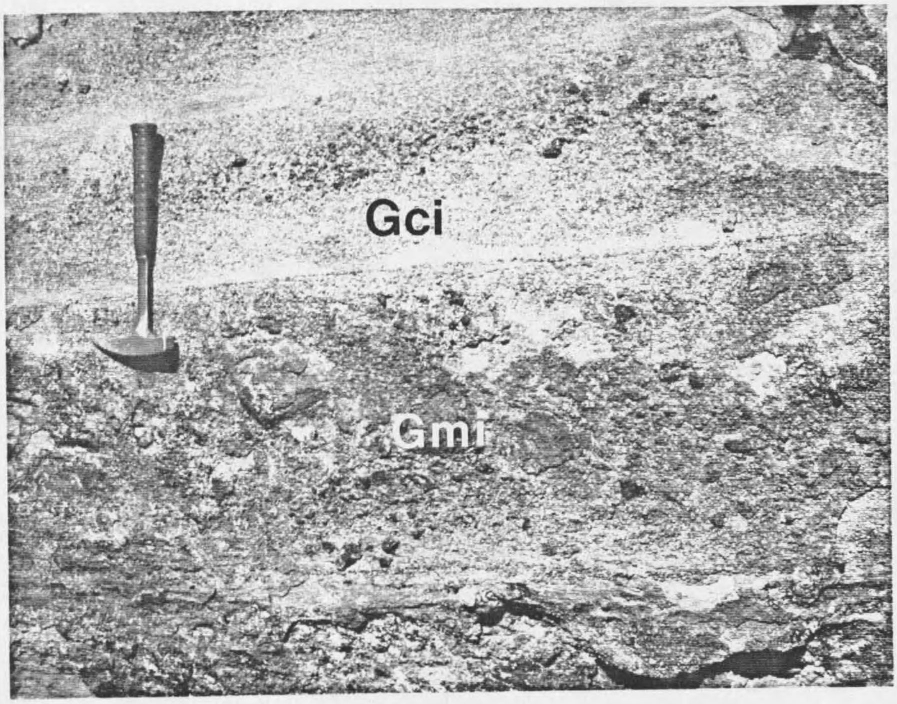

Figure 15. Interbedded conglomerate units deposited in a medial alluvial fan setting.Gmi - matrix-supported, inversely graded pebble to cobble conglomerate; Gci - inversely graded clast supported granule to pebble conglomerate. Hammer for scale.

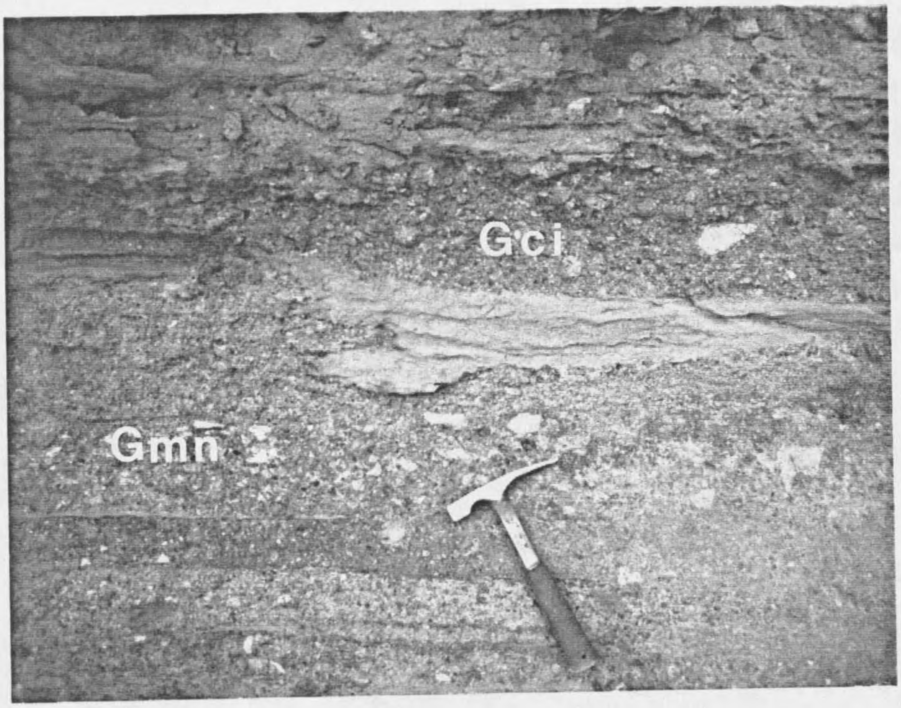

Figure 16. Interbedded sandstone and conglomerate deposited in a medial alluvial fan setting. Gmn - matrix-supported normally grade pebble to cobble conglomerate; Gci - inversely graded clast supported pebble to cobble conglomerate. Hammer for scale.

Matrix-Supported, Ungraded Conglomerate (Gmu)

Description : This facies is composed of matrix-supported, massive, ungraded conglomerate (Gmu). The framework consists of moderately to very poorly sorted, angular to rounded, blade and equant shaped, granule, pebble, cobble, and boulder sized gravel in a very poorly sorted matrix composed of muddy sand to mud (Figure 10). Although this facies is matrix-supported, a wide range in gravel content gives rise to both clast-rich (> 50% clasts) and clast-poor (< 50% clasts) varieties. Clast-rich deposits form tabular to sheet-like beds 5 to 250 centimeters thick and up to 150 meters wide (perpendicular and oblique to flow direction) (Figure 13). Some fill broad scours (Figure 10). These units lack internal stratification and commonly grade laterally into graded conglomerate (Gmn, Gmi) towards the center of the deposits and into clast-supported,massive, ungraded (Gcu) or graded conglomerate (Gcn, Gci) along the fringes of the deposits. They are interbedded with all other lithofacies types and commonly overlain by horizontally stratified sandstone (Sh) and conglomerate (Gh) and laminated mudstone (Fl).

Clast-poor deposits also form tabular to sheet-like beds 3 to 200 centimeters thick and up to 120 meters in lateral extent (perpendicular and oblique to flow direction) (Figure 10). Some fill broad scours. The basal contact is typically sharp. These units commonly grade laterally into massively bedded sandstone (Sm) or matrix-supported graded conglomerate (Gmn, Gmi) and are intercalated with all other types of lithofacies. Most commonly they are overlain by horizontally bedded sandstone (Sh) and laminated mudstone (Fl). Matrix-supported, ungraded conglomerate is present in the thick, laterally continuous sequences of laminated mudrock (Fl) and in these areas load structures and disharmonic folding are common in the mudrock. Mudcracks are recognizable in laminated mudstone (Fl) found at the tops of both clast-rich and clast-poor facies. Root traces are common.

Interpretation : Matrix-supported, ungraded conglomerate (Gmu) is interpreted as the deposits of subaerial plastic debris flows and subaqueous sediment gravity flows. Clast-rich flows were transported under laminar conditions as noted by the lack of stratification and absence of scour at the base of the deposits (Fisher, 1971; Enos, 1977). Cohesion and dispersive pressure were the primary mechanisms of sediment support. The tabular nature of these deposits suggests that subaerial debris flows deposited material over an unconfined surface (Rodine and Johnson, 1976; Waresback and Turbeville, 1990). Lateral textural variability in the deposits resulted from lateral changes in flow rheology such that flows were more fluid along the edges (Shultz, 1984).

Clast-poor matrix-supported, ungraded conglomerates were deposited as both subaerial and subaqueous sediment gravity flows. Subaerial deposits commonly grade laterally into matrix-supported, coarse tail normally- or inversely-graded conglomerate (Gmn, Gmi). These lateral gradations suggest that the sediment was transported as relatively fluid debris flows where material is supported by the cohesive nature of the matrix (Naylor, 1980). Tabular unit geometry and association with horizontally stratified sandstone (Sh), mudcracks and root traces suggest that clast-poor, matrix-supported, ungraded conglomerate units were deposited in a subaerial environment where flow was not confined to channels. Reworking of the tops of the depositional units by sheetflow and pedogenesis were important processes between flow events.

Subaqueous deposition by density or turbidity flow is probable where these facies are associated with very thick laminated mudstone (Fl) units (5 - 45 meters). Lateral gradations into massive normally graded sandstone (Sn) and granule-pebble normally graded clast-supported conglomerate (Gcn) have been recognized in turbidite sequences

(Walker, 1978). The presence of disharmonic folding, contorted bedding, and load structures in the underlying laminated mudstone (Fl) units suggests that deposition occurred over a water saturated surface (Mastalerz, 1990).

Matrix-Supported, Normally Graded Conglomerate (Gmn)

Description : Matrix-supported, massive, normally graded conglomerate units are composed of moderately to poorly sorted, subangular to rounded, blade and equant shaped, granule, pebble, cobble, and boulder (< 1.5 meters in diameter) sized clasts in a poorly sorted matrix composed of muddy sand to mud (Figure 16). These deposits form tabular to sheet-like beds 4 to 200 centimeters thick and up to 200 meters wide (perpendicular and oblique to flow direction), have a well-defined planar basal contact, and fill pre-existing topography (Figure 13). They commonly grade laterally into clast-poor matrix-supported, ungraded (Gmu) and inversely graded conglomerate (Gmi) and are intercalated with all other types of lithofacies. Most commonly, these units are overlain by horizontally bedded sandstone (Sh) and laminated mudstone (Fl). Matrix-supported, normally graded conglomerate units are present within the thick, laterally continuous laminated mudrock (Fl) units. In these instances, load structures and disharmonic folding are common in the underlying laminated mudrock (Fl).

Interpretation : Matrix-supported, normally graded conglomerate (Gmn) is interpreted as the deposits of subaerial fluid, unconfined debris flows and subaqueous density flows. Subaerial deposits are interbedded with horizontally stratified sandstone and mudrock (Sh, Fl) units the surfaces of which often have mudcracks and root traces. These deposits commonly grade laterally into clast-poor matrix-supported, ungraded and inversely graded conglomerate (Gmu, Gmi) indicating that the sediment was supported by matrix cohesion while being transported as relatively fluid debris flows (Naylor, 1980). Tabular unit geometry and the presence of sheetflow deposits overlying units of matrix-supported, normally graded conglomerate (Gmn) suggest that deposition occurred on an unconfined depositional surface.

Subaqueous deposition by density or turbidity flow is probable where this facies is associated with thick laminated mudstone (Fl) units. This interpretation is supported by the presence of disharmonic folding, contorted bedding, and load structures in the underlying laminated mudstone (Fl) units suggesting that the depositional surface was water saturated (Mastalerz, 1990). In addition, lateral gradation of matrix-supported, normally graded conglomerate (Gmn) into massive, ungraded sandstone and granule-pebble conglomerate (Sm, Sn, Gmu) is a relationship documented from turbidite deposits (Walker, 1978) and indicative of subaqueous deposition.

Matrix-Supported, Inversely Graded Conglomerate (Gmi)

Description : This facies consists of massive, inversely graded conglomerate (Gmi). It is composed of poorly to very poorly sorted, angular to subrounded, blade and equant granule, pebble, cobble, and boulder (<2.5 meters in diameter) sized clasts in a matrix of very poorly sorted muddy sand to mud (Figure 15). These units are typically 7 to 20 centimeters thick and up to 100 meters wide. Stratification is absent except for occasional shear fabrics near the base. The basal contact is typically sharp and planar. Coarse tail grading is predominant and can disappear laterally such that the unit becomes either matrix-supported, ungraded (Gmu) or clast-supported and ungraded (Gcu) (Figure 12). Clast content within a single depositional unit changes laterally as some units are more matrix-supported near their centers. Matrix-supported, inversely graded conglomerate

(Gmi) is interbedded with all other lithofacies types and most commonly overlain by horizontally (Sh) and low angle stratified sandstone (Sl) and horizontally stratified mudrock (Fl). Small scour and fill sequences composed of trough cross-stratified sandstone and granule - pebble conglomerate (St, Gt) are common on the down-flow side of clasts protruding from the upper surfaces of the depositional units (Figure 17).

Interpretation : Matrix-supported, inversely graded conglomerate (Gmi) is interpreted as the deposits of subaerial viscous debris flows. Sediment was transported under laminar flow conditions as noted by the lack of traction-induced stratification and absence of scour at the base of the deposits (Fisher, 1971; Enos, 1977). Inverse grading suggests that kinetic seiving was common enough to cause vertical clast segregation and dispersive pressure was high enough to support larger clasts above the base of the bed (Larsen and Steel, 1978; Costa, 1984). The tabular nature of the deposits suggests that these debris flows deposited material on an unconfined surface (Rodine and Johnson, 1976; Waresback and Turbeville, 1990).

Lateral Gradations in Massive Conglomerate Lithofacies

Lateral textural variations within massive conglomerate units are caused by changes in flow rheology. Basal friction and dewatering within the flow can cause an increase in yield strength and flow plasticity (Shultz, 1984). This effectively increases matrix content and may cause transitions from normal to ungraded to inversely graded fabrics within a single massive unit. Dilution of a debris flow would cause a decrease in yield strength and the flow would become either ungraded, normally graded, or inversely-to-normally graded (Rodine and Johnson, 1976) depending upon the initial state of the flow.

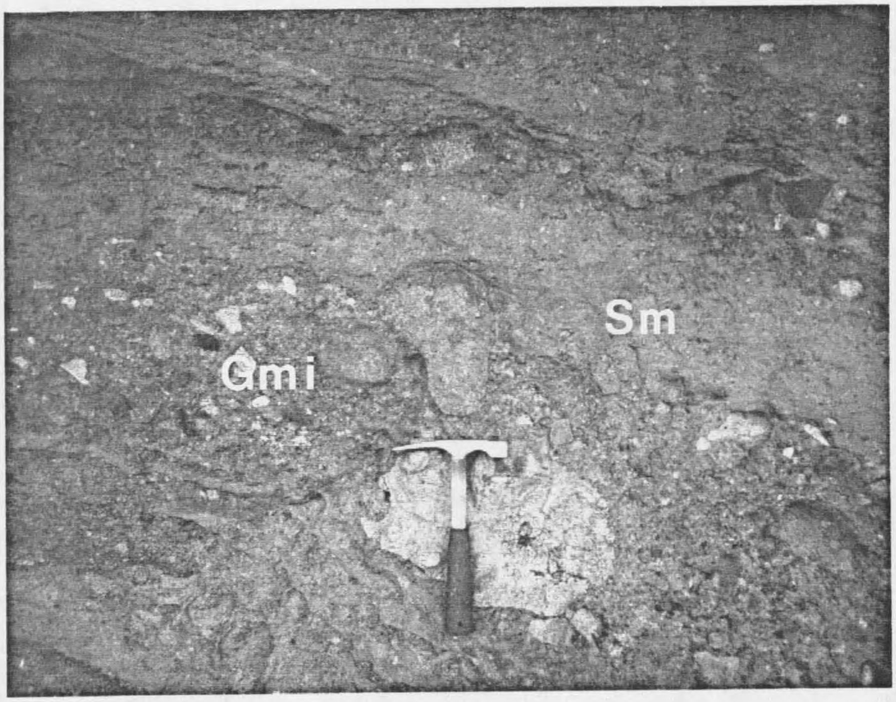

Figure 17. Interbedded sandstone and conglomerate deposited in a medial alluvial fan setting. Gmi - matrix-supported, inversely graded pebble, cobble, and boulder conglomerate; Sm - massive, ungraded sandstone. Hammer for scale.

Horizontally Stratified Conglomerate (Gh)

Description : Horizontally stratified conglomerate (Gh) units are composed of granule to cobble sized gravel with sandy to sandy mud matrix. Beds are tabular with thicknesses ranging from 10 to 300 centimeters and lateral extent from 10 to 250 meters. Horizontally stratified conglomerate (Gh) interbedded with horizontally stratified sandstone commonly fills broad, shallow scours (1 meter deep and 15 meters wide) (Figure 18). This facies is frequently part of fining-upward sequences (Figures 11 and 13) where it is underlain by matrix- and clast-supported, massive, graded (Gmn, Gmi, Gcn, Gci) and ungraded (Gmu, Gcu) conglomerate and overlain by horizontally stratified sandstone (Sh), ripple-cross stratified sandstone (Sr), and horizontally laminated mudstone (Fl).

Interpretation : Horizontally stratified conglomerate (Gh) was deposited under upper flow-regime plane bed conditions. Horizontally stratified conglomerate (Gh) with a sandy matrix is indicative of streamflow while units with more clay-rich matrix may be suggestive of hyperconcentrated flow (Smith, 1986). The tabular to sheet-like nature of individual units suggests deposition occurred during periods of unconfined turbulent flow over broad, low-relief depositional surfaces. This type of high-energy and sediment charged flow is termed sheetflow (Miall, 1977). The presence of this facies in tabular fining-upward sequences indicates that unconfined debris flow events were followed by turbulent unconfined sheetflow capable of reworking material at the tops of the debris flows. The presence of interbedded horizontally stratified conglomerate (Gh), horizontally and low-angle stratified sandstone (Sh), ripple-cross stratified sandstone (Sr), and horizontally laminated mudstone (Fl) filling broad, shallow scours (Bull, 1972; Nilsen, 1982; Mack and Rasmussen, 1984) suggests that in-filling of surface topography occurred

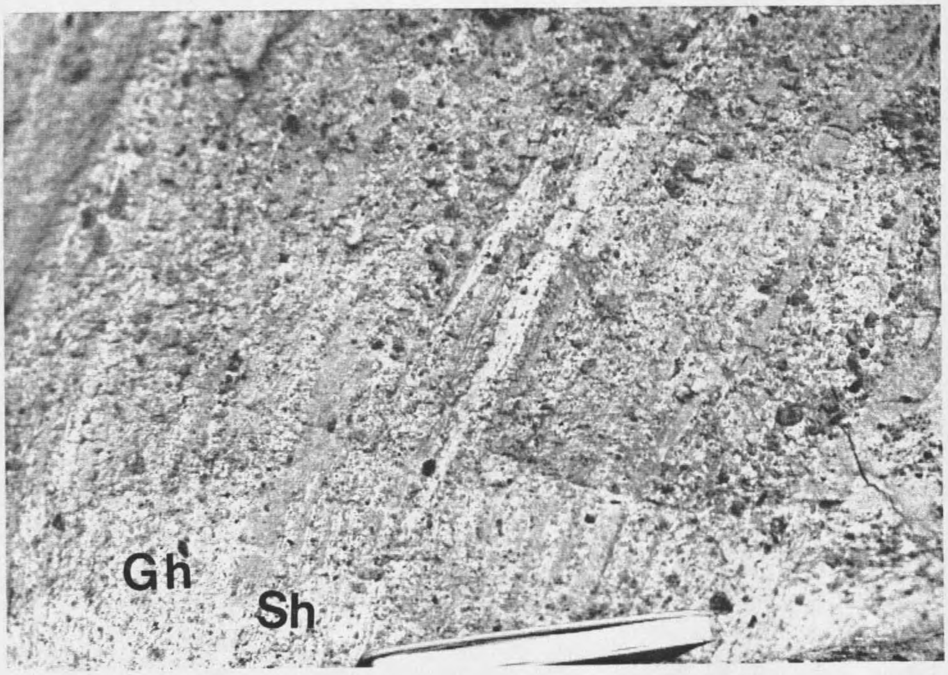

Figure 18. Tilted interbedded horizontally stratified sandstone (Sh) and conglomerate (Gh). Edge of fieldbook (15 cm) for scale.

under fluctuating flow conditions typical of turbulent sheetflow (Davis, 1938; Hogg, 1982; Elliot and Wells, 1982; Ballance, 1984; Golia and Stewart, 1984).

Trough Cross-Stratified Conglomerate (Gt)

Description : Trough cross-stratified conglomerate is rare, making up less than one percent of Member 1 of the Horse Camp Formation. It is generally composed of moderately sorted, subangular to well rounded, equidimensional, granule, pebble, and cobble sized clasts. Matrix is generally sand to muddy sand. Sets are associated with trough cross-stratified sandstone (St), horizontal and low-angle stratified sandstone (Sh/Sl), horizontally stratified conglomerate (Gh), and ripple cross-stratified sandstone (Sr). Troughs are scoured into underlying lithofacies and truncate massive, graded (Sn, Si) and ungraded sandstone (Sm) and all massive conglomerate facies (Gmu, Gmn, Gmi, Gcu, Gcn, Gci). Isolated troughs are most common and are generally between 0.5 to 1 meter deep and less than 1 to 3 meters wide. Cross-strata range from 3 to 7 centimeters thick and up to 3 meters wide. The lower bounding surface of troughs is usually overlain by a pebble and cobble lag. The overlying sets generally conform to the basal scour surface and cross-strata are well below the angle of repose.

Larger cosets (1 to 2 meters thick and 3 to 5 meters wide) composed of numerous troughs are present in the southern portion of study area near the base of Member 1 at section I. Foresets are 2 to 8 centimeters thick and up to 5 meters wide and are interstratified with trough cross-stratified sandstone. Individual troughs truncate each other.

Interpretation : Trough cross-stratified conglomerate is interpreted as the deposits of diffuse gravel sheets (Hein and Walker, 1977) or bedload pulses (Reid and Frostick,

1986) emplaced during peak flow in channels (Todd, 1989). Foresets which conform to the shape of the scour and are at angles less than the angle of repose formed by filling of shallow scours by successive migration of diffuse gravel sheets (Middleton and Trujillo, 1984; Schmitt and others, 1991). The common association of trough cross-stratified sandstone (St) with trough cross-stratified conglomerate (Gt), horizontal and low-angle stratified sandstone (Sh/Sl), and ripple cross-stratified sandstone (Sr) suggests deposition occurred during energy fluctuations in small ephemeral braided streams (McGowen and Garner, 1970; Miall, 1977). Truncation of laterally continuous massive sandstone and conglomerate by scours filled with trough cross-stratified sandstone and conglomerate indicates that the small ephemeral streams cut into a low-relief surface characterized by hyperconcentrated and debris flow deposition.

The large cosets in the southern portion of the study area are the deposits of either scour-filling by diffuse gravel sheets during periods of rapid channel switching ormigrating gravel bedforms on the base of a longer-lived perennial but small braided stream system (Galay and Neill, 1967; Rust, 1978; Fahnestock and Bradley, 1973).

Massive Ungraded Sandstone (Sm)

Description : Massive, ungraded sandstone units are typically composed of fine to coarse grained, moderately to poorly sorted sand with occasional granule, pebble and cobble outsized clasts (Figure 17). Beds are tabular ranging from 2 to 50 centimeters thick and extending laterally from 5 to 100 meters. Basal contacts are sharp and subplanar (Figure 19). These units are associated with all other types of lithofacies. They are commonly overlain by horizontally bedded sandstone (Sh) and laminated mudrock (Fl) in which mudcracks and root traces are common. Load structures and disharmonic folding are commonly found where this facies overlies laminated mudrock (Figure 11).

Interpretation : Massive ungraded sandstone (Sm) facies are interpreted as being the deposits of unconfined sheet-like sandy hyperconcentrated flow (Smith, 1986), debris flow (Ballance, 1984), or density modified grain flow (Lowe, 1982) capable of carrying outsized clasts as large as cobbles. The presence of mudcracks and root traces in overlying deposits of laminated mudrock (Fl) indicate these units were deposited under subaerial conditions. Although few fluid escape structures or signs of biotubation were evident, massive bedding could also result from either liquefaction or bioturbation (Collinson and Thompson, 1988, p. 100-101). Subaqueous deposition by density or turbidity flow is probable where this facies is associated with thick, laterally continuous laminated mudstone (Fl) sequences (Mastalerz, 1990) and soft sediment deformation are common.

Normally Graded Sandstone (Sn)

Description : Massive, normally graded sandstone units are generally composed of fine to coarse grained, moderately to poorly sorted sand (Figure 19). This facies is associated with all other types of lithofacies including thick sequences of laminated mudrock. Normally graded sandstone is often found at the base of fining upward sequences where it is overlain by horizontally stratified sandstone (Sh) and mudrock (Fl) in which mudcracks and root casts are common (Figure 11). Basal contacts are sharp. The upper contact is characterized by small scale (1 to 3 centimeters) scour and fill deposits. Bed geometry is tabular ranging from 5 to 30 centimeters thick and extending from 10 to 75 meters laterally.

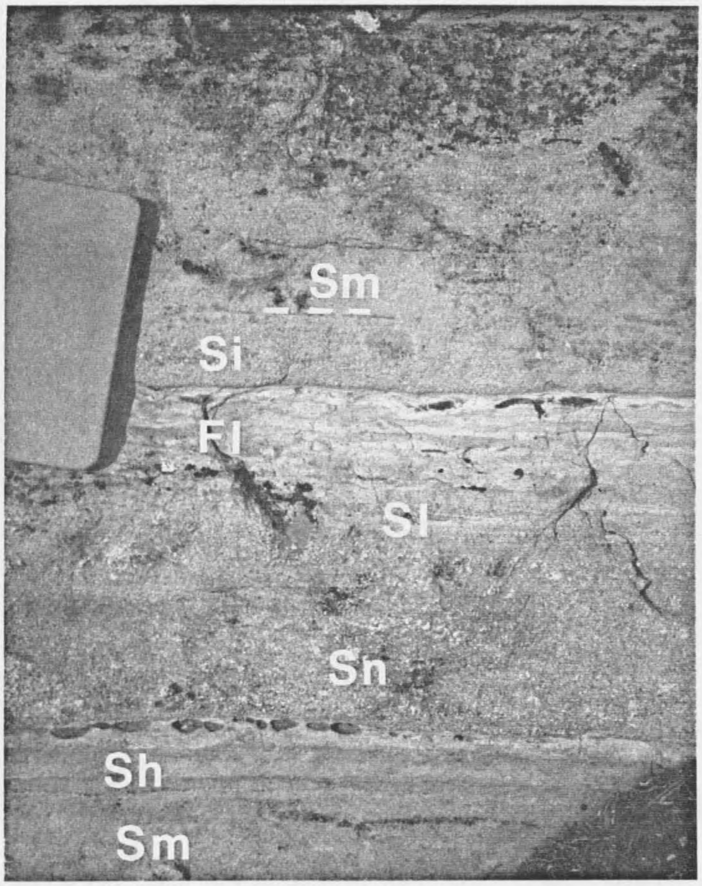

Figure 19. Interbedded sandstone and mudstone deposited on a sandflat. Sm - massive, ungraded sandstone; Sh - horizontally stratified sandstone; Sn - normally graded sandstone; Si - inversely graded sandstone; Fl - laminated mudstone. Edge of fieldbook (15 cm) for scale.

Interpretation : Normally graded massive sandstone units (Sn) are deposits of subaerial and subaqueous decelerating sediment gravity flows over unconfined surfaces (Hubert and Hyde, 1982). Where associated with the thick units of laminated mudstone (Fl) normally graded sandstone are the deposits of density or turbidity currents (Allen, 1984; Mastalerz, 1990). The common occurrence of this facies in fining upward sequences overlain by horizontally laminated sandstone (Sh) and mudrock (Fl) with associated mudcracks and root traces suggests deposition in a subaerial environment by either hyperconcentrated (Ballance, 1984) or sandy debris flow (Lowe, 1982) on an unconfined depositional surface.

Inversely Graded Sandstone (Si)

Description : Massive, inversely graded sandstone units are composed of moderately to poorly sorted, fine to coarse grained sand with occasional granule, pebble, and/or cobble outsized clasts (Figure 19). Beds are tabular ranging from 3 to 35 centimeters thick and extending from 5 to 60 meters laterally. Basal contacts are sharp and subplanar. The tops of depositional units are characterized by small scale (1 - 3 centimeters) scour and fill deposits of sand and granules. This facies is associated with all other lithofacies types except the thick laminated mudstone sequences. Inversely graded sandstone is commonly located at the base of fining upward sequences composed of horizontally stratified sandstone (Sh) and mudrock (Fl) in which mudcracks and root casts are common.

Interpretation : Massive inversely graded sandstone (Si) units are deposits of unconfined sandy debris flows (Ballance, 1984) or noncohesive grain flows where grains are activated by dispersive pressure and grading developed by kinetic sieving (Lowe, 1982;

Collinson and Thompson, 1988, p. 101). These flows appear to have been nonerosive. The presence of inversely graded sandstone (Si) at the base of fining upward sequences where they are commonly overlain by horizontally laminated sandstone (Sh) and mudrock (Fl) with associated mudcracks and root traces indicates that following deposition of a massive, inversely graded sandstone bed, its upper surface was reworked by turbulent sheetflow (Miall, 1977). Subsequent ponding of water on the depositional surface allowed for deposition of horizontally laminated mudrock (Fl) and eventual subaerial exposure led to development of dessication cracks.

Horizontal and Low-Angle Stratified Sandstone (Sh/Sl)

Description : Horizontally stratified and low-angle stratified sandstone units are composed of either moderately to well sorted, fine- to medium-grained sand or moderately sorted, medium- to very coarse-grained sand and granule-pebble sized gravel. These two lithofacies are grouped because they generally grade into each other and form under similar conditions as discussed below (Figure 20). Horizontal and low-angle stratified moderately sorted, medium- to very coarse-grained sandstone units are deposited as tabular units 10 to 300 centimeters thick and 10 to 250 metersin lateral extent. This facies commonly fills broad, shallow scours (less than 1 meter deep and 5 meters wide) (Figure 18). Thin sheetlike units (less than 5 centimeters thick, 1-25 meters in lateral extent) of horizontally laminated moderately sorted, fine- to medium-grained sandstone (Sh) overlain by lenses of laminated mudstone (Fl) are commonly found above horizontally stratified conglomerate (Gh) (Figure 18), massive sandstone (Sn, Si, Sm) and conglomeratic units (Gmu, Gmn, Gmi, Gcu, Gcn, Gci) (Figure 11, 13).

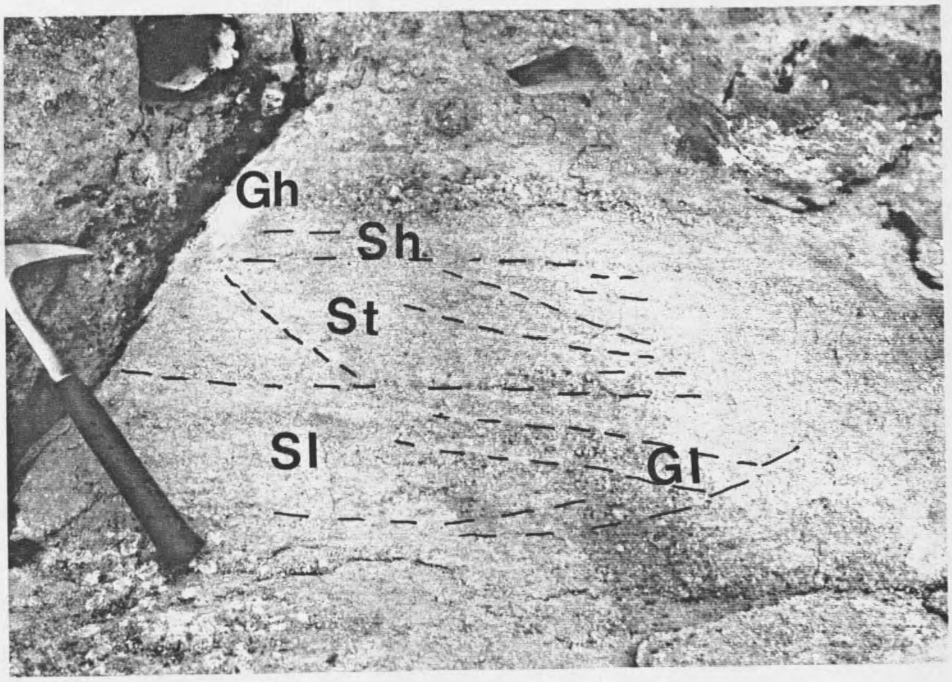

Figure 20. Shallow scour (35 cm deep) filled with low-angle stratified sandstone (Sl) and granule to pebble conglomerate (Gh), trough cross-stratified sandstone (St), and horizontally stratified sandstone (Sh) and granule, pebble conglomerate (Gh). Hammer for scale.

Interpretation : Fine- to medium-grained horizontally laminated sandstone and associated laminated mudstone were deposited under upper flow-regime plane bed conditions (Hogg, 1982; Guy and others, 1990). The sheet-like geometry of the depositional units suggests that the flow was unconfined and turbulent over broad, low-relief depositional surfaces. Scour and fill deposition of sediment on top of massively bedded units indicates reworking of sediment deposited by earlier hyperconcentrated and debris flow events. Medium- to very coarse-grained horizontally laminated pebbly sandstone is deposited under lower flow-regime plane bed conditions during waning of sheetflow events (Bull, 1972; Nilsen, 1982; Mack and Rasmussen, 1984). The common association of these two types of horizontally and low-angle stratified sandstones suggests that they develop under pulsating flow conditions typical of turbulent sheetflow on an alluvial fan depositional surface (Davis, 1938; Elliot and Wells, 1982; Ballance, 1984; Golia and Stewart, 1984).

Ripple Cross-Stratified Sandstone (Sr)

Description : Ripple-cross stratified sandstone is composed of moderate to well sorted very fine to medium grained sand and is associated with all other lithofacies. Symmetrical, flat-topped ripples on bedding surfaces of medium to very fine sand are common in thick sequences of laminated mudstone (Fl). Asymmetrical ripples and climbing ripples are found interbedded with thin discontinuous sequences of laminated mudstone (Fl), horizontally laminated sandstone (Sh), and trough-cross stratified sandstone (St), and bounding all types of massive sandstone and conglomerate depositional units. Unit thickness ranges from 0.5 to 3 centimeters and lateral extent from 0.25 to 2 meters.

Interpretation : Symmetrical, flat-topped ripples associated with thick sequences of laminated mudstone (Fl) are the result of surface wave activity in lacustrine settings or leveling off by wind erosion (Collinson, and Thompson, 1982, p. 67; Fouch and Dean, 1982; Pettijohn and others, 1987, p. 110). Assymetrical ripples that occur in conjunction with thin discontinuous sequences of laminated mudstone (Fl), horizontally laminated sandstone (Sh), trough-cross stratified sandstone (St), and bounding all types of massive sandstone and conglomeratic units developed during lower flow regime waning flood flow on the depositional surface (Pettijohn and others, 1987, p. 110-111; Collinson and Thompson, 1988, p. 63; Waresback and Turbeville, 1990).

Trough Cross-Stratified Sandstone (St)

Description : Trough cross-stratified sandstone is rare, making up less than one percent of Member 1 of the Horse Camp Formation. It is made up of coarse- and medium-grained, moderately- to poorly-sorted sandstone; granules and pebbles are locally abundant. Troughs truncate massive sandstone (Sm, Sn, Si) and conglomerate (Gmu, Gmn, Gmi, Gcu, Gcn, Gci) units. Sets are associated with trough cross-stratified conglomerate (Gt), horizontal and low-angle stratified sandstone (Sh/Sl), horizontally stratified conglomerate (Gh), and ripple cross-stratified sandstone (Sr) (Figure 20). Solitary troughs scoured into underlying units are most common and are generally between 0.1 to 0.75 meters thick and from 1 to 3 meters wide. These scours truncate massive, graded (Sn, Si) and ungraded sandstone (Sm) and all massive conglomerate facies (Gmu, Gmn, Gmi, Gcu, Gcn, Gci). The lower bounding surface of troughs is usually overlain by a coarse sand, granule, and/or pebble lag with overlying sandstone sets conforming to the basal scour surface. Isolated troughs are filled with individual sets that range from 1 to

3 centimeters in thickness and up to 1 meter in width. Foresets dip at angles typically less than the angle of repose.

In the southern portion of the study area there is a large coset of cross-cutting troughs approximately 3 meters thick and up to 5 meters wide (the "torrential trough cross-beds" of Moores (1968). Individual troughs range from 0.25 to 1.5 meters thick and from 1 to 3 meters wide. These troughs are filled with individual sets that range from 1 to 3 centimeters thick and 0.25 to 2 meters wide.

Interpretation : Trough cross-stratified sandstone was deposited under plane bed flow conditions which developed on a scoured surface (DeCelles and others, 1983). The low-angle of repose of the foresets indicates that the foresets did not develop by avalanching down the lee face of a migrating dune (DeCelles and others, 1983). The common association of trough cross-stratified sandstone (St) with trough cross-stratified conglomerate (Gt), horizontal and low-angle stratified sandstone (Sh/Sl), and ripple crossstratified sandstone (Sr) suggests deposition occurred during energy fluctuations in a small ephemeral braided stream (Rust, 1978).

Laminated Mudrock (Fl)

Description: This facies is composed of thinly bedded to thinly laminated, pastel pink, green, yellow and white claystone, siltstone, and mudstone. Two subfacies of laminated mudrock are recognized based on distinctive geometry, composition, and sedimentological characteristics.

The first type consists of thinly laminated siliciclastic siltstone, mudstone and claystone sequences that range in thickness from 0.25 to 5 centimeters and extend laterally from 1 to 15 meters (Figures 5, 11, and 19). It is typically noncalcareous and very rarely silicified. Mudcracks and root traces are common. This subfacies is commonly present at the top of fining upward sequences which include (from bottom to top) massive, graded and ungraded sandstone (Sm, Sn, Si) and clast- and matrix-supported conglomerate (Gcu, Gcn, Gci, Gmu, Gmn, Gmi) overlain by horizontally stratified sandstone (Sh) and granule conglomerate (Gh).

The second laminated mudrock subfacies is laminated to thinly bedded, siliciclastic mudstone and claystone. It is typically calcareous and well-silicified. Wavy bedding, burrows and grazing traces are common (Figure 21). These fine-grained sequences can be as much as 9 meters thick and range in lateral extent from 5 to 45 meters for thicker sequences.

Interpretation : These two distinct sequence geometries suggest different depositional mechanisms for each. The common presence of the thinner, less laterally continuous facies at the top of fining upward sequences suggests that deposition took place during waning flood flow conditions on a subaerial depositional surface. Laminated mudrock (Fl) was deposited where silt and clay settled out of very shallow ponded water (Fouch and Dean, 1982; Nilsen, 1982; Ballance, 1984; Blair, 1987).

The thicker and more laterally continuous mudrock facies is commonly bioturbated, siliceous, and calcareous suggesting deposition in standing water (Surdam and Wolfbaurer, 1975). This facies displays soft-sediment deformation features where it is interstratified with clast-supported, ungraded (Gcu) and normally graded (Gcn) conglomerates and massive, ungraded (Sm) and normally graded (Sn) sandstone. Theses relations are indicative of subaqueous deposition (Fouch and Dean, 1982; Dean and Fouch, 1983).

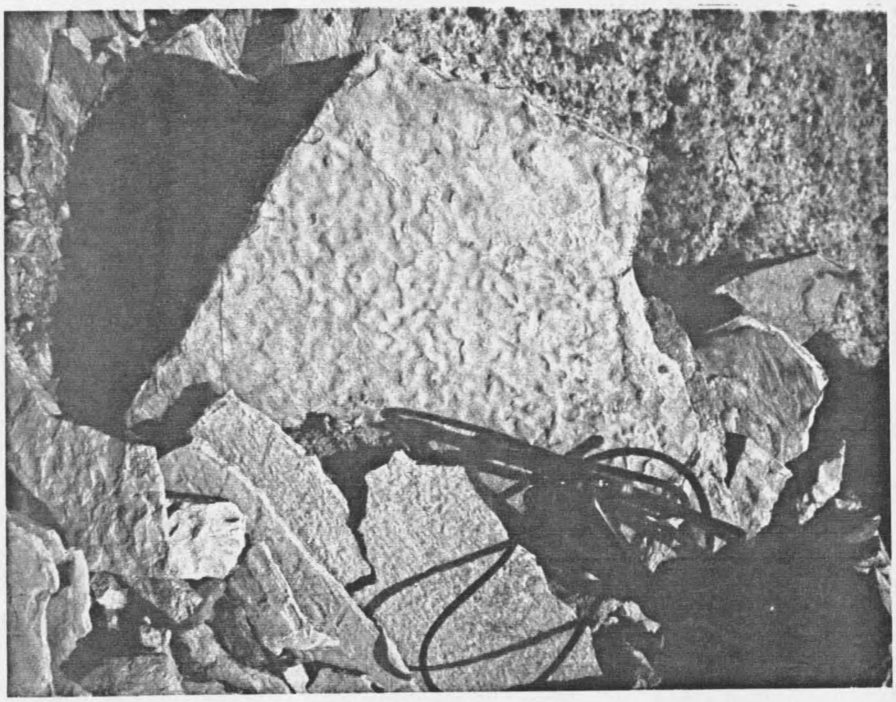

Figure 21. Bioturbated silicified laminated mudstone (Fl). Sunglasses for scale.

Lithofacies Assemblages and Depositional Environments

Consideration of lithofacies types, lithofacies assemblages, and bed geometries leads to recognition of three different major environments of deposition for the sedimentary rocks of Member 1 of the Horse Camp Formation. These include alluvial fan which is divided into proximal, medial and distal subenvironments, sandflat, and lacustrine. In general, conglomerate and sandstone were deposited on alluvial fans and sandflats by episodic sediment transport events. Thick (up to 100 meters) lenses dominated by mudrock represent shallow lacustrine deposits. The geographic positions of the environments that characterize Member 1, as evidenced by both lateral and vertical facies variations changed temporally with tectonically-driven changes in location of dominant highlands (Figure 22).

Proximal Alluvial Fan Deposits

Facies Assemblages. Proximal alluvial fan facies assemblages are composed of laterally continuous (Figure 23), massively bedded, clast- or matrix-supported, cobble and boulder conglomerates (Gcu, Gcn, Gci, Gmu, Gmn, and Gmi) (Figure 24). These units are up to 1.5 meters thick, extend laterally up to 120 meters, and have planar to broadly concave-upward basal contacts.

Interbedding of massive bedded coarse facies units is common. More frequently, however, individual conglomeratic units are abruptly overlain by 1 to 30 centimeter thick fining upward sequences of stratified conglomerate, sandstone, and/or mudrock (Figure 13). Facies within the fining upward sequences include horizontal and low-angle cross-

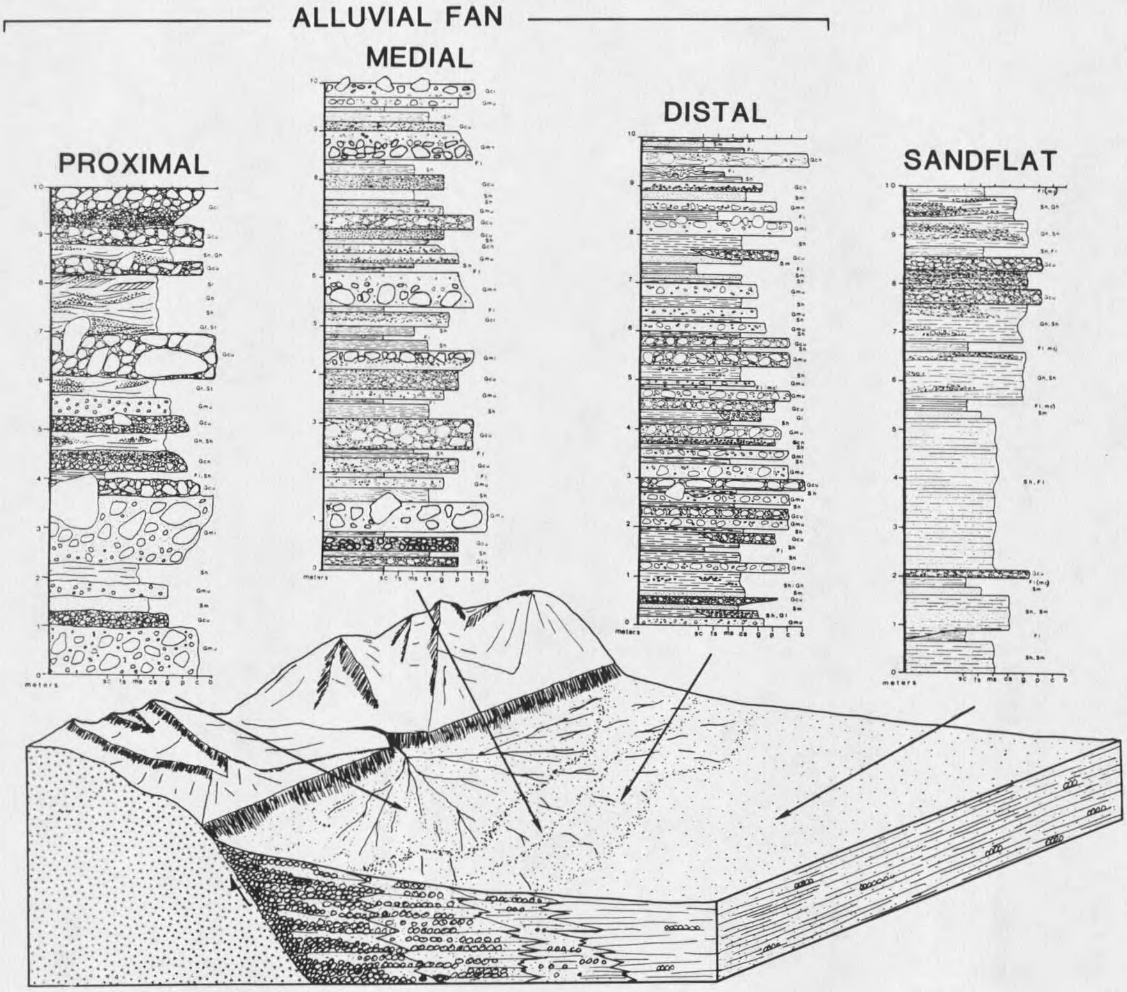

Figure 22. Schematic block diagram showing the characteristic distribution of proximal, medial, and distal alluvial fan subenvironments and sandflat environments and lithofacies assemblages off of the footwall block. Lacustrine environment would be more distal from the sandflat.

Figure 23. Proximal alluvial fan depositional sequence. Note lateral continuity of the beds. Fieldbook for scale.

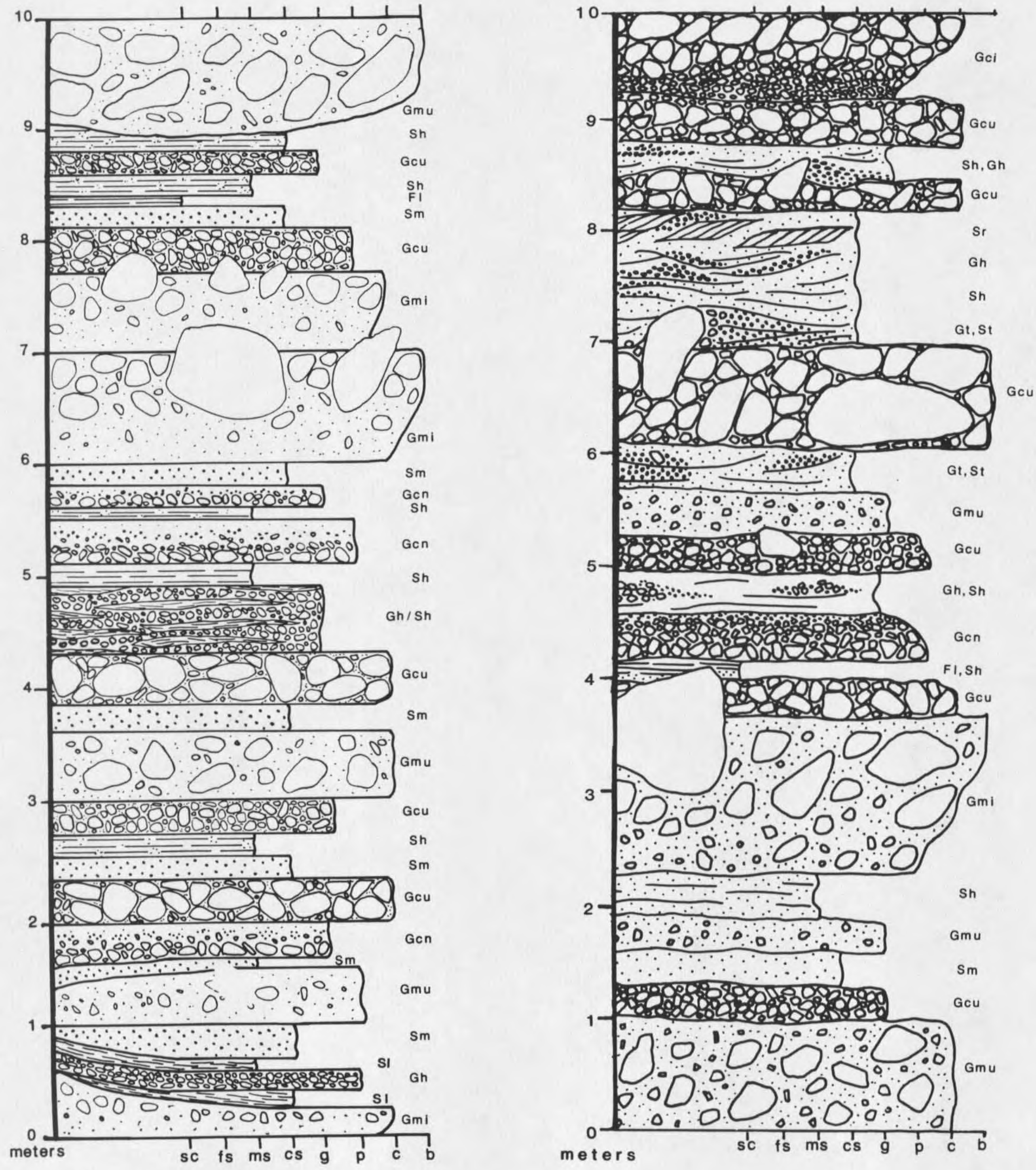

Figure 24. Detailed lithofacies profiles showing representative proximal alluvial fan lithofacies assemblages. Profile on left is from measured section H; profile on right from measured section C.

stratified conglomerate (Gh, Gt), horizontal and low-angle stratified and ripple cross-stratified sandstone (Sh, Sl, Sr), and laminated mudrock (Fl).

Proximal facies are interbedded with megabreccia deposits at Sections C and F and two lenticular (4 to 9 meters thick and up to 45 meters wide) bodies of bioturbated, silicified and marly laminated mudrock (Fl) (Figure 6 and Plates 1 and 2). Within these fine-grained sequences are 10 to 50 centimeter thick beds of clast-supported, massive, ungraded and normally graded conglomerate and sandstone. At Section F there is an unusually large solitary boulder (20 meters in diameter) engulfed by laminated mudrock which shows intense soft sediment deformation at the base of the boulder (Plate 1, Section F).

Interpretation. The coarse clastic (cobbles to large boulders) and texturally immature deposits of Member 1 are considered to have been deposited on the proximal portion of an alluvial fan (Elliot and Wells, 1982; Mack and Rasmussen, 1984) (Figure 22). The tabular to sheetlike geometry of massively bedded conglomeratic units suggests deposition took place by debris and hyperconcentrated flow over an unconfined to slightly scoured surface (McGee, 1897; Davis, 1938; Blair, 1987). The common presence of boulder sized material within the deposits is indicative of deposition near the channel intersection point on the alluvial fan (Whipple and Dunne, 1992). The coarse grained nature of the facies combined with the lack of channel fill deposits suggests that the intersection point was relatively high on the fan surface and implies that sedimentation rates were relatively high.

Sheetflood depostion of the massively bedded conglomerates was followed by reworking of sediment on the surface by sheetflow (Ballance, 1984). Conversely, as Harrison and Fritz (1982) suggest, massive conglomerate overlain by stratified material may also represent the deccelerating phase of an episodic sedimentation event rather that post-flood reworking of the fan surface. Sedimentology studies of Holocene alluvial fans of Mt. Everts in Yellowstone National Park suggest that either of these two models are feasible (Schmitt and others, in press).

Lenses of mudrock and very fine-grained sandstone represent the deposits of small ponds that developed in close proximity to landslide deposits on the proximal portions of alluvial fans (Krieger, 1977). These ponds were inhabited by burrowing organisms. Silicified layers are interstratified with layers of marly, analcime-rich mudstone suggesting that the ponds were probably somewhat alkaline (Surdam and Wolfbauer, 1975). The water chemistry was controlled by the dissolution of abundant volcanic glass eroded from adjacent highlands composed of older volcanic rocks (Surdam and Eugster, 1976).

Medial Alluvial Fan Deposits

Facies Assemblages. Medial alluvial fan facies assemblages resemble proximal assemblages but are typically finer grained, more thinly bedded, and the beds are more laterally continuous (Figure 23) (Gloppen and Steel, 1981). These assemblages are composed predominantly of massively bedded, clast-supported pebble to small boulder conglomerate with subordinate amounts of massively bedded, matrix-supported pebble to small boulder conglomerate (Figure 25). Individual conglomerate units are laterally extensive up to 150 meters and are generally less than 0.5 meters thick. Conglomeratic units are occasionally interbedded with each other but more commonly individual depositional units are overlain by fining upward sequences of horizontally stratified granule to pebble conglomerate and coarse-grained sandstone, massive and ripple cross-stratified sandstone, and finely laminated mudrock with plant root traces and mudcracks. Small scour and fill features composed of low-angle cross-stratified sandstone and granule

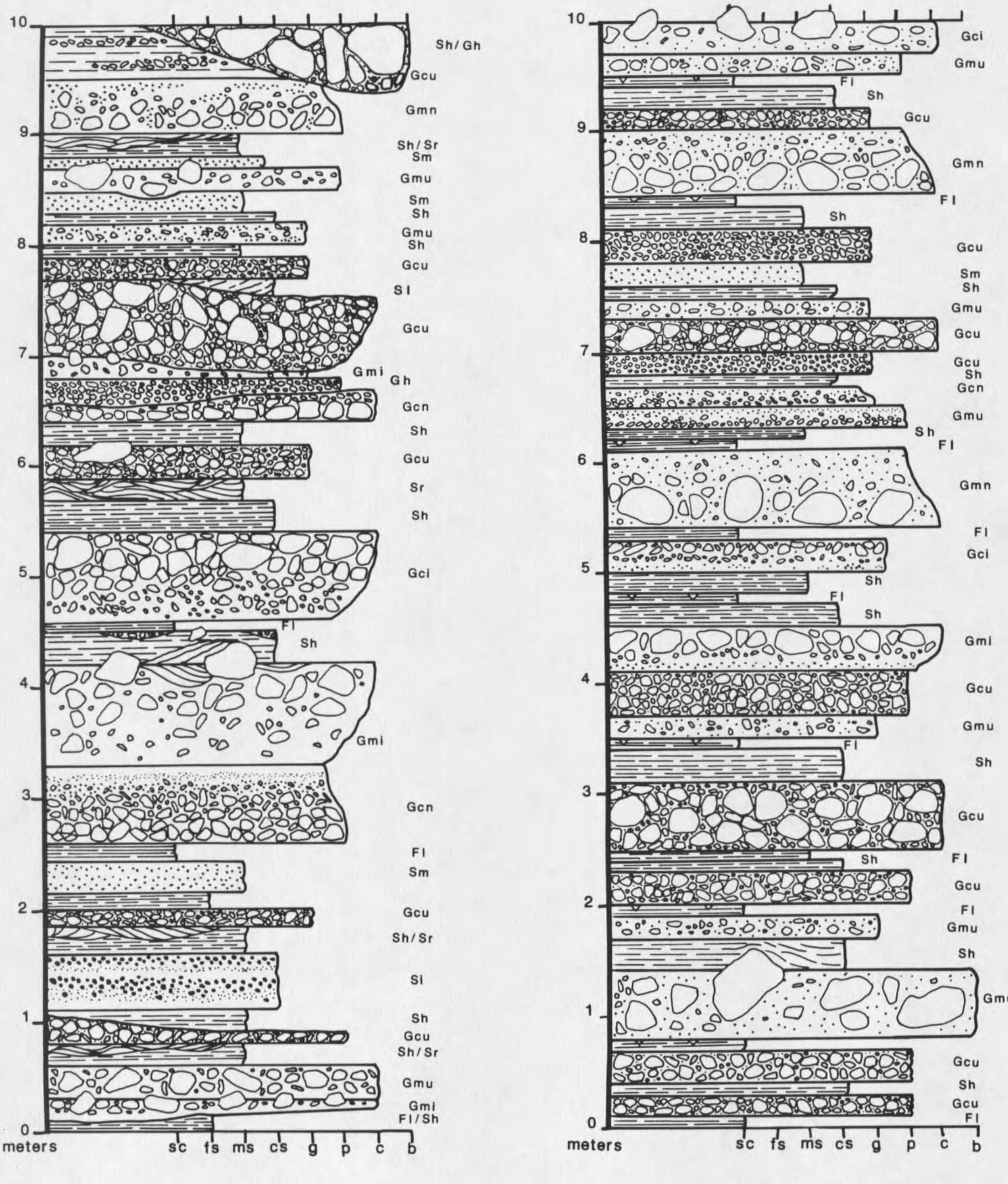

Figure 25. Detailed lithofacies profiles showing representative medial alluvial fan lithofacies assemblages. Profile on left is from measured section B; profile on right from measured section G.

conglomerate are common. Local lenses (4 to 6 meters thick and 20 meters wide) of laminated mudrock are present but rare.

Interpretation. Finer-grained assemblages and thinner more laterally continuous beds suggest that these units were deposited on the medial portion of an alluvial fan (Gloppen and Steel, 1981; Golia and Stewart, 1984; DeCelles and others, 1991). The tabular nature and massive bedding characteristic of the conglomerate units are indicative of deposition during sheetflooding events by unconfined debris and hyperconcentrated flow (Ballance, 1984; Mack and Rasmussen, 1984). During stages of waning flood flow or in subsequent events, coarse-grained sand, granules, and pebbles of the mass flow deposit were reworked by traction transport causing development of fining upward sequences which abruptly overlie the conglomerate unit (Harrison and Fritz, 1982; DeCelles, 1991). Scour and fill deposition on the downslope side of large clasts protruding from the underlying massive beds led to development of shadow structures. The repetition of laterally continuous mass flow deposits overlain by fining upward conglomerate and sandstone is indicative of episodic sedimentation on an alluvial fan surface rarely traversed by braided stream channels. Because the beds are laterally continuous and there is an overall decrease in the amount of scour, the medial portion of an alluvial fans typically has lesser topographic relief than the proximal portion (Blair, 1987; Whipple and Dunne, 1992). The lack of topographic relief inhibits ponding of water which results in the deposition of fewer associated mudrock lenses.

Distal Alluvial Fan Deposits

Facies Assemblages. Distal alluvial fan assemblages are finer grained than medial assemblages. Maximum clast size rarely exceeds cobble and typically ranges from pebble to coarse-grained sand. Individual depositional units are typically less that 0.3 meters thick and extend laterally up to 200 meters. There is very little pronounced scour and fill (Figure 26). Massively bedded conglomerate and conglomeratic sandstone occasionally fill very broad, shallow troughs (less than 0.25 meters deep and 10 meters wide). Shadow structures composed of horizontal to low-angle stratified sandstone and granule conglomerate are present on the downflow side of larger clasts. Mudcracks and soft sediment deformation features are very common.

These assemblages are composed predominantly of interbedded, sheetlike, granule to cobble, massively bedded, matrix- and clast-supported conglomerate units (Gcu, Gcn, Gmu, Gmn, Gmi). Individual depositional units are commonly overlain by fining upward sequences composed of horizontal and low-angle stratified sandstone (Sh, Sl) and granule conglomerate (Gh, Gl), rippled and massive sandstone (Sr, Sm), and finely laminated mudrock (Fl) in which mudcracks and soft sediment deformation features are common.

Interpretation. The interbedded nature of thin, massively bedded pebble-granule conglomerate with horizontally stratified sandstone and granule conglomerate suggests that deposition occurred by sheetflooding over the distal reaches of the alluvial fan (Blair, 1987) (Figure 26). During initial stages of flooding, debris and hyperconcentrated flows deposited thin, laterally continuous sheets of matrix- and clast-supported conglomerate (Elliot and Wells, 1982). This was followed by sheetflow capable of traction transport of material from the medial to the distal portions of the fan while reworking the surface of the mass flow deposits (Ballance, 1984). The final stages of sedimentation included the deposition of finely laminated mud which often ultimately developed dessication cracks. Sheetflood and sheetflow deposition of sediment over the distal portions of the fan was episodic (Hogg, 1982; DeCelles and others, 1991). Unlike the medial and proximal assemblages, soft sediment deformation is common in laminated mudrock beneath

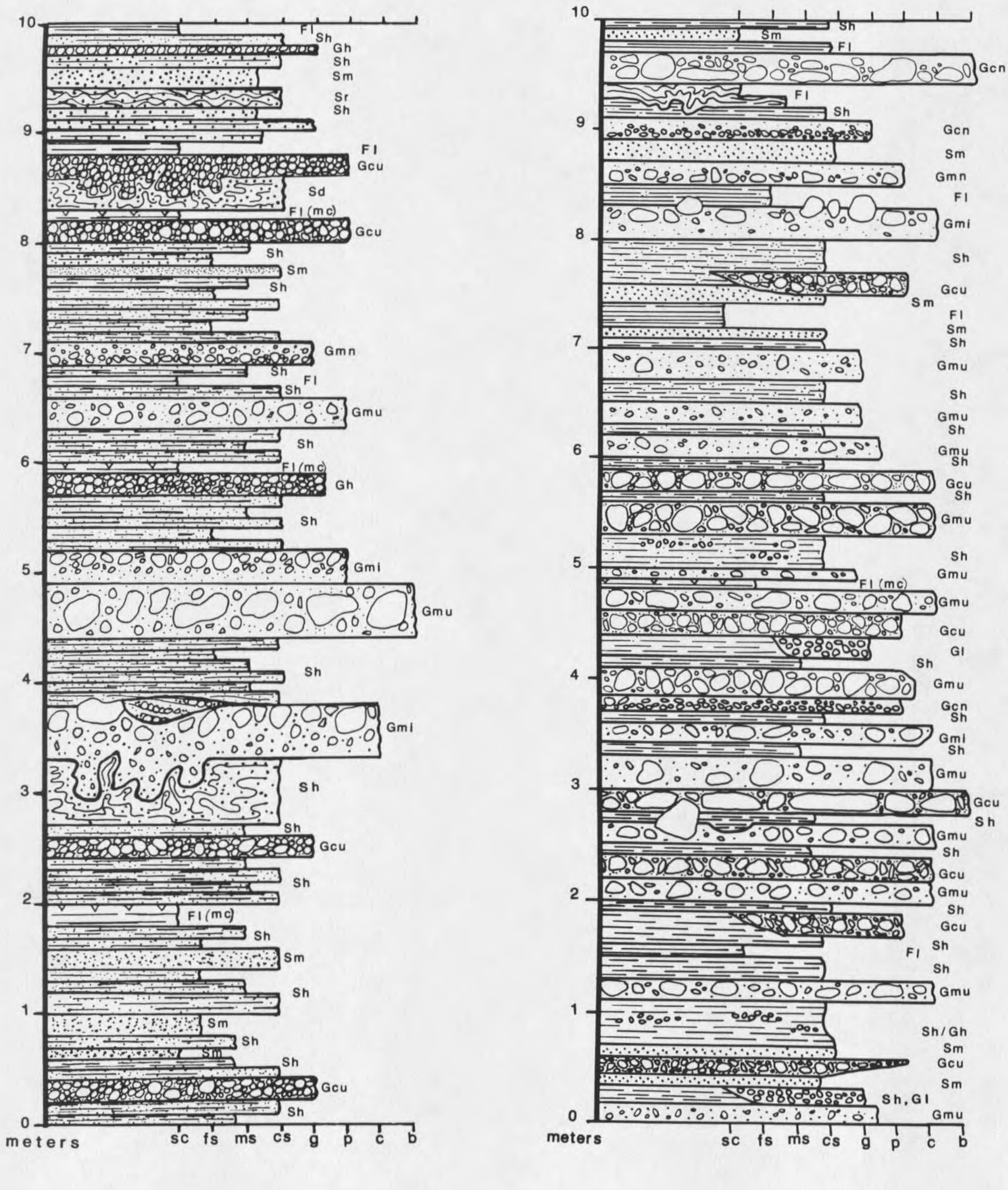

Figure 26. Detailed lithofacies profiles showing representative distal alluvial fan lithofacies assemblages. Profile on left is from measured section A; profile on right from measured section I.

conglomeratic units. This suggests that the surface of deposition was often wet enough for the mud to behave plastically. Frequent development of mudcracks and soft sediment deformation is a characteristic of areas where deposits of distal alluvial fan, sandflat, and lacustrine environments interfinger (Fouch and Dean, 1982).

Sandflat Deposits

Facies Assemblages. The sandflat environment is represented by medium- to very coarse-grained horizontally and low-angle stratified and massive sandstone (Sh, Sl, Sm) interstratified with lesser amounts of granule to pebble horizontally stratified conglomerate (Gh) and laminated mudrock (Fl) with mudcracks (Figure 27). Minor facies include thin, massively bedded and low-angle to trough cross-stratified granule to pebble conglomerate (Gcu, Gmu, Gt) and rippled sandstone (Sr). Individual beds are 0.1 to 1 meter in lateral extent and less than 3 centimeters thick. However, units composed of horizontally and low-angle stratified and massive sandstone and granule-pebble conglomerate (Sh, Sl, Sm, Gh) can be up to 3 meters thick and at least 200 meters wide. Scour and fill structures are common in these facies. Scours are typically relatively small (less than 0.25 meters deep and 2 meters wide) but those filled with low-angle to trough cross-stratified granule and pebble conglomerate (Gt) are up to 1 meter deep and 5 meters wide.

Interpretation. The finer-grained conglomeratic texture, interstratification of abundant horizontally bedded sandstone with granule-pebble conglomerate (Ballance, 1984), and lateral continuity of facies (Hubert and Hyde, 1982) suggests that this assemblage represents a sandflat environment (Figure 22). Horizontally stratified units were deposited when the adjacent fan was flooded causing sheetflow over the sandflat (Davis, 1938; Blair, 1987). Sheetflow capable of scour and fill led to the development of

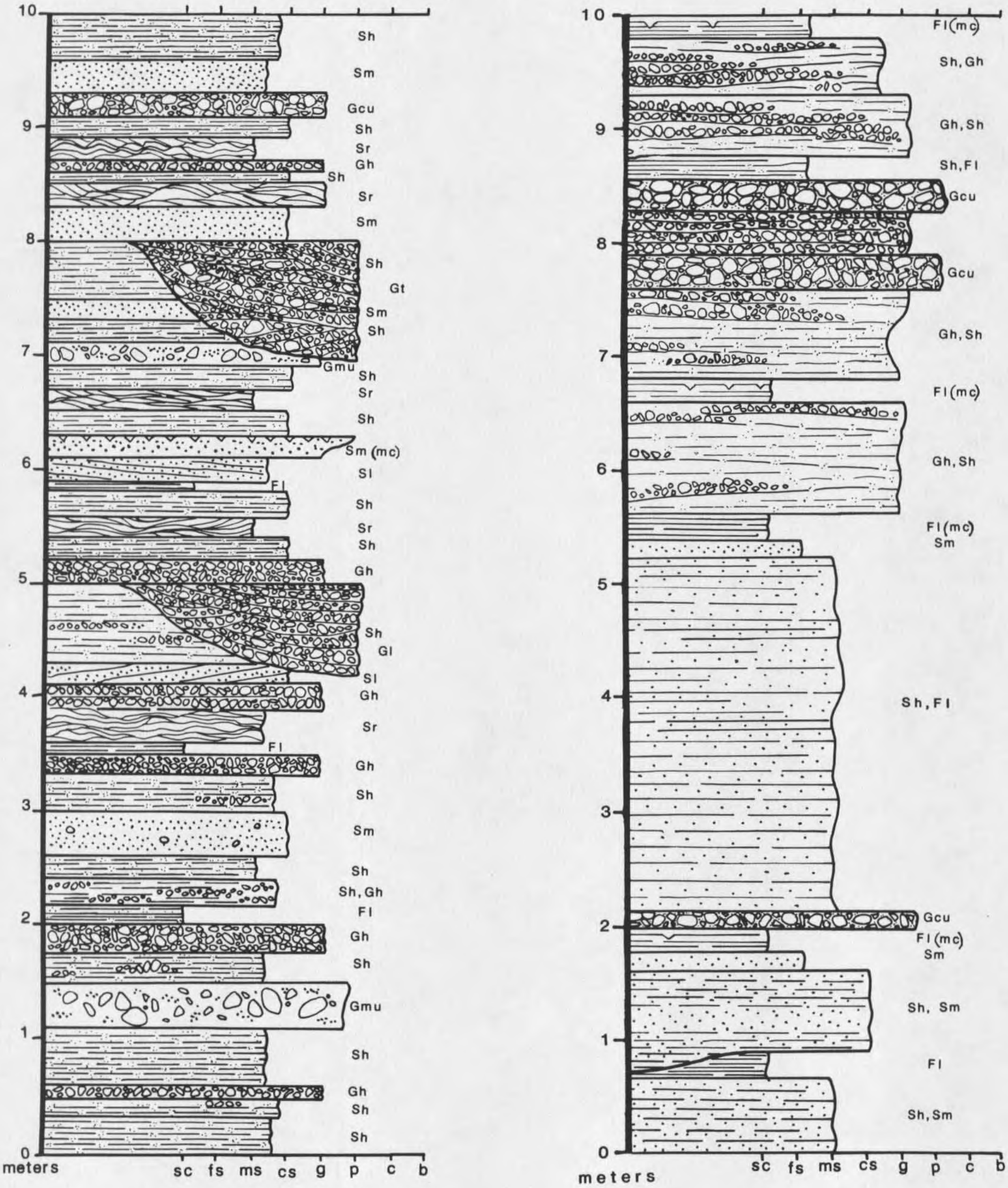

Figure 27. Detailed lithofacies profiles showing representative sandflat lithofacies assemblages. Profile on left is from measured section D; profile on right from measured section G.

small channels filled with granule and pebble conglomerate (Hogg, 1982). Sheetflow facies commonly interfinger with thick (up to 20 meters), laterally persistent beds (several hundred meters wide) of laminated mudstone and massive sandstone suggesting that there was some lateral shifting of the sandflat and adjacent lacustrine environments through time.

Lacustrine Deposits

Due to the poor exposure of mudrock facies detailed analyses of complete lithofacies assemblages were not performed. However, observations from small scattered outcrops allow for limited interpretation of a lacustrine environment.

Facies Assemblages. Lacustrine lithofacies assemblages are composed predominantly of white, yellow, pale green, red, and dark brown and gray calcareous fissile mudstone, siltstone, and very fine-grained sandstone. Horizontal laminae and ripple cross-laminae are common. Stratification is often manifested by light and dark layering within the beds. Grazing tracks and burrows are common on bedding surfaces while mudcracks are rare. A few beds of massive, normally graded and ungraded clast-supported granule and pebble conglomerate and sandstone are interstratified with mudrock layers. The largest lens of this assemblage is 100 meters thick and 1 kilometer in lateral extent and is centered between Sections A and D. This lenticular unit overlies and interfingers with a sequence of sandflat deposits.

Interpretation. The great thickness (up to 100 meters) and lateral continuity (up to 1 kilometer) of these mudrock deposits indicate that they were deposited in a small alkaline lacustrine system at least 1 kilometer in diameter with water depths of perhaps only a few meters. Bioturbation and sedimentary structures are indicative of a shallow, oxygenated lake (Galloway and Hobday, 1983, p. 195-196). Sedimentation in this type of system is controlled by sheetflooding of adjacent alluvial fans and sandflats which causes influxes of fine sand, silt, and clay. Extreme sheetflooding can potentially produce small subaqueous density flows composed of coarser material. Sand ripples are symmetrical and flat-topped indicating that they developed as wave ripples. Mudcracks formed at the margins of the lakes as the level of the water dropped.

Summary of Depositional Environments

Member 1 of the Horse Camp Formation was deposited in a temperate, semiarid (Axelrod, 1957, 1962) terrestrial alluvial fan - sandflat - lacustrine setting (Figure 22). The earliest stages of sedimentation were characterized by the development of an alluvial fan system. The lower 20 to 60 meters of Member 1 are composed of sediment deposited in distal alluvial fan and sandflat environments (Plate 1). Above these distal deposits, medial and proximal assemblages make up 50 to 300 meters of section. The upper 150 to 200 meters of Member 1 were deposited in a variety of depositional environments. In the southern part of the study area (Plate 1, Sections G, H, and I), these strata are composed of proximal, medial, and distal alluvial fan facies. These assemblages interfinger to the north with sandflat and lacustrine facies which are typical of the central portion of the study area (Plate 1, Section D). Finally, the uppermost part of Member 1 in the northern part of the study area is composed of medial to distal alluvial fan, sandflat, and lacustrine assemblages overlain by megabreccias which were emplaced as landslides.

MEGABRECCIAS

Introduction

Sedimentary breccia and megabreccia deposits are commonly associated with basin margin sequences in the Basin and Range province (Woodford and Harriss, 1928; Noble, 1941; Jahns and Engel, 1950; Longwell, 1951; Burchfiel, 1966; Moores, 1968; Langenheim and others, 1971; Krieger, 1977; Miller and John, 1988; Yarnold and Lombard, 1989). Throughout the region these deposits may be composed of up to 2×10^{10} m^3 of brecciated rock and rock debris interbedded with conglomerate, sandstone, mudstone, and limestone (Figure 28) (Harrison and Falcon, 1937; Pierson and Costa, 1987). Interstratification with basin-fill sequences and their lenticular nature suggest that megabreccias may have been emplaced as landslides (Burchfiel, 1966; Krieger, 1977). If this is the case, recognition of these deposits could prove exceptionally useful in determining tectono-sedimentary histories of extensional basins of western North America by providing information on relief, proximity, location and bedrock composition of adjacent highlands.

Azimuth of transport direction and paleoslope can be determined by analysis of striations, directional folds, and structural imbrication of clasts near the base of the deposit (Yarnold and Lombard, 1989). Megabreccias are often composed of stratigraphically intact sections of rock that reflect the bedrock lithology of the source area with greater detail than is present in finer-grained deposits.

Because exposure of the three megabreccias in Member 1 is not complete, determination of total volume and paleorelief is not possible (Figure 29) (Melosh, 1987). However, transport direction and source area composition are determinable. Member 1 megabreccias reflect the composition of their Oligocene volcanic source area. Measurement

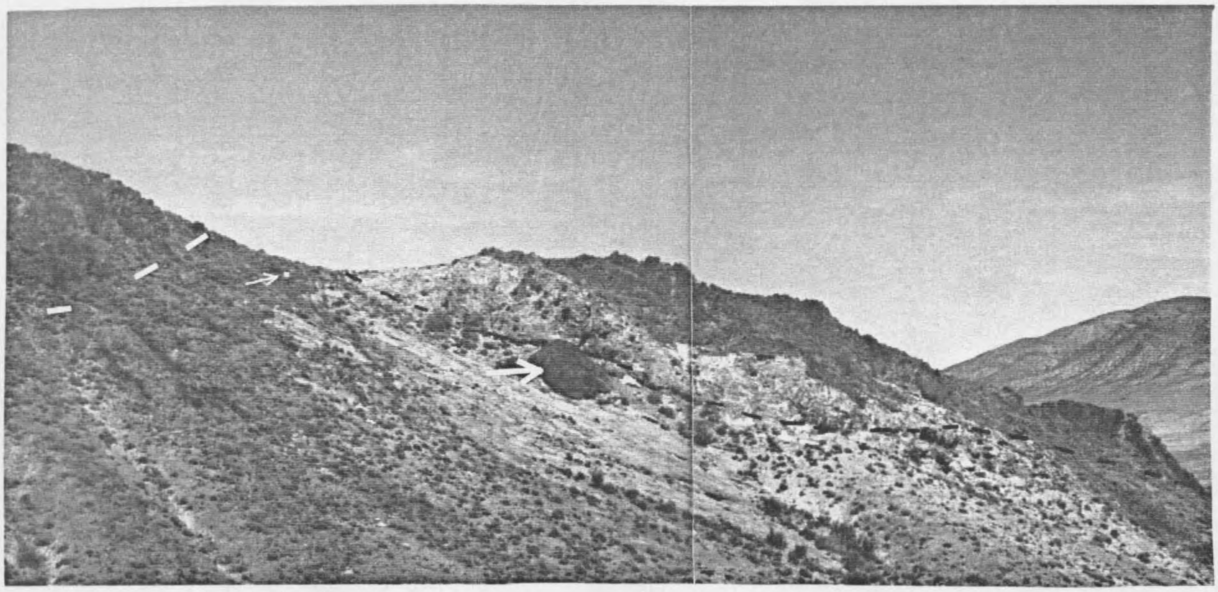

Figure 28. Panorama looking east of the two stratigraphically lower slide blocks composed of Railroad Valley Rhyolite and Windous Butte Formation. White dashed line at base of lowest block. Small white arrow pointing to Jim Schmitt (2 meters tall). Black dashed line at base of middle block. Large white arrow pointing to large boulder of brecciated Windous Butte Formation engulfed in lacustrine strata.

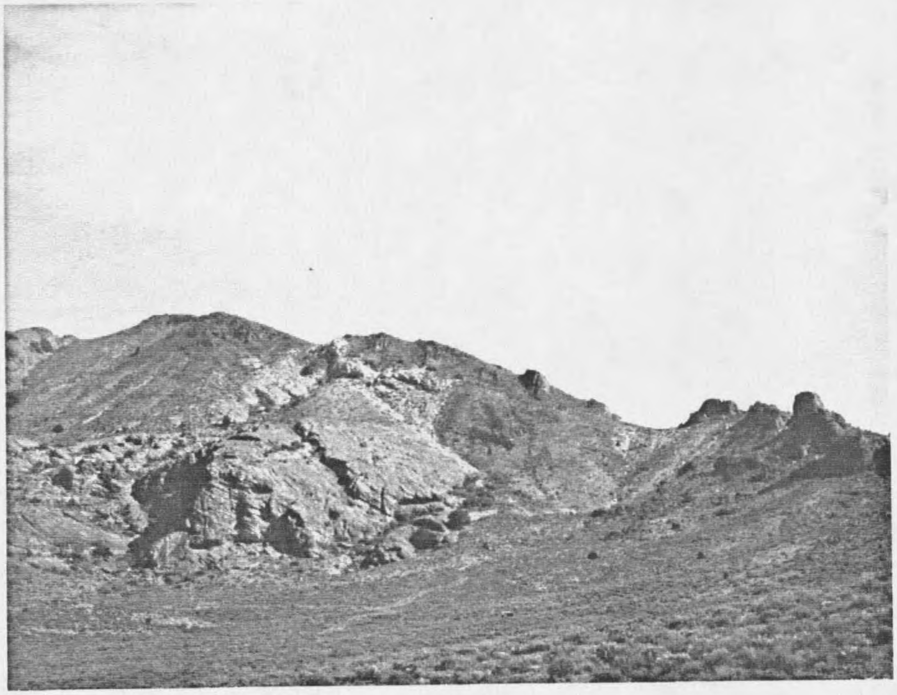

Figure 29. View northward from Section B towards Sections C and F. The ridge is capped by the three megabreccia blocks. The stratigraphically lowest (oldest) on the left and the highest (youngest) on the right.

of directional folds and structurally imbricated clasts at the base of the uppermost deposit provides information on the direction of landslide movement. Analysis of megabreccia lithofacies allows for further interpretation of transport direction and means of landslide emplacement.

Definition and Interpretation of Megabreccia Lithofacies

Yarnold and Lombard (1989) summarize characteristics commonly recognized in megabreccia deposits of western North America and the Middle East (Figure 30) anddivided megabreccia deposits into three major components including: 1) an interval of deformed substrate (DS) below the base of the deposit, 2) a discontinuous zone of substrate mixed with megabreccia material (MZ), and 3) the breccia sheet. The breccia sheet forms the largest volume of the deposit and is characterized by differing degrees of brecciation. A matrix-rich disrupted zone (DZ) overlies the mixed zone near the base of the breccia sheet (Longwell, 1951; Shreve, 1968 ; Anderson, 1978). Comminuted slip surfaces (CSS), surfaces where rock flour is formed, are common in the disrupted zone. These surfaces commonly separate zones of differential brecciation within the portion of the breccia sheet overlying the disrupted zone. Differential brecciation includes jigsaw breccia (JB), crackle breccia (CB), and massive, nonbrecciated blocks (MNB) (Harrison and Falcon, 1937; Longwell, 1951; Shreve, 1968 ; Burchfiel, 1966; Watson and Wright, 1969; Krieger, 1977; Drewes, 1977; Anderson 1978; Johnson, 1978; Balcer, 1984; Kerr, 1984). The top of the deposit is often characterized by a coarse boulder cap (BC) (Norton, 1917; Harrison and Falcon, 1937; Hadley, 1964; Marangunic and Bull, 1968; Watson and Wright, 1969; Plafker and Ericksen, 1978; Kerr, 1984; Hewitt, 1988). In Member 1 of the Horse Camp Formation, extremely coarse monolithologic conglomerate of the same composition as the megabreccias lies along strike of the megabreccia deposits. These

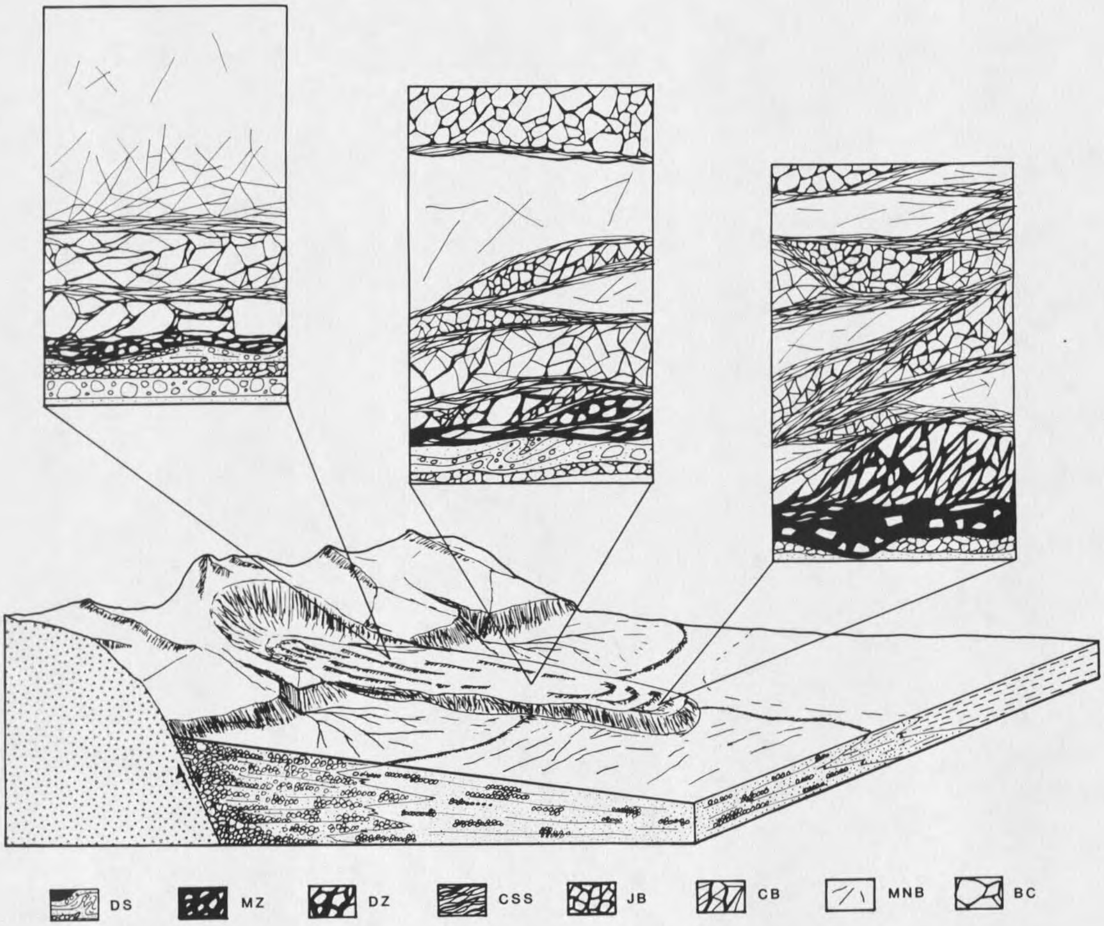

Figure 30. Schmatic block diagram showing the longitudinal changes within a megabreccia block. Degree of brecciation increases distally. DS - deformed substrate; MZ - mixed zone; DZ - disrupted zone; CSS - comminuted slip surfaces; JB - jigsaw breccia; CB - crackle breccia; MNB - massive nonbrecciated block; BC - bouldery cap.

aprons of sediment are interstratified with finer basin-fill sediment and interpreted as debris shed off the megabreccias. They are also described in this section.

In this study, the above characteristics are described and interpreted using megabreccia lithofacies to determine the depositional nature, transport direction, and tectonic implications of the megabreccias recognized at the top of Member 1 of the Horse Camp Formation.

Deformed Substrate (DS)

Description : Up to 4 meters of sedimentary strata underlying megabreccia deposits have been scoured and entrained into the mixed zone (Figure 31) or severely folded (Figures 32 and 33). Scours range from 0.05 to 2 meters in depth and are 1 to 7 meters long. Scouring is present most commonly in coarse-grained sandstone and conglomerate units. Slabs of coarse-grained sandstone and conglomerate up to 0.5 meters thick have been entrained from the underlying, undeformed strata and incorporated into the mixed zone as imbricated blocks (Figure 31). Dip of imbricated blocks is to the north - northwest. Where underlying strata are composed of fine-grained sandstone and mudrock folding is very common. Folds involve up to 2 meters of strata, are overturned to recumbent, and verge to the south - southeast (Figures 32 and 33).

Strata are deformed below the base of all three megabreccia blocks. However, folding is recognized only in conjunction with the largest megabreccia deposit located near the top of Member 1 in (from north to south) sections F, C, E, B, A, and D (Plates 1 and 2 and Figures 6 and 34). Because of the large size and longitudinal orientation of the exposure of this particular megabreccia, most of the recorded deformation of the substrate was located at the base of this deposit. The thickest (4 meters) section of deformed substrate lies between sections C and E where the breccia sheet is thinnest. The zone of

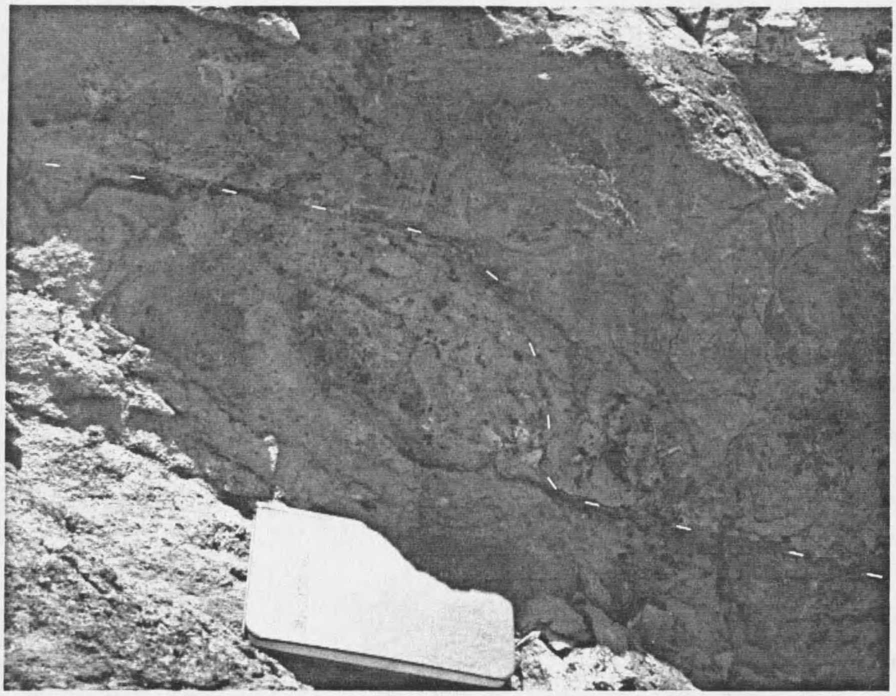

Figure 31. Effects of scouring at the base of a megabreccia. White dashed line at base of megabreccia. Note the counterclockwise rotation of the cobble. Fieldbook for scale (15 cm long).

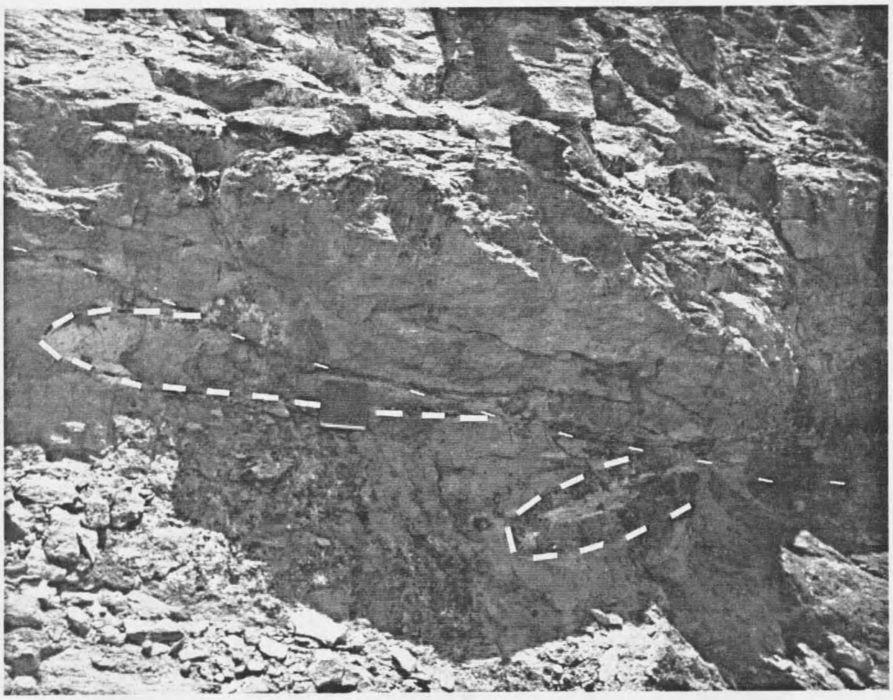

Figure 32. Deformation of substrata. Sandstone and mudstone layers outlined in white dashed lines were folded and sheared off by the overlying block. Fieldbook for scale (15 cm long).

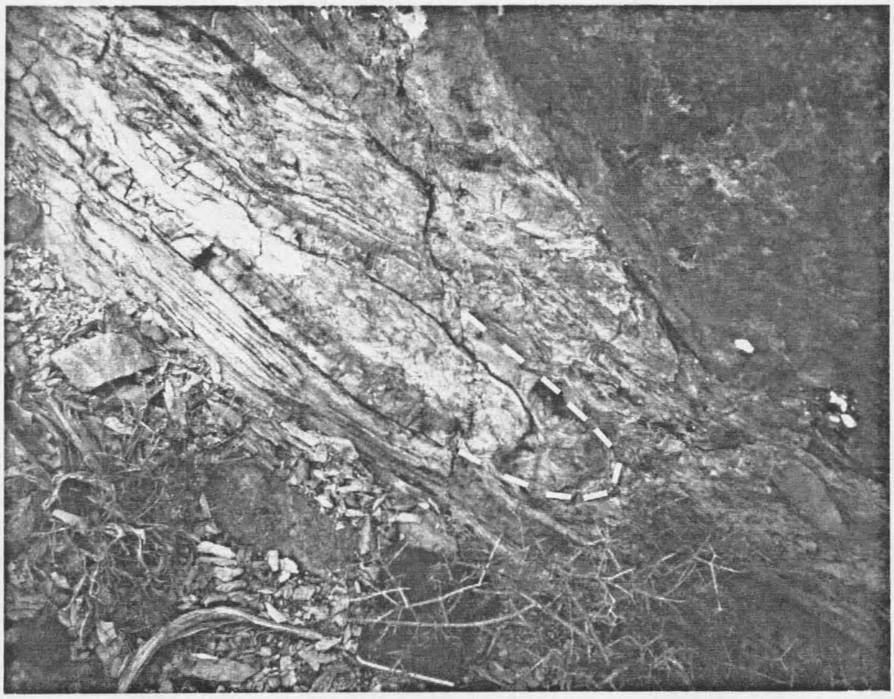

Figure 33. Intense folding of mudstone layer. Hinge of fold outlined by white dashed line. Actual distance across photo is approximately 1 meter.

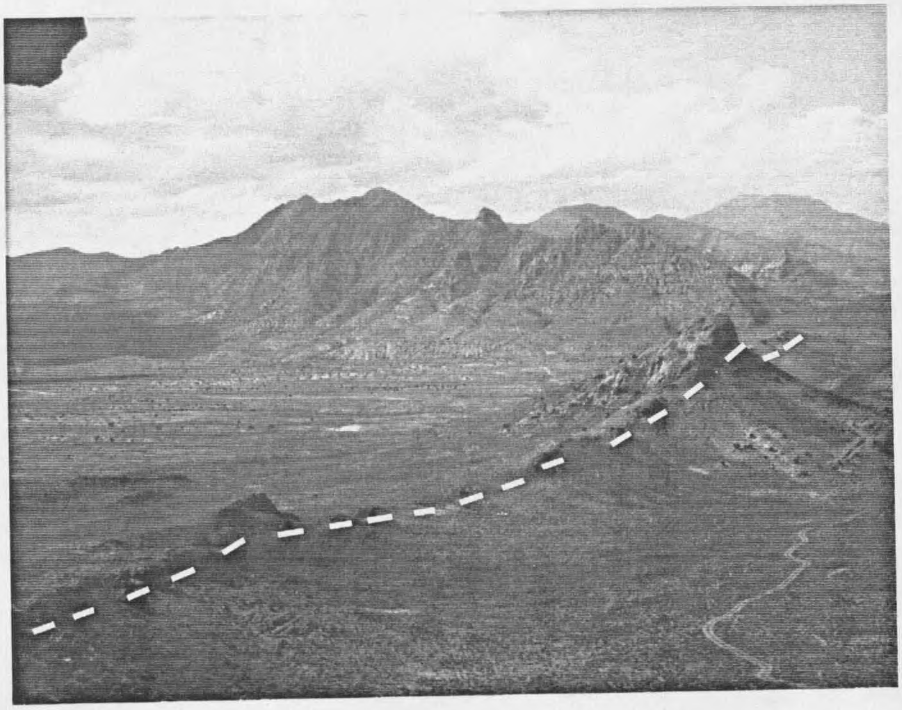

Figure 34. View to the south from Section F of outcrop of stratigraphically highest megabreccia. Strata dip to the east. Megabreccia ridge trends to the south parallel to direction of megabreccia transport. White dashed line delineates the base of the megabreccia.

deformed substrate is thinnest (2 centimeters) at the base of the middle block along section F. Where the mixed zone (described below) is very thin or absent, deformation of underlying strata is characterized by comminuted slip surfaces that are generally subparallel to basal contacts. These surfaces extend laterally up to ten meters, have 1 to 20 centimeter thick intervals of rock flour, and often exhibit slickensides.

Interpretation : Deformation of strata underlying megabreccia deposits is a result of the shearing forces along the base of landslides during transport (Melosh, 1987). Intensely folded fine-grained sandstone and mudstone deformed ductilely in response to shear forces. Folds are south vergent indicating a north to south transport direction (see Paleocurrent and Paleoslope section below). Coarser-grained sandstone and conglomerate show more brittle behavior by being scoured and entrained into the mixed zone as either disaggregated sediment or slabs of rock. Comminuted slip surfaces present in the substrate appear to have been zones of detachment during transport (Watson and others, 1969; Krieger, 1977).

Mixed Zone (MZ)

Description : The mixed zone consists of matrix-supported, siltstone to conglomeratic sandstone derived from both the substrate and overlying breccia sheet (Figure 31). It is a lenticular to tabular discontinuous zone (0 to 5 meters thick and 0 to 25 meters long) that is massive or banded. Textural layering tends to be subparallel to the base of the deposit. The basal contact is sharp with a few comminuted slip surfaces (Figure 35). The upper contact of the mixed zone is gradational to undulatory with up to 2 meters of relief. Load structures are common at this horizon beneath the main bulk of the breccia sheet. Clastic dikes up to one meter thick derived from the mixed zone extend up to 5

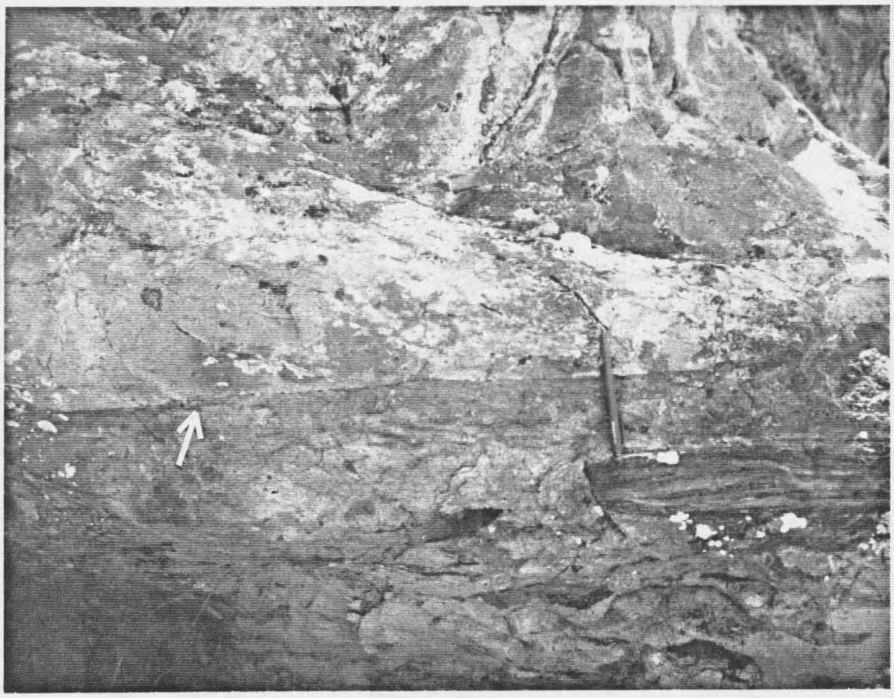

Figure 35. Mixed zone at the base of megabreccia block (white arrow points to base).
Note imbricated slab directly below pencil..

meters into the overlying breccia sheet (Figure 36). Beneath the two older blocks at the northern end of the study area (Section F), the mixing zone is very thin (0 to 15 centimeters) and extends up to 100 meters laterally with well-developed shearing fabric. Within the stratigraphically highest megabreccia deposit, the mixing zone is thicker (0 to 5 meters) and extends laterally up to 150 meters. Within this deposit, the thickness of the mixed zone and number of comminuted slip surfaces increase towards the south.

Interpretation : The mixed zone is interpreted to be the result of scouring, entrainment, and comminution during deposit runout. Material derived from both the substrate and megabreccia is present in the mixed zone. This combination of material indicates matrix was incorporated from both sources during landslide transport. Basal protrusions on the breccia sheet and positive topographic features on the depositional surface may be locally sheared off during landslide runout (Ericksen and Plafker, 1970). Banding of material may be the result of accretion of material to the substrate (Yarnold and Lombard, 1989). As evidenced by cross-cutting relationships, clastic dikes are derived from the mixed zone. These dikes were probably emplaced before movement stopped as is suggested by their straight, curved or contorted paths (Yarnold and Lombard, 1989).

Southward thickening of the matrix zone at the base of the largest megabreccia deposit is due to an increase in scouring of substrate and brecciation of landslide material. The southward increase in the amount of sediment in the mixed zone is a result of longer transport distance suggesting a north to south direction of movement.

Clastic Dikes (CD)

Description: Clastic dikes are composed of siltstone to matrix-supported conglomeratic sandstone derived from the mixed zone (MZ) (Figure 36). These dikes have

Figure 36. Clastic dike extending into the megabreccia block. Hammer for scale.

straight, curved, or contorted outlines and are oriented subvertically. Clastic dikes are up to 5 meters in length and less than 10 centimeters wide.

No clastic dikes were documented in the two stratigraphically lower megabreccia blocks present in Section F. A full spectrum of sedimentary dike morphologies are present in the highest megabreccia block. Clastic dikes are generally absent in the northernmost exposures of this block at Sections F and C. To the south, between Sections C and E clastic dikes are generally straight or contorted (Figures 36 and 37). The number of dikes increases southward in conjunction with thickening of the mixed zone.

Interpretation : Because the mixed zone forms during transport and is the source for clastic dikes, these dikes probably formed during dilation of fractures in the later stages of transport and at the time of emplacement of the megabreccia sheet. Cross-cutting relations and deformation of the dikes suggest that contorted dikes formed earliest and were deformed by continued movement of the breccia sheet. Dikes that curve in the direction of transport are better defined and probably formed during transport but later than contorted dikes (Johnson, 1978). Straight dikes probably formed at the time of emplacement. These dikes are not strongly controlled by brecciation, but rather by dilation induced during the emplacement phase (Yarnold and Lombard, 1989). The southward increase in clastic dike abundance is correlative with an increase in mixed zone thickness and degree of brecciation towards the south. This increase in source material and increase in dilation allows for an increase in the number of dikes present to the south.

Breccia Sheet

The breccia sheet makes up the largest volume of the megabreccia deposit. As defined by Yarnold and Lombard (1989) it is composed of a disrupted zone (DZ) near the

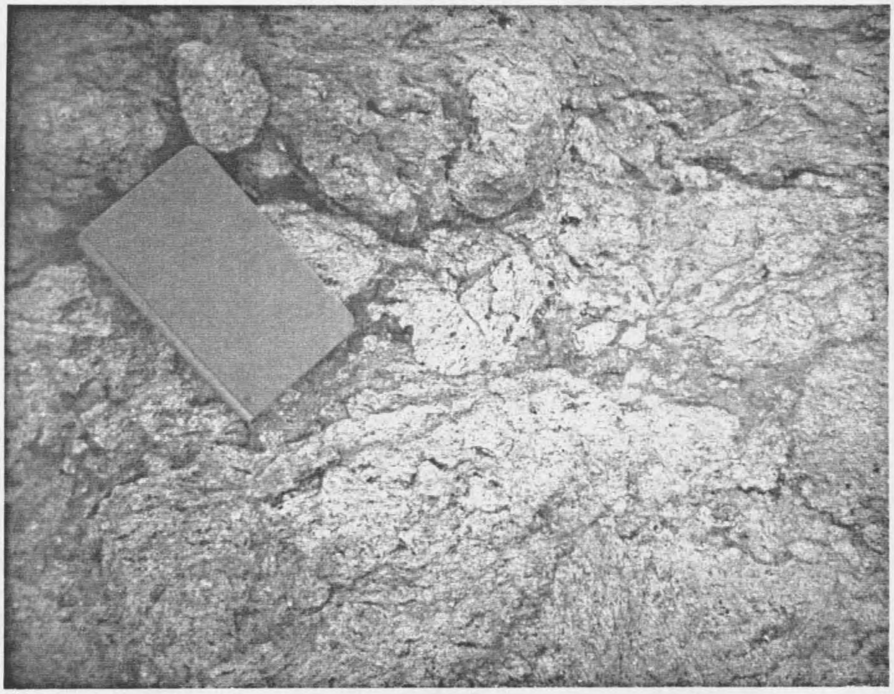

Figure 37. Disrupted zone with contorted clastic dikes. Fieldbook for scale (15 cm long).

base which is overlain by the matrix-poor zone (MPZ) cross-cut by numerous comminuted slip surfaces (CSS) and topped by a coarse boulder cap (BC). These features will be discussed individually.

Disrupted Zone (DZ)

Description : The disrupted zone is composed of Oligocene volcanic clasts 2 to 15 centimeters in diameter derived from the matrix-poor zone. Clasts are surrounded by very poorly sorted silty sandstone matrix derived from adjacent clasts and from clastic dikes extending from the mixed zone (Figure 37). Clasts are slightly imbricated with apparent dip to the north. Although contacts with underlying and overlying zones are gradational, comminuted slip surfaces commonly separate the disrupted zone from the mixed zone and the matrix-poor zones.

The disrupted zone is typically lenticular to tabular ranging from 0 to 7 meters thick and extending as much as 150 meters laterally. This zone thickens from 0 to 7 meters from north to south in the largest block but is thin to nonexistent (0 to 20 centimeters) in the smaller blocks. The disrupted zone in the largest block is well defined between Sections C and E and becomes very prevalent at Sections B and A.

Interpretation : The disrupted zone develops in response to intense brecciation and shear which increase with increasing distance of transport. The composition of this zone, its gradational relationship to the matrix-poor zone, and its southward increase in thickness suggest that in the earliest stages of movement, the disrupted zone resembled the overlying matrix-poor zone (Hsu, 1975; Yarnold and Lombard, 1989). Within the disrupted zone, the increase in number of cross-cutting clastic dikes and slip surfaces to the south suggests north to south transport (Melosh, 1987).

Comminuted Slip Surfaces (CSS)

Description : Slip surfaces occur throughout the megabreccia and in the underlying substrate (Figure 38). Flat, imbricated slices of rock are separated by thin anastomosing fractures filled with rock flour. Slickensides are common on the surfaces of the rock slices. Except at the southern end of the largest block, slip surfaces are subparallel to the base of the deposit. At the southern end, near Section A, slip surfaces dip north 10 to 24^{o} relative to the underlying strata.

Comminuted slip surfaces occur throughout the megabreccia deposit. Slip surfaces are poorly developed but present in the mixed zone and in the substrate where the mixed zone is thin (0 to 30 centimeters). They are most common near the base of the breccia sheet in the disrupted zone where they increase in thickness and number upwards. In the overlying matrix-poor zone their occurrence is restricted and they separate different lithologic packages and zones of differential brecciation.

Interpretation : Comminuted slip surfaces are direct manifestations of progressive simple shearing within the megabreccia deposit (Twiss and Moores, 1992, pg. 304 - 308). Shear stress is applied by the moving block and is transmitted to the depositional surface. Effects of stress are concentrated in the mixed zone and disrupted zone. The prevalence of slip surfaces in the disrupted zone and dramatic decrease in the number of slip surfaces in the matrix-poor zone suggests that most of the shearing took place within the disrupted zone. The slip surfaces separating lithologic packages in the matrix-poor zone act as laminar shear surfaces that developed during transport. Those separating zones of differing degrees of brecciation may be accommodation surfaces separating differing amounts of disruption. The north dipping comminuted slip surfaces present at Section A may represent

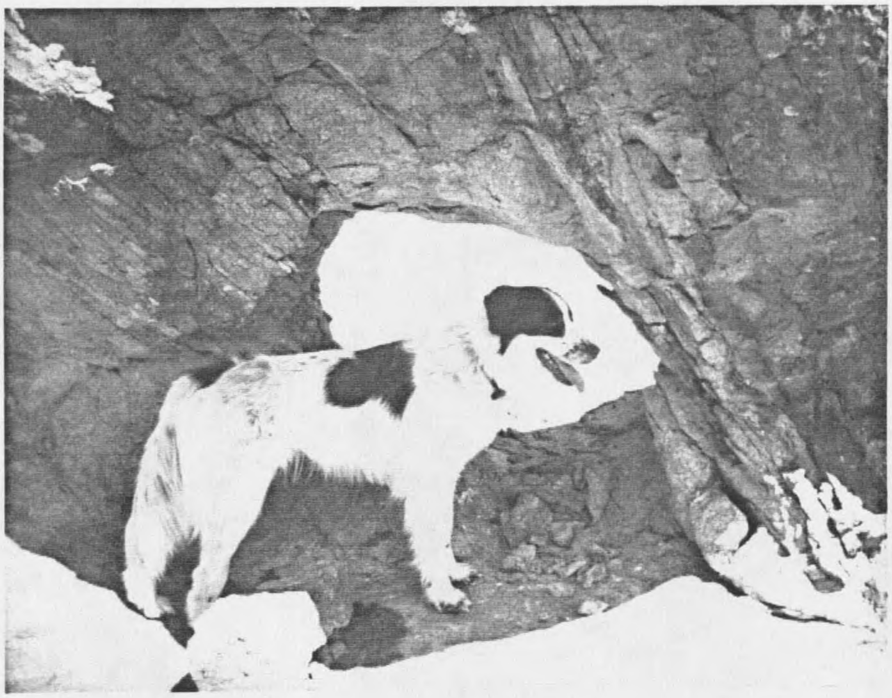

Figure 38. Comminuted shear surfaces dipping to the right. Annie the dog for scale (70 cm high).

"distal ramping". These surfaces develop as the most distal end of the breccia block comes to a stop. The moving material behind the distal portion is forced to ramp over the stationary material. Similar features have been recognized in the Black Canyon (Longwell, 1951; Anderson, 1978) and the Cross Hill breccias (Drewes, 1977; Balcer, 1984) in Arizona.

Matrix Poor Zone (MPZ)

Description : The matrix-poor zone is composed of Oligocene volcanic rocks brecciated to varying degrees. This brecciation is described by Yarnold and Lombard (1989) as jigsaw breccia, crackle breccia, and massive nonbrecciated blocks. These zones of brecciation are divided by comminuted slip surfaces.

Jigsaw breccia (JB) is a brecciation facies in which rock fragments are separated by a thin band of matrix but are not significantly rotated (Figure 39). Matrix is derived from adjacent clasts except in rare cases where it was introduced from the underlying sediments. Zones of jigsaw breccia (JB) are 5 to 12 meters thick and up to 200 meters long. This facies is also referred to as mosaic breccia by Laznicka (1988).

Crackle breccia (CB) is a facies of severely shattered rock in which the fracture bounded fragments show little to no matrix, separation, or rotation (Figure 40). Zones of crackle breccia (CB) range up to 15 meters thick and 150 meters long.

The few comminuted slip surfaces recognized in the matrix poor zone are located near the southern extent of the largest megabreccia block. These zones of shearing range from 0 to 3 meters thick and extend up to 20 meters laterally.

Massive and non-brecciated (MNB) blocks appear to be intact and strongly resemble in-situ outcrops of the source rock (Figure 41). These blocks are up to 40 meters

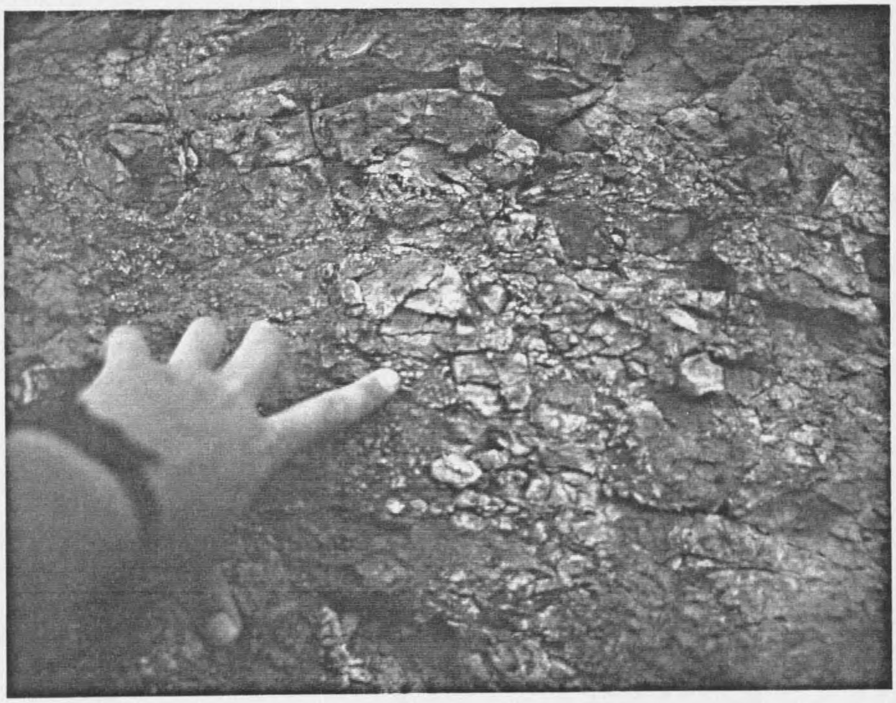

Figure 39. Jigsaw breccia composed of pebble to cobble sized clasts that have undergone minimal rotation in a sandy matrix.

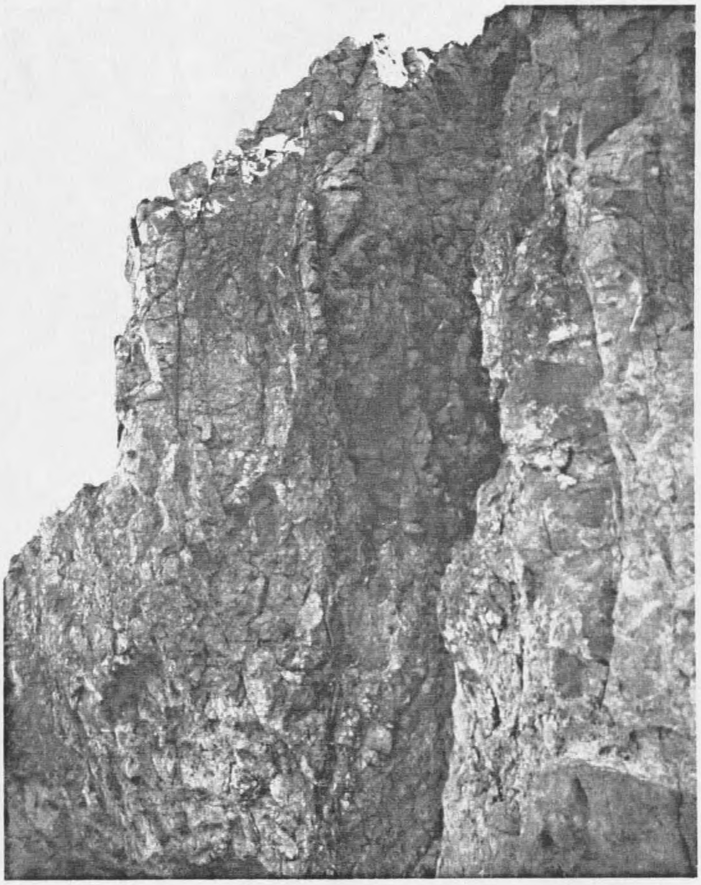

Figure 40. Cliff of crackle breccia composed of very angular cobble to boulder sized clasts that have not undergone rotation and are separated by a layer of very thin sandy matrix. Distance across the base of the photo is approximately 5 meters.

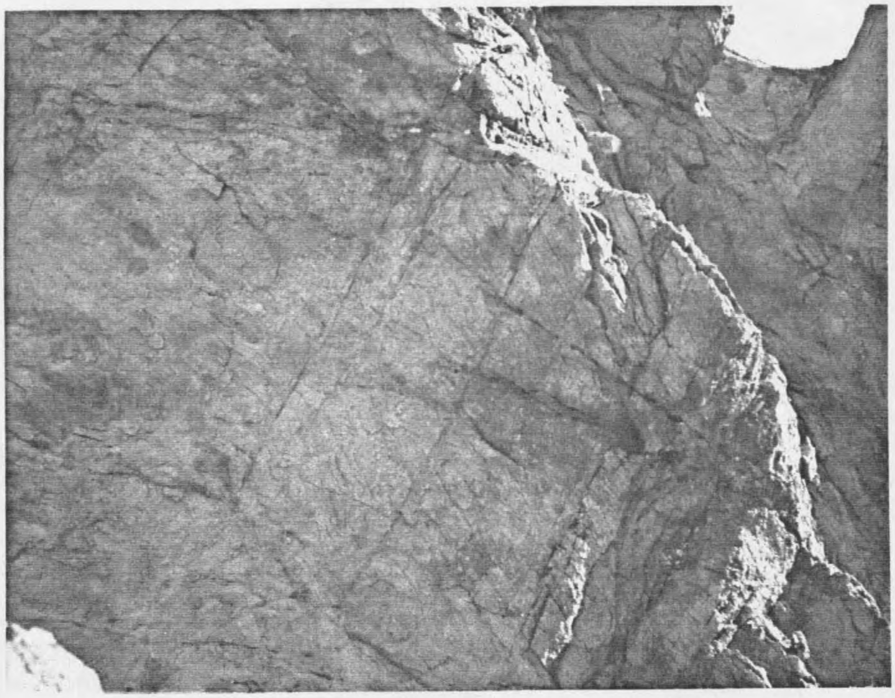

Figure 41. A cliff of massive nonbrecciated Railroad Valley rhyolite within the megabreccia block. Distance across the base of the photo is approximately 8 meters

thick and 125 meters long. The largest blocks form the north - south striking ridge that marks the top of Member 1 in the northern half of the study area.

While the thickness of the matrix-poor zone remains relatively consistent within the two smaller blocks in section F in the northern portion of the field area, the overall thickness of the largest megabreccia deposit increases from north to south. The two smaller deposits range in thickness from 20 to 25 meters. The matrix poor zone in the largest deposit is 45 to 150 meters thick. This deposit is thinnest at Sections F and C, thickest between Sections E and B, and gradually thins to approximately 120 meters at Section A. A thin megabreccia deposit (4 meters) located at the top of section D lies to the south along strike with the megabreccia deposit found at Section A and may represent material eroded from that deposit.

<u>Interpretation</u> : The varying degrees of brecciation within the matrix-poor zone represent differences in magnitude of shear stresses in the breccia sheet. The most severely brecciated material is jigsaw breccia. This material deformed during transport during which time the matrix developed. Crackle breccia developed at the time of emplacement when shattering of the rock takes place without clast rotation. Massive nonbrecciated blocks are transported as coherent blocks on zones of shearing. The southward thickening of the largest deposit is typical of an increase in material at the distal portion of large rock avalanches or landslides transported and deposited without obstruction (Yarnold and Lombard, 1989).

<u>Boulder Cap (BC)</u>

<u>Description</u> : The coarse boulder cap is composed of angular to subrounded, Oligocene volcanic boulders to large cobbles derived from the top of the megabreccia. The

interstitial matrix is derived from adjacent clasts. This minor facies is present at Sections E, B, and A.

Interpretation : The boulder cap may represent the bouldery surface recognized on the surface of historical rock-avalanches (Hadley, 1964). It may also be the result of erosional and pedogenic processes wearing down the surface of the deposit (Hewitt, 1988).

Longitudinal Trends

Features resembling those listed above have been recognized in many megabreccia deposits elsewhere. Yarnold and Lombard (1989) realize the ubiquitous nature of these characteristics and develop a predictive model to aid in recognizing and reconstructing ancient rock-avalanche deposits. This model assumes a semiarid alluvial fan-playa depositional setting but allows for some modification depending upon individual study site characteristics. The model describes three typical stratigraphic sections for the proximal, medial, and distal portions of large rock-avalanche lobes (Figure 30). The following is a comparison of the model of Yarnold and Lombard (1989) with description and interpretation of the north to south longitudinal changes from within the stratigraphically highest megabreccia deposit in Member 1.

Proximal Stratigraphy

Most proximal deposits are characterized by coarse basin margin (alluvial fan) facies overlain by a thin mixed zone. The contact has very little relief and because of the coarse nature of the underlying facies, substrate deformation is characterized by scouring and entrainment of sediment. The overlying breccia sheet is thin with very poorly developed shear zones, general absence of clastic dikes, and dominance of jigsaw and crackle breccia facies.

The two small megabreccia blocks and northern portion of the largest megabreccia strongly resemble this description. The two smaller blocks are thin breccia sheets (20 to 25 meters) with thin comminuted slip surfaces and composed of jigsaw and crackle breccia. They are underlain by very thin mixing zones (1 to 5 centimeters) and deposited over medial alluvial fan deposits. The basal contacts have very low relief.

Because megabreccia deposits create their own topography, fine-grained sandstone and mudrock commonly surround the breccia sheet. These finer-grained facies are deposited in standing water in ponds that developed on the margins and surface of the landslide. Although the megabreccias of Member 1 of the Horse Camp Formation generally overlie relatively coarse-grained strata, the stratagraphically middle megabreccia deposit interfingers with and is overlain by finer-grained sandstone and mudrock facies. At Section F the highest breccia sheet overlies finer-grained rocks. Its emplacement resulted in extreme deformation of these strata by the shear forces generated by transport of the deposit. Above the deformed substrate, the mixing zone is 1 to 1.5 meters thick with incorporated slabs of sandstone. The breccia sheet is thinnest (40 to 45 meters) in this area. Where the breccia sheet overlies coarser deposits, the mixing zone is thinner (1 to 30 centimeters). The breccia sheet is composed of jigsaw and crackle breccia with thin, discontinuous comminuted slip surfaces. Clastic dikes are prevalent where the deposit overlies finer-grained sandstone and mudrock.

Medial Stratigraphy

According to the model of Yarnold and Lombard (1989) medial deposits typically overlie substrate facies composed of alluvial fan to sandflat sediments depending upon the position of local facies boundaries. Deformation of these sandstone and mudstone units may be significant. The contact between the substrate and a thin mixed zone typically shows minor to moderate relief. The mixed zone is the source for well-developed clastic dikes which intrude into the overlying, relatively thin breccia sheet. Typically, the breccia sheet has a poorly developed matrix-rich disrupted zone with comminuted slip surfaces common at the base.

The stratigraphy of the largest breccia sheet in Member 1 at Sections E and B strongly resembles the medial stratigraphy of other megabreccia deposits as described above. The underlying sedimentary strata are composed of sandstone and conglomerate deposited in alluvial fan and sandflat environments. Degree of deformation of substrate is moderate where exposed. The mixed zone is 0.5 to 3 meters thick with up to 1 meter of relief. Clastic dikes 0.1 to 0.5 meters wide and less than 3 meters long are well developed and extend into the disrupted zone (1 to 3 meters thick) at the base of the breccia sheet. The disrupted zone is dominated by clastic dikes that penetrate comminuted slip surfaces.

Distal Stratigraphy

The model described by Yarnold and Lombard (1989) is based upon a basinward transition from coarse marginal to fine-grained basin center facies. Thus, the distal stratigraphy of a megabreccia deposit is strongly controlled by the presence of fine-grained basin sediments. Folding, contortion, and/or imbrication of relatively fine-grained sandflat or lacustrine sediments can be intense at the rock avalanche-substrate interface. This contact can exhibit significant relief and is characterized by a thick mixed zone which acts as a source for clastic dikes. Dikes protrude several meters into the overlying thick breccia sheet which displays a well-developed disrupted zone and laterally extensive comminuted slip surfaces. These slip surfaces commonly dip toward the direction of the source (Figure 30) and have been interpreted as "ramp-type structures" developed as the megabreccia came to a halt.

Near Section A the southernmost exposure of the largest megabreccia overlies alluvial fan and sandflat sandstone and conglomerate. This is characteristic of distal deposits on the large radius alluvial fans on which the landslides were deposited. Features within the megabreccia outcrop at Section A suggest that this is the distal portion of the largest megabreccia in Member 1. The basal contact is mostly covered but exposed portions of the mixed zone are moderately thick (2 to 3 meters) and basal contact relief is significant (greater than 4 meters). Clastic dikes (0.25 to 2 meters thick) extend more than 5 meters thick into the breccia sheet often parallel to comminuted slip surfaces that dip 15 to 25^{o} to the north. Brecciation is most intense in this area and is characterized by jigsaw breccia and shear zones up to 5 meters which separate zones by crackle breccia and massive non-brecciated blocks.

Emplacement of Megabreccias

The described features of Member 1 megabreccias are typical of deposits elsewhere that have been interpreted as landslides. Analyzing data from studies of Pleistocene and Holocene landslides, Campbell (1989) proposes a model that suggests long-runout landslides move downslope on a lubricating active particle layer. This model suggests that the larger the mass moving downslope, the greater the kinetic energy involved, the longer time required for the active layer to dissipate, and thus, the larger the runout distance. Comparisons of Pleistocene and Holocene landslides and ancient megabreccia deposits suggest that similar mechanisms were probably operational during the emplacement of the megabreccia deposits. Campbell's model provides an explanation for vertical and longitudinal trends in characteristics recognized in the megabreccias of Member 1 of the Horse Camp Formation. The active particle layer may be preserved as the mixing zone which is thickest in the most distal reaches of the megabreccia.

PALEOCURRENTS AND PALEOSLOPE

Sediment transport direction indicators are rare in Member 1 of the Horse Camp Formation. In order to determine the general direction of flow throughout the member, it was necessary to use shadow structures (Karcz, 1968) (Figure 8). Direction of flow could not be quantified from the shadow structures because they are rarely exposed in three-dimensions. However, general flow direction could be qualifiably determined. For the lower portion of Member 1, shadow structures indicate that direction of flow was from the northwest and southwest. For the upper portion of Member 1 shadow structures suggest direction of flow was from the north in the northern part of the study area (Sections F, C, E, B, and A) and from the south in the southern portion of the study area (Sections G, H, and I).

Other paleoslope/paleocurrent data collected include trend and plunge of trough axes, and trend and plunge of folds found in deformed strata underlying megabreccia deposits. Substrata found beneath the base of megabreccia deposits are often deformed by the shear forces generated by megabreccia transport. This deformed zone is characterized by isoclinal and recumbent folding of mudrock and sandstone facies and structural imbrication of 1 meter thick slices of coarse sandstone and conglomerate facies (Yarnold and Lombard, 1989). Vergence of folds and dip of imbrication are potentially useful indicators of megabreccia transport direction (Kerr, 1984; Yarnold and Lombard, 1989).

Deformational folds and imbricated blocks are present at the base of the largest slide block found at the top of Member 1 in the northern half of the field area. Folding involved beds of mudrock and sandstone 25 to 40 centimeters thick (Figures 32,33). The trend and plunge of 14 isoclinal and recumbent folds were measured, plotted on a stereonet, and corrected for tectonic rotation (Figure 42.a). Folds are south vergent suggesting megabreccia transport was from north to south.

Five to 10 centimeter thick blocks of coarse sandstone and granule - pebble conglomerate were structurally imbricated with observed dip to the north. Exposures of imbrication were rare and two-dimensional; therefore, no data of this type were collected.

Less than 1% of Member 1 is composed of trough cross-stratified sandstone and/or conglomerate. Because of the limited number of exposures, a total of only 23 trough axes was measured (Figure 42.b). These were direct measurements of three-dimensional exposures in conglomerate and sandstone trough cross-stratified units (Gt, St). Eleven measurements of trough axes were taken near the base of Member 1 at Section H in the southern part of the field area. These troughs of interstratified sandstone and granule-pebble-cobble conglomerate range from 1 to 2 meters deep and 2 to 5 meters wide. Measurements plotted on a stereonet and corrected for tectonic rotation indicate that the sediment deposited in the measured troughs was transported form west to east (Figure 42.b).

Near the top of Member 1 at Section D, the trend and plunge of 12 three-dimensional exposures of trough axes were measured in trough cross-stratified medium- to coarse-grained sandstone. Troughs are 1 to 1.5 meters deep and 2 to 5 meters wide. The trend and plunge of the measured trough axes were plotted on a stereonet and corrected for tectonic rotation. These data suggest sediment was transported from north to south (Figure 42.b).

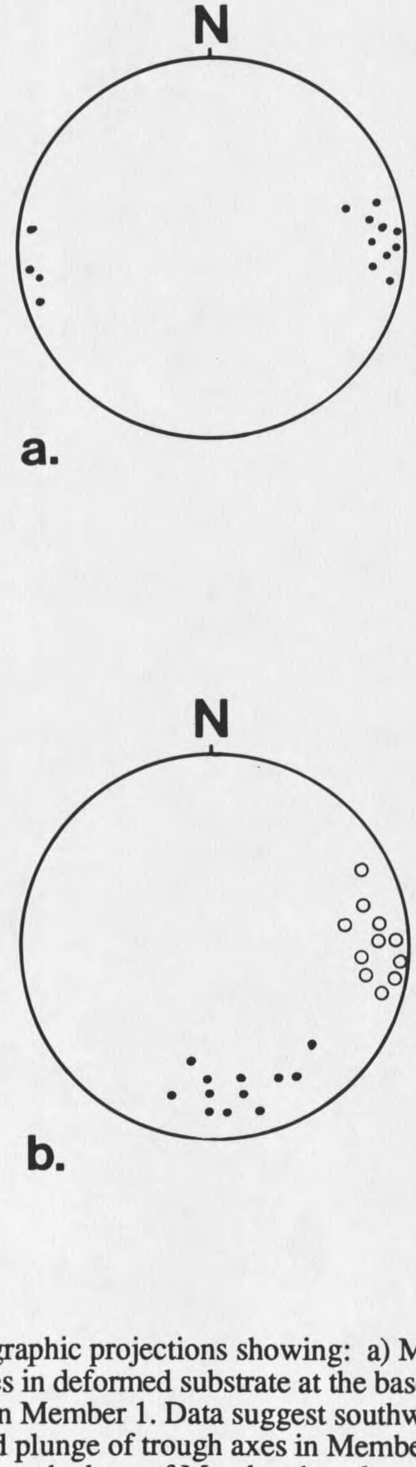

Figure 42. Equal area stereographic projections showing: a) Measured trend and plunge of south vergent fold axes in deformed substrate at the base of the stratigraphically highest megabreccia in Member 1. Data suggest southward transport of the block. b) Measured trend and plunge of trough axes in Member 1. o denotes trough measurements from near the base of Member 1; • denotes trough measurements obtained near top of Member 1.

PETROGRAPHY

Conglomerate

Composition

The conglomerates of Member 1 of the Horse Camp Formation are composed predominantly of Oligocene volcanic clasts with some Paleozoic carbonate and quartzite clasts. Clast size ranges from granule to boulder with granule and pebble sized clasts most common. Clasts are typically subangular to rounded and equant to bladed in shape. Shape and roundness may be controlled by parent lithology which would control clast durability and pre-transport shape.

Eight different clast types were identified in this study. Clast count data are tabulated in Table 2. Six of these represent Oligocene volcanic units including the: 1) Railroad Valley Rhyolite (Trv), 2) Blind Springs Formation (Tbs), 3) Stone Cabin Formation (Tsc), 4) Windous Butte Formation (Twb), 5) Needles Range Formation (Tnr), and 6) Shingle Pass Formation (Ts). These clasts were discriminated in hand sample by relative percentages of quartz, potassium feldspar and plagioclase (Scott, 1965). Clasts of Railroad Valley Rhyolite and Windous Butte Formation are subangular to rounded and are typically well silicified and therefore quite durable. Clasts of Blind Springs, Stone Cabin, Needles Range, and Shingle Pass Formations are silicified to a lesser degree and hence not as durable (some are quite friable). These clasts are subrounded to well rounded.

Clasts of Paleozoic limestone, dolostone, sandstone, and quartzite were identified based on various physical properties such as hardness (especially for the quartzite clasts), color, internal structures, fossil content, and compostition (limestone and dolostone). Paleozoic carbonate and sandstone clasts are subangular to well rounded and appear to be somewhat durable. Paleozoic quartzite clasts are angular to subrounded as they are typically less affected by abrasion during transport due to their inherent hardness.

Oligocene Volcanic Rocks. Clasts derived from Oligocene volcanic rocks were identified based on the relative percentages of distinguishing phenocrysts as described by Scott (1965). Hand samples of each volcanic unit in the area were collected for comparison.

The Railroad Valley Rhyolite is the source for 0 to 90% of clasts found in individual depositional units within Member 1 of the Horse Camp Formation. These clasts are found in each measured section and are represented in all but one clast count grid. Clasts derived from this unit are composed of approximately 30% phenocrysts set in a fine groundmass (less than 0.05 millimeters). Phenocrysts are composed of 40% quartz, 40% plagioclase, 10% sanidine, and 10% mafic minerals (biotite, hornblende, and magnetite). These clasts are typically silicified and white, light gray, pale pink, and purple in color.

The Blind Springs Formation is a very minor contributor of gravel sized clasts (0 - 6.3%) because it is composed of relatively soft red fluvial sandstone and conglomerate derived from Railroad Valley Rhyolite and green lacustrine sandstone and mudstone (Scott, 1965). Clasts from the Blind Springs Formation are represented in two sites within Section G and are identified based on texture and composition. These clasts are somewhat silicified to slightly calcareous, typically rounded to well rounded, conglomeratic sandstones containing granules and pebbles of Railroad Valley Rhyolite. Clasts from the Stone Cabin Formation (described below) are found in the same general locality as those derived from the Blind Springs Formation.

Clasts from the Stone Cabin Formation are recognized in Sections G, H, and I and make up 0 to 13% of conglomerate in these sections. Stone Cabin clasts are somewhat silicified, mottled pink and yellow, and are composed of 43% phenocrysts, 45% of which are quartz, 30% sanidine, 20% plagioclase and traces of biotite and magnetite (Scott, 1965).

The most dominant source of clasts to Member 1 is the Windous Butte Formation. This unit is the source of 13 to 100% of the clasts found in the study area and generally accounts for more than 65% of all clasts counted. Gravel weathered from the Windous Butte Formation is represented in all clast count grids in every section measured. Clasts from this source are well silicified; pale apple green, forest green, or dark gray in color; and composed of 33% phenocrysts in a fine matrix. Clasts were differentiated from other rhyolitic clasts based on the relative percentage of phenocrysts. Phenocryst abundance as described by Scott (1965) include 25% quartz, 30% sanidine, 35% plagioclase, and 10% mafic minerals (biotite, hornblende, and magnetite).

Clasts from the Needles Range Formation are found only in the southern portion of the study area and were represented in two clast count sites where they make up less than 2% of the total number of clasts counted. Scott (1965) describes the Needles Range Formation as a pale red to pale purple ignimbrite composed of 35% phenocrysts: 20% quartz, 5% sanidine, 50% plagioclase, 15% biotite (the high percentage of large (2 - 5 millimeters) biotite flakes is distinguishing), and 10% hornblende.

Clasts from the Shingle Pass Formation are found only in the southern portion of the study area and are represented in two clast count localities along Section I where they make up less than 2% of all counted clasts. These devitrified, pale red clasts are composed of 12% phenocrysts in a glass shard - pumice matrix (Scott, 1965). Phenocrysts consist of 10% quartz, 60% sanidine, 25% plagioclase, and 5% mafic minerals (biotite, hornblende, pyroxene, and magnetite).

Paleozoic Rocks. Clasts derived from Paleozoic carbonate rocks and quartzite are less abundant than Oligocene volcanic clasts. Because many clasts are pebble and cobble sized, it is difficult to identify the formation from which individual clasts came; therefore, carbonate clasts are separated into two groups, limestones and dolostones. Quartzites are easily identified based on their color and mineralogy.

Limestone clasts are generally pale to dark gray mudstone to fine grained grainstone and recrystallized carbonates. They typically lack visible stratification and fossils although a few clasts contained crinoid stem sections (Mississippian Joana Formation), brachiopods, or Receptaculites (Ordovician Pogonip Group). Local limestone sources include the Cambrian Pole Canyon Limestone, Lincoln Peak Formation, and Windfall Formation, Ordovician Pogonip Group, Devonian Guilmette Formation, Mississippian Joana Formation, and Pennsylvanian Ely Limestone.

Dolostone clasts are medium gray to black or brown; some are sucrosic or mottled. None of these clasts contain fossils and they lack stratification. Sources for the dolostone clasts include the Cambrian Windfall Formation, Silurian Fish Haven and Laketown Dolomites, and Devonian Sevy and Simonson Dolomites and Guilmette Formation.

Quartzite and sandstone clasts are bright white and tan to dark gray, respectively. The quartzite clasts do show some slight stratification whereas the sandstones (which are very rare) are generally massive. Sources for the quartzite clasts include the Cambrian Prospect Mountain Quartzite and, more probably, the Ordovician Eureka Quartzite. Sources for sandstone clasts include the Mississippian Chainman Formation or sandstones from the undifferentiated Permian section.

Composition Modes

Conglomeratic units within Member 1 of the Horse Camp Formation are composed predominantly of clasts derived from Oligocene volcanic units with some contribution from older Paleozoic carbonates, quartzites and sandstones. Percentages of Paleozoic clasts change relative to the percentage of Oligocene volcanic clasts with distance above the base of the section as shown by graphs plotting these trends for each measured section in Figure 43. Table 3 contains a tabulation of the relative percentages of the different clast types in Member 1 conglomerates.

Because of the dominance of volcanic clasts, changes in the percentage of Paleozoic clasts throughout Member 1 are more diagnostic of changes in provenance; therefore, discussion of conglomerate clast compositional trends will focus on the changes in the percent of Paleozoic clasts. There is a general increase in the percent of Paleozoic clasts above the base of Member 1 and near the northern and southern margins of the basin (Figure 43). The conglomerates found within 200 meters of the base of Member 1 are composed of greater than 95% Oligocene volcanic rocks. Near the top of Member 1, Paleozoic clasts make up as little as 5% near Section A and as much as 54% near Section D. Clasts derived from Paleozoic rocks make up a significant percentage of total clasts at north and south margins of Member 1. Member 1 strata in the north contain as much as 44% Paleozoic clasts; in the south this value is as high as 40 to 50%.

Sandstone

Texture

Sandstones were sampled from measured sections A, B, C, E, and F and from outcrops between sections C and E of Member 1 of the Horse Camp Formation. Thesesamples show a great variety of textures from moderately sorted, horizontally stratified, fine to medium-grained lithic arkose, feldspathic litharenite, and litharenite to very poorly sorted, massive bedded very fine to very coarse-grained lithic arkose, feldspathic litharenite and litharenite. Generally, sandstones are texturally immature with a high percentage of clay matrix (some of which may be diagenetic), contain very angular to subrounded grains (a product of grain durability and shape prior to transport), and are

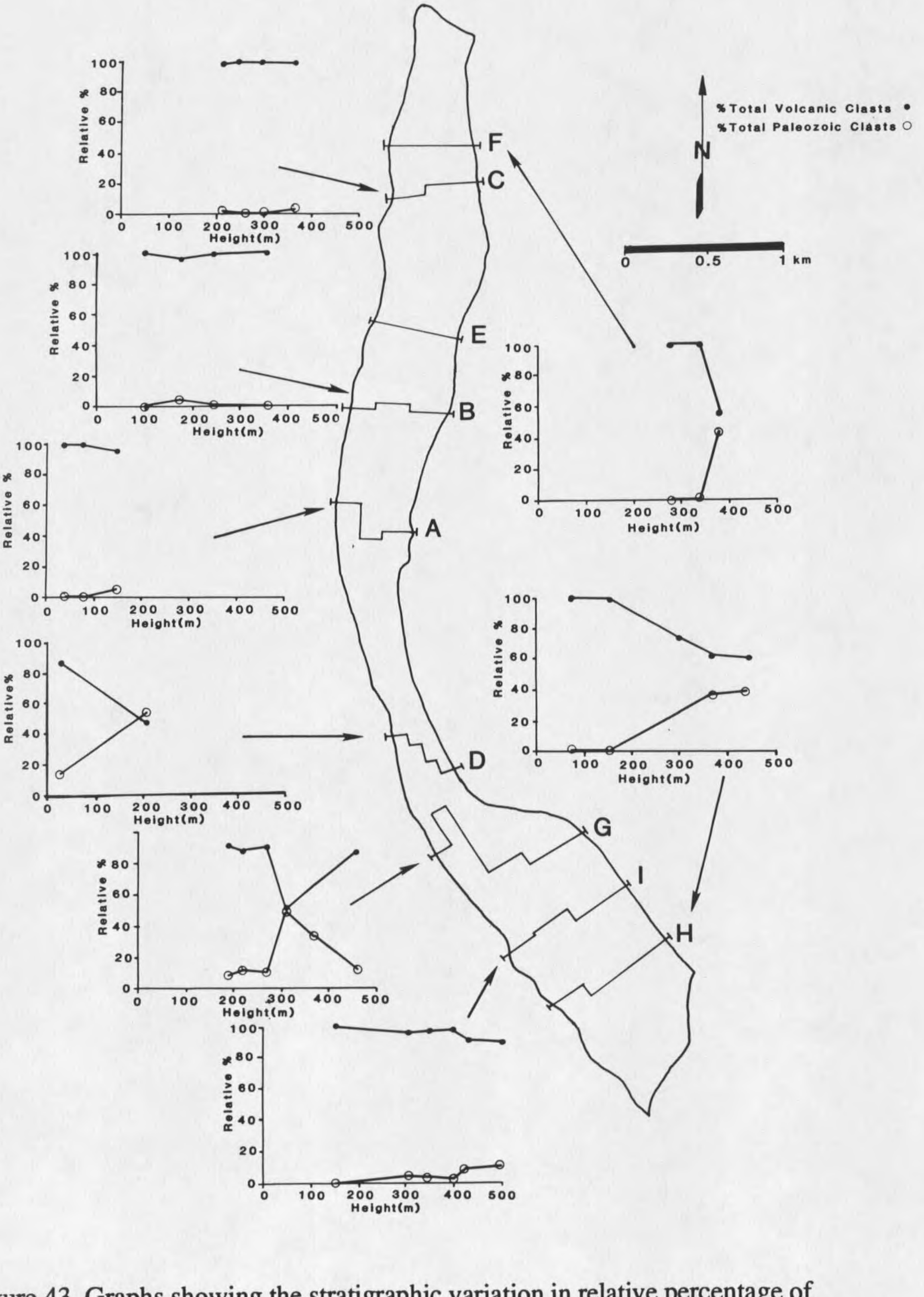

Figure 43. Graphs showing the stratigraphic variation in relative percentage of conglomerate clast lithologies for measured sections of Member 1 of the Horse Camp Formation. Base of section is to the left.

typically poorly to very poorly sorted. Grain to grain contacts are tangential and long for mineral grains and most rock fragments, and concavo-convex for some rock fragments.

Post-burial history of Member 1 sandstones of the Horse Camp Formation involves a complex sequence of diagenetic processes including cementation and dissolution or replacement of framework grains. Determining specific diagenetic trends are not within the scope of this study; however, the following is a brief description of observed diagenetic textures. Various cements are present including: 1) authigenic clay development around lithic fragments, and 2) pore-filling hematite, microcrystalline quartz, poikilotropic and fine crystalline calcite, and possibly two types of zeolites (massive, clear, isotropic, non-potassic, and fine crystalline cement, possibly analcite; and a potassic, fibrous, crystalline variety). Framework grain alteration includes: 1) dissolution of potassium feldspar, plagioclase, and volcanic rock fragments creating some secondary porosity, and 2) replacement of potassium feldspar by calcite and clay; biotite and hornblende by hematite; plagioclase by zeolite (?) and clay; and volcanic rock fragments by microcrystalline quartz (relict crystals are visible), clays, and zeolite (?).

Framework Grain Composition

Framework grains including quartz, feldspar, and lithic fragments are identified using the methods described by Folk (1980, p. 62 - 89) and Pettijohn and others (1987, p. 29 - 47). Primary framework grains as defined by Dickinson (1970) include monocrystalline and polycrystalline quartz (Qm and Qp), potassium feldspar and plagioclase (F), and lithic fragments (L) which include both sedimentary and volcanic rock fragments (Ls and Lv). In addition total quartzose grains (Q) is calculated from the sum of monocrystalline and polycrystalline quartz (Q = Qm + Qp), and the total lithic fragment component (Lt) is determined from the sum of polycrystalline quartz and lithic fragments (Lt = Qp + L). Point count data are presented in Table 4.

Monocrystalline Quartz (Qm). Monocrystalline quartz grains are single quartz crystals with straight to slightly undulose extinction. Most commonly, crystals are whole or fragmented and lack prismatic faces, are hexagonal with geometrically straight edges with some rounded corners, or have corrosion embayments. These features are indicative of a volcanic source for most of the quartz (Folk, 1980, p. 66 - 76). Quartz grains with strong undulose extinction, weak polygonization, and with abraded quartz overgrowths are extremely rare suggesting that very little of the quartz came from metamorphic or sedimentary sources (Young, 1976).

Polycrystalline Quartz (Qp). Polycrystalline quartz includes single grains composed of chert, chalcedonic chert, and composite quartz. Chert grains are most common and are composed of microcrystalline equidimensional quartz grains less than 10 microns in diameter. These grains have round, somewhat spherical, radiating crystal agglomerations suggesting that they may be highly silicified volcanic rock fragments with quartz filled amygdules or devitrification spherules. Slightly less common are grains of chalcedonic chert composed of radiating, fibrous crystals. These grains may represent microcrystalline quartz vug fillings from volcanic rock fragments. Composite quartz grains are very rare (less than 1% of total quartz component) and are composed of mosaics of sutured, elongate, and straight boundaried crystals usually appearing quite fractured. The fracturing in these grains may have developed by volcanic shocking (Scott, 1965).

Feldspar (F). Thin sections were stained for potassium feldspar to help in differentiating sanidine from quartz. Sanidine is the most common feldspar and is recognized by its reception to cobaltinitrite stain, low optic axial angle (always less than 30°), and, more uncommonly, by Carlsbad, Manevach and Baveno twinning. Plagioclase is present in lesser amounts and is recognized by very common albite twinning. Plagioclase crystals are too altered to determine albite - anorthite composition.

Lithic Fragments (L). Lithic fragments include both sedimentary and volcanic rock fragments. Volcanic rock fragments are the most predominant framework grain of the sandstones of Member 1. These grains are typically aphanitic or porphyritic with phenocrysts of quartz, sanidine, plagioclase, biotite, hornblende, and opaque minerals. Some grains are slightly to intensely silicified. Some volcanic fragments have a devitrified glass shard texture. Sedimentary grains are far less common and include grains of quartzarenite or quartzite, siliciclastic mudstone, and limestone fragments. The quartzarenites or quartzites are fine-grained with either hematite or silica cement and quartz overgrowths. Siliciclastic mudstones are difficult to distinguish from aphanitic volcanic rock fragments except when they are laminated and contain rounded quartz grains. Limestone fragments are very rare possibly due to post-burial alteration. Those grains identified as carbonate fragments were small, well rounded grains of micrite.

Sandstone Composition Modes

Forty-three sandstones were analyzed petrographically and point-counted using the relative percentages of framework grains (as described above). These sandstones plot as elliptical clusters on compositional QmFLt, QFL, and QpLsLv ternary diagrams (Figures 44, 45, and 46, respectively). Sandstones are composed of up to 83% lithic fragments (greater than 90% volcanic lithic fragments), typically less than 30% feldspar, and 1 to 31% quartz. Tuffaceous sandstones found near top of Member 1 are composed of 42 to 69% feldspar, 17 to 31% rock fragments, and 8 to 28% quartz. Sandstones range in composition from litharenite to feldspathic litharenite with rare lithic arkose (classification by Folk, 1980, p. 127).

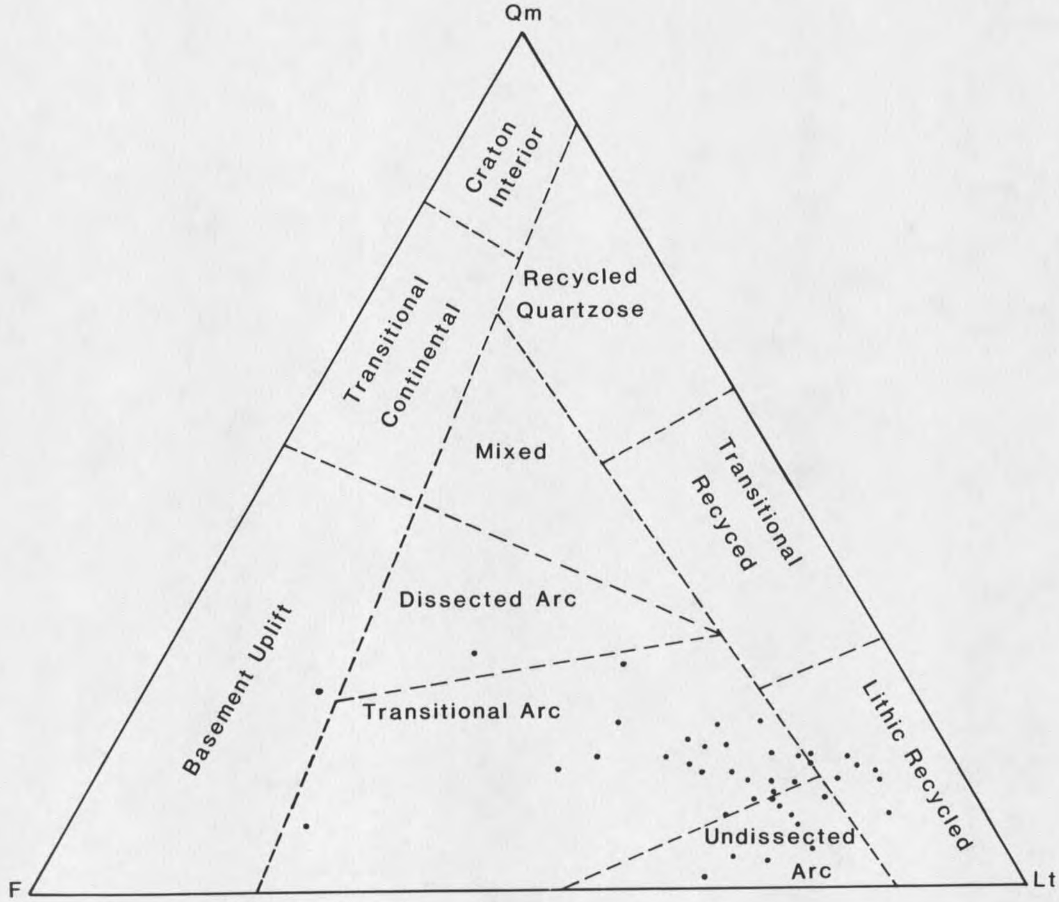

Figure 44. QmFLt ternary diagram showing the provenance of Member 1 sandstones. Note that sandstones plot primarily in the lithic recycled, undissected arc, and transitional arc provenance fields. Provenance fields after Dickinson and others (1983).

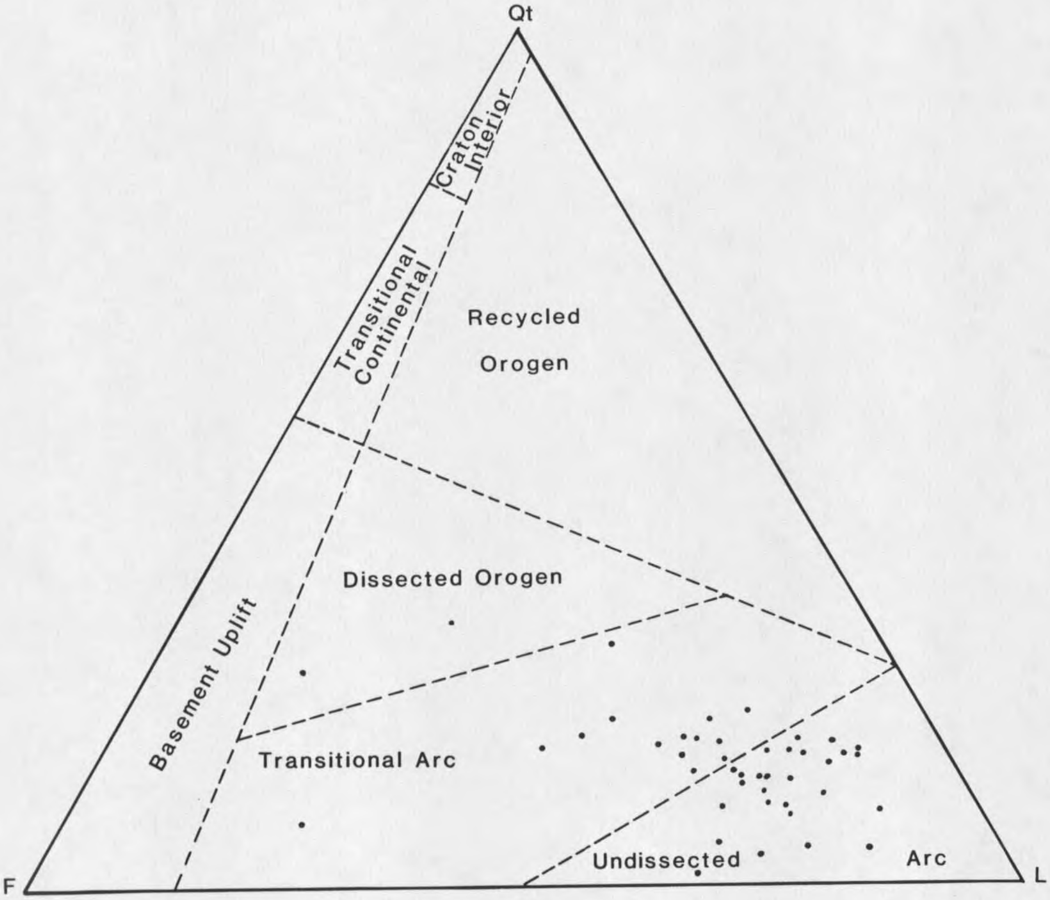

Figure 45. QtFL ternary diagram illustrating the provenance of Member 1 sandstones. Undissected and transitional arc fields contain the majority of the plotted sandstone compositions. Provenance fields after Dickinson and others (1983).

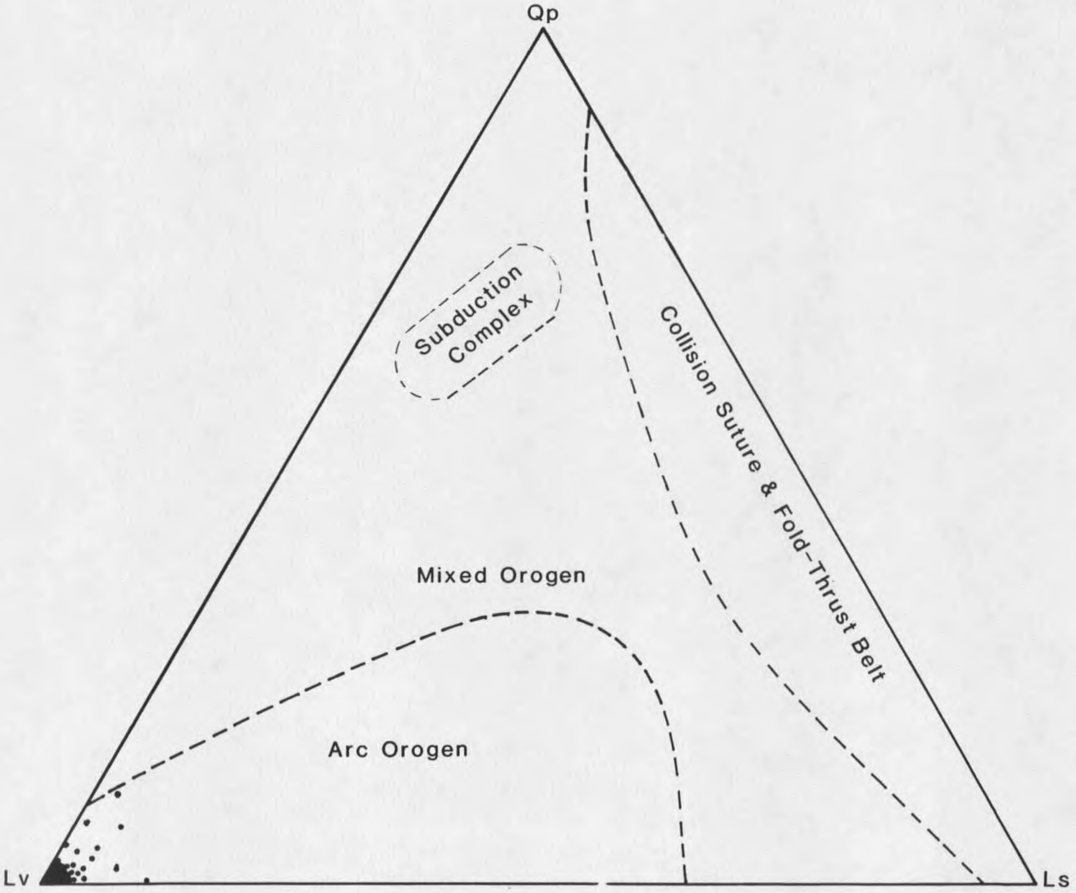

Figure 46. QpLvLs ternary diagram showing arc orogen provenance of Member 1 sandstones. Provenance fields after Dickinson and others (1983).

Litharenites are volcanic-arenites characterized by subequal amounts of quartz and feldspar (Qm = 5 - 20%, F = 8 - 27%). Lithic fragments are predominantly volcanic rock fragments (Lv = 75 - 100%) with small amounts of polycrystalline quartz (Qp = 0 - 7%) and sedimentary rock fragments (Ls = 0 - 10%). Feldspathic litharenites are composed of 46 -72% lithic fragments, 20 - 40% feldspar grains, and 1 - 26% quartz grains. The lithic component is composed of 88 - 100% volcanic rock fragments, 0 -10% sedimentary rock fragments, and 0 - 7% polycrystalline quartz.

Sandstone compositions do not change significantly from the northern to the southern part of Member 1 of the Horse Camp Formation. There is an increase in the amount of feldspar and quartz at approximately 350 to 380 meters above the base of Member 1 due to the presence of tuffaceous sandstones. Figure 47 shows the vertical trends of sandstone composition in relation to sample locations. Table 5 is a tabulation of relative percentages of sandstone grains comparing total quartz, feldspar, and lithic fragments; monocrystalline quartz, feldspar, and total lithic fragments; and polycrystalline quartz, lithic sedimentary fragments, and lithic volcanic fragments.

The sandstones sampled in the lower 350 meters of Member 1 are litharenites with some feldspathic litharenites. At this horizon, there is an apple green lithic arkose which is interpreted as a reworked airfall tuff. Above this unit, the sandstone compositions change to litharenite with some feldspathic litharenite. Although, petrographic analysis of sandstones along sections D, G, I, or H was not completed because of time and cost restrictions, careful hand sample identification was performed. These hand samples were classified predominantly as feldspathic litharenites and litharenites.

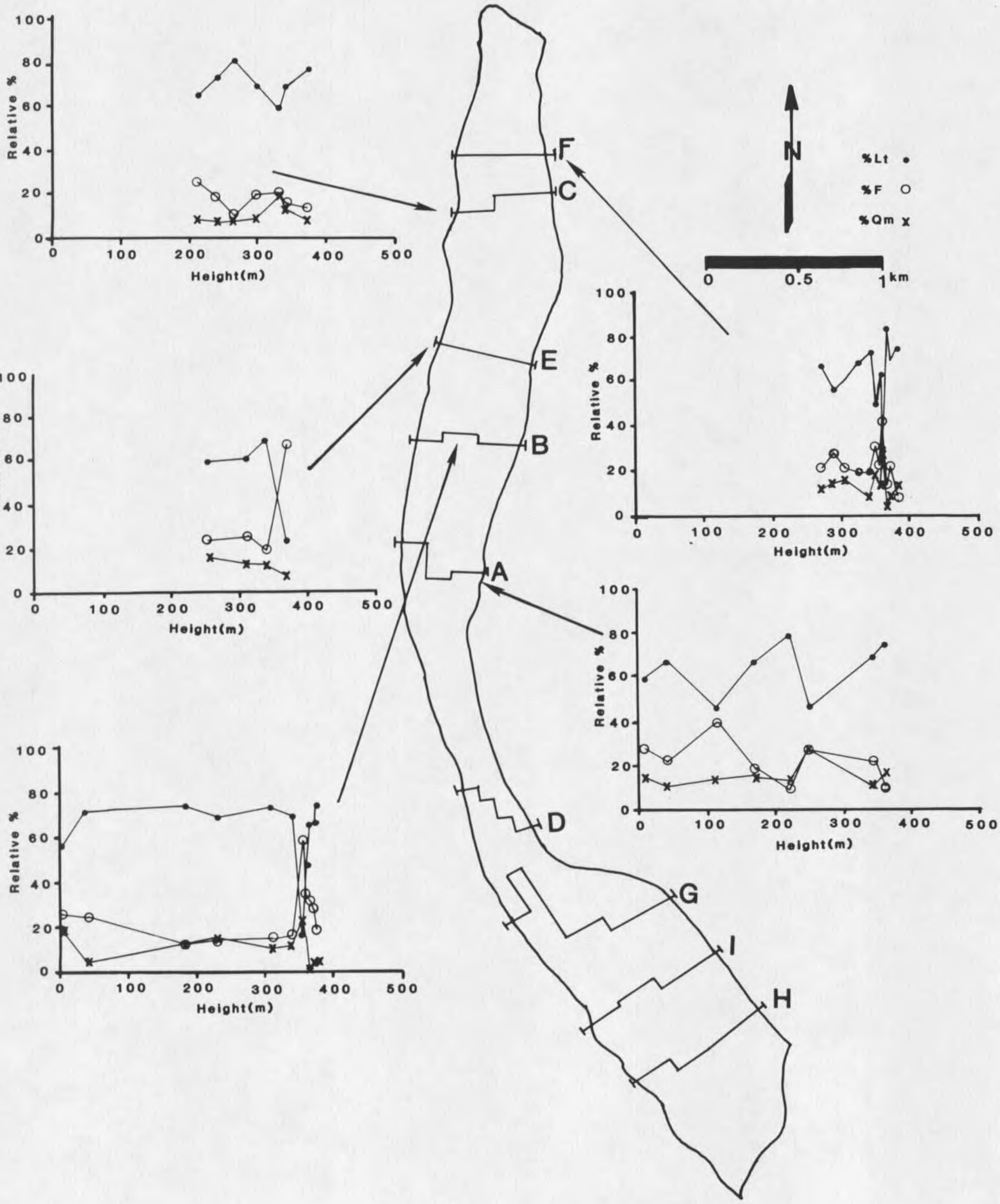

Figure 47. Graphs showing the vertical changes in sandstone composition for selected measured sections of Member 1 of the Horse Camp Formation.

PROVENANCE

Member 1 of the Horse Camp Formation was deposited in a basin with a temporally changing provenance. Changes are recognized by analyzing the directionallity of paleoslope and paleocurrent indicators, sandstone and conglomerate composition, and petrofacies and lithofacies distribution. A volcanic petrofacies makes up the lower 200 meters of Member 1 and records the first stage of basin development (Figures 43, 47). The second stage of basin development is represented by a mixed volcanic - sedimentary petrofacies comprising the upper 300 to 350 meters.

The stratigraphically lower volcanic petrofacies is defined by conglomerate and sandstone composed predominantly of volcanic debris (> 95%). Paleocurrent and composition data indicate the volcanic petrofacies was locally derived from western source terrains composed primarily of Oligocene volcanic rocks and minor Paleozoic rock. These sediments were deposited in a distal alluvial fan and sandflat environment. In the northern portion of the study area, the clasts in the volcanic petrofacies were derived from Railroad Valley Rhyolite and Windous Butte Formation. There is a notable absence of clasts from the Blind Springs, Stone Cabin, Calloway Well, Needles Range, and Shingle Pass Formations, and Currant Tuff. These potential source rocks are also absent in the two older megabreccia blocks present at Section F which are composed of Railroad Valley Rhyolite directly overlain by Windous Butte Formation.

The absence of clasts of Blind Springs, Stone Cabin, Calloway Well, Neddles Range, and Shingle Pass Formations, and the Currant Tuff in the conglomerate and megabreccia suggests that these units were missing from the source terrain as well. Scott (1965) describes a dome of Railroad Valley Rhyolite directly overlain by Windous Butte Formation with notable omission of the other Oligocene volcanic rocks at the north end of

Ragged Ridge. Drill hole data from some oil wells in Railroad Valley to the west indicate that the dome of Railroad Valley Rhyolite and overlying Windous Butte Formation extends to the west beneath Railroad Valley (Vreeland and Berrong, 1979). These are the only known locations where the Railroad Valley Rhyolite and Windous Butte Formation comprise the entire Oligocene section (Moores and others, 1968). Therefore the conglomerate and megabreccias composed of sediment derived exclusively from these two formations are interpreted to have been shed off of this terrain directly to the west.

Indirect evidence supports the idea that the sediments comprising the volcanic petrofacies of Member 1 in the southern end of the study area may have been transported from west to east. Data from drill holes further to the south and west of those discussed above indicate that there are places in the subsurface of Railroad Valley where much of the Oligocene section, including the Railroad Valley Rhyolite and Windous Butte Formation, has been eroded away (Bortz and Murray, 1979). The detritus eroded from these areas may have been deposited in the incipient Horse Camp basin.

The mixed volcanic - sedimentary petrofacies comprises the upper 300 to 350 meters of Member 1 of the Horse Camp Formation. It is defined by the presence of greater than 5% Paleozoic sedimentary clasts in addition to volcanic clasts. This change in petrofacies corresponds to a change in paleocurrent data indicating a significant shift from a western source area to northern and southern source areas which provided sediment to the basin. This transition is recorded in the distribution patterns of basinal facies (Figure 43, 47; Plate 1) (Mack and Rasmussen, 1984).

The mixed volcanic - sedimentary petrofacies of the northern portion of Member 1 was derived from the White Pine Range to the north. Composition, paleoslope and paleocurrant information, and lithofacies characteristics distinguish these rocks from those in the underlying 200 meters. Along with an increase in the percentage of Paleozoic clasts, a change in source area composition is noted in the stratigraphically highest landslide deposit. This deposit is composed of the entire Oligocene section, unlike the two underlying blocks, suggesting that it came from an area where all Oligocene volcanic units were present, possibly to the north. Paleocurrent and paleoslope data reflect a change in sediment transport direction from eastward to southward. The north to south sediment transport trend is reflected in sedimentary facies distribution patterns. Within 3 to 5 kilometers, proximal, medial, and distal alluvial fan facies interbedded with landslide deposits grade southward into sandflat and lacustrine facies (Section D). The source area was approximately 5 to 9 kilometers to the north given the present location of the White Pine Range.

The lacustrine deposits are located within 3 to 4 kilometers of a southern source area and interfinger with sandflat and distal alluvial fan facies. These facies are limited in lateral extent, rapidly grading southward into medial and proximal alluvial fan assemblages. Proximal and medial alluvial fan facies are composed of 15 to 50% Paleozoic clasts and are restricted to within 2 to 3 kilometers of the source area (Plate 1). Four angular unconformities divide this sequence of proximal deposits into three unconformity bounded packages and strongly implicate an active tectonic regime.

TECTONIC IMPLICATIONS

Early Tectonic History of the Horse Camp Basin

Member 1 of the Horse Camp Formation is composed of two distinct petrofacies which record a temporal change in sediment source areas. The older volcanic petrofacies is composed of laterally continuous alluvial fan sandstones and conglomerates derived from a western source terrane composed of Oligocene volcanic rocks (Figure 48). The large lateral extent and vertical persistence in the lithofacies assemblages of the volcanic petrofacies suggests that the alluvial fan radius were relatively large (5 to 15 kilometers) (Heward, 1978; Bull, 1984). In extensional basins such as Death Valley (Hooke, 1967) and the rift basins of east Africa (Tiercelin, 1987), large radius alluvial fans are most commonly deposited off of the hanging wall block on the inactive side of half-graben basins (Leeder and Gawthorpe, 1987; Alexander and Leeder, 1990). The source terrain for the lower petrofacies was either a tilted fault block (Wernicke and Burchfiel, 1982) or a hanging wall of a listric normal fault (Gibbs, 1984).

Dickinson (1991) suggests that planar and listric normal faults are equally plausible when interpreting sedimentary sequences deposited in extensional settings. During structural evolution of the Catalina metamorphic core complex of Arizona, a complex system of planar and listric normal faults controlled the development of numerous small half-graben subbasins filled with Neogene alluvial fan assemblages (Dickinson, 1991). The depositional evolution of the Tertiary Sacramento Pass Formation, an alluvial fan and lacustrine assemblage in the Snake Range of Nevada is interpreted by Grier (1983) to have

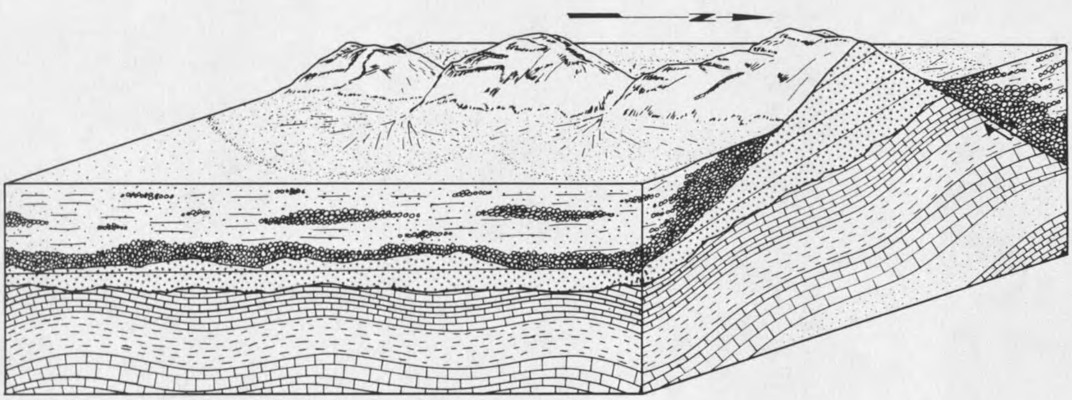

Figure 48. Schematic block diagram showing the distribution of alluvial fan assemblages and the location of the western source for the volcanic petrofacies.

been controlled exclusively by high angle normal faults separating tilted fault blocks. Reconnaisance work by Schmitt (personal communication, 1992) suggests that listric faults may also have played a role in the evolution of Sacramento Pass Formation. In the Whipple Mountains of California fault blocks produced by high-angle normal faulting sole at depth into the Whipple Mountain detatchment (Nielson and Beratan, 1990). This smaller scale faulting controlled the evolution of assymetric half-grabens. Long radius Neogene alluvial fans were deposited off of the hanging wall and short radius alluvial fans were deposited off of the footwall of the high angle normal faults (Beratan, 1991).

The volcanic petrofacies of Member 1 was very likely deposited in a half graben which developed in response to planar or listric normal faulting (Figure 48). The distribution of the alluvial fan assemblages indicates that west dipping faults controlled the half graben. If these faults are located east of the present exposures, possibly where the Horse Range is today, then the source of Member 1 may have been a hanging-wall rollover anticline. If the west dipping faults are located to the west, then the source for Member 1 was the backside of a tilted footwall block.

The younger mixed petrofacies of Member 1 is composed of Tertiary volcanic and Paleozoic sedimentary detritus derived from separate source areas to the north and south. A dip-sip component on the activated Ragged Ridge fault allowed for down-to-the-south tilt of the basin floor and caused a dramatic change in basin paleogeography and sediment dispersal patterns during later Member 1 time. A high rate of subsidence on the southern margin of the basin is recorded by at least four intraformational angular unconformities and a rapid northward transition from coarse-grained alluvial fan to lacustrine facies assemblages (Figure 49) (Blair and Bilodeau, 1988). The alluvial fans were of short radii (less than 5 kilometers) suggesting that they were deposited near the active basin-bounding fault, the Ragged Ridge fault. These fans would be analogous to the alluvial fans on the eastern side of Death Valley which are shed off of the adjacent, active footwall (Hooke, 1967). Tilting along the Ragged Ridge fault produced extensional progressive unconformities during periods of accelerated slip. These taper toward the center of basin subsidence and bound packages of alluvial fan sediment deposited during periods of lesser magnitude fault displacement (Anadon and others, 1986). Large radius (5 to 15 kilometers) alluvial fans and long runout landslides were deposited on the north side of the basin as the hanging wall was tilted to the south (Figure 49) (Leeder and Gawthorpe, 1987; Alexander and Leeder, 1990). Dickinson (1991) suggests that the long runout landslides which produce megabreccias are commonly generated by rockslides along bedding planes tipped to progressively steeper angles on evolving hanging wall blocks. This would support the hypothesis that the mixed petrofacies was deposited in a half graben basin that tilted to the south (Figure 49).

The exact timing of tectonic events is not well known at this time. However, future radiometric dating of tuffaceous units throughout Member 1 will provide a more precise temporal record of unconformity development and fault activity.

Influence of Transverse Structures on Member 1 Deposition

There is no evidence suggesting that transverse structures influenced deposition of the lower petrofacies. However, development of progressive unconformities in active basin margin facies assemblages indicates that transverse structures became increasingly dominant during the later stages of Member 1 development. Displacement along the west-striking high-angle Ragged Ridge fault on the southern boundary of the Horse Camp basin controlled dispersal of sediment during the deposition of the upper mixed petrofacies. Uplift of the northern Grant Range relative to the Horse Camp basin provided a source for mixed volcanic and sedimentary clasts and acted to restrict southward drainage.

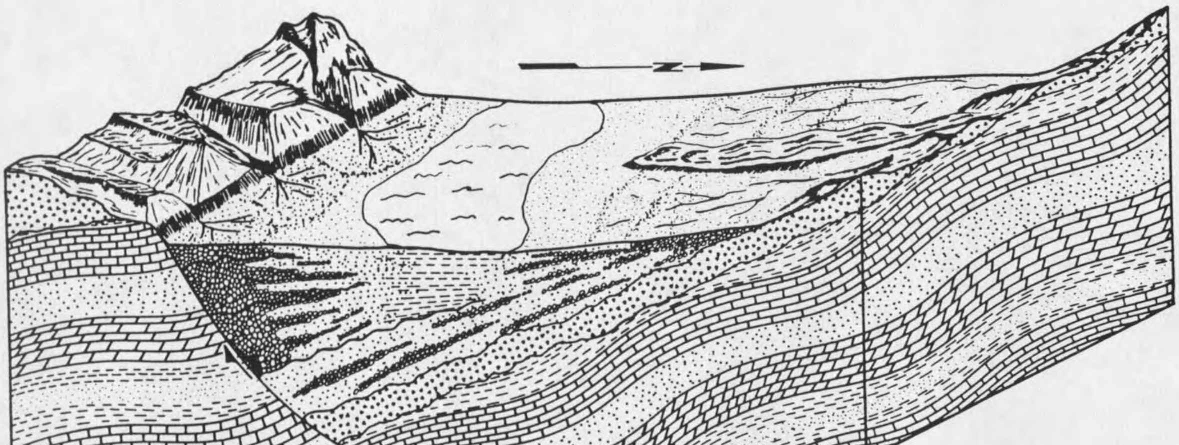

Figure 49. Schematic block diagram depicting the paleogeography and paleotectonic setting of the mixed petrofacies.

A thick sequence of coarse-grained sediment deposited along the Ragged Ridge fault indicates that offset was significant enough to rule out torsional offset between two north-striking normal faults in the Horse Camp basin (Faulds and others, 1992). Rather, the Ragged Ridge fault may have developed as an accommodation zone between two areas of differing magnitudes or rates of extension, presumably the Horse and Grant Ranges (Gibbs, 1984). However, evidence from the Blue Ribbon and Timpiute lineaments of southeastern Nevada indicates that transverse structures typically develop coeval with volcanism and associated north-south extension in the Basin and Range province (Bartley and others, 1992; Axen and others, 1993). If applicable to east-central Nevada, this observation suggests that the Ragged Ridge fault initially developed earlier, coeval with Oligocene volcanism and acted as a barrier to north-south propagation of developing Miocene - Pliocene normal faults.

During subsequent Neogene east-west extension, north-striking normal faults in the White Pine, Horse, and Grant Ranges would have propagated until they intersected older west-striking transverse faults such as the Currant Summit fault zone, Ragged Ridge fault, and Stone Cabin fault zone. The older transverse zones connected the normal faults by acting as lateral steps between the normal faults. Most likely extension would be accommodated by oblique- to dip-slip motion on these transverse faults. Each of the progressive unconformities in the mixed petrofacies of Member 1 of the Horse Camp basin records a period of normal to normal-oblique displacement on the Ragged Ridge fault. In this setting, the sedimentary sequence is preserved in the hanging wall of the transverse fault (Gibbs, 1984; Bartley and others, 1992).

Preliminary study of Member 2 of the Horse Camp formation indicates that the Ragged Ridge fault continued to be active during the deposition of a few hundred more meters of sediment. However, deposition of the upper two-thirds of Member 2 appears to have been more controlled by the Currant Summit fault zone at the southern end of the

White Pine Range. This would suggest that the accommodation of differential extensional rates or magnitudes in this region was shifted northward to the Currant Summit fault zone.

Rolling Hinge Model

It was not feasible to test the rolling hinge model by studying Member 1 of the Horse Camp Formation. Because this model reflects the regional structures in an extended orogen over a relatively long period of time (millions of years) (Spencer 1984), analysis of the entire formation is necessary to determine the effects of isostatic rebound in the footwall of the normal fault system controlling deposition of the Horse Camp Formation.

If the Horse Camp Formation was deposited in an area influenced by a rolling hinge mechanism, certain predictions can be made. From east to west, the age of basins located between the Horse Range and Railroad Valley should decrease. The oldest basins would be nearest to the breakaway zone (presumably in the Horse Range) and the basin nearest the active fault margin would be the youngest (Miller and John, 1988). An elongate basin with exposed Oligocene volcanics occurs between the two ridges of Paleozoic strata that make up the Horse Range. This basin is bounded on its east side by a high angle normal fault (possibly the breakaway zone) and may in fact be the oldest basin in the Horse Range although it is presently undated. The next basin to the west is the Horse Camp basin in which the Horse Camp Formation is exposed. Although Member 1 contains no evidence suggesting that it was deposited in a tectonic environment dominated by a rolling hinge (internal unconformities suggesting isostatic uplift or an eastern source), the uplift of Members 1 and 2 may be the result of flex and subsequent fault rotation of the footwall of a normal fault rooted to the west in the Horse Range (Buck, 1988; Hamilton, 1988; Wernicke and Axen, 1988). Members 3 and 4 are the youngest units of the Horse Camp

Formation and may represent deposition in the "youngest basin" between the Horse Range and Railroad Valley.

The hypothesis that the Tertiary structure of this region was controlled by a rolling hinge mechanism could be tested. Accurate chronostratigraphy of the Horse Camp Formation would provide a basis for understanding the timing of events which characterized the evolution of the Horse Camp Formation and its surrounding orogen. Detailed analysis of the sedimentology and stratigraphy of Members 2, 3, and 4 and structural mapping of the southern White Pine, Horse, and northern Grant ranges would permit interpretation of depositional environments, areas of active uplift, and timing relations of faults.

REFERENCES CITED

Alexander, J. and Leeder, M.R., 1987, Active tectonic control on alluvial architecture, in Ethridge, F.G., Flores, R.M., and Harvey, M.D.,eds., Recent developments in fluvial sedimentology: Society of Economic Paleontologists and Mineralogists Special Publication 39, p. 243-252.

Alexander, J. and Leeder, M.R., 1990, Geomorphology and surface tilting in an active extensional basin, SW Montana, USA: Journal of the Geological Society, London, v. 147, p. 461-467.

Allen, J.R.L., 1984, Parallel lamination developed from upper-stage plane-beds: a model based on the larger coherent structures of the turbulent boundary layer: Sedimentary Geology, v. 39, p. 227-242

Anadon, P., Cabrera, L., Colombo, F., Marzo, M., and Riba, O., 1986, Syntectonic intraformational unconformities in alluvial fan deposits, eastern Ebro Basin margins (NE Spain): International Association of Sedimentologists Special Publication no. 8, p. 259-271.

Anderson, R.E., 1978, Geologic map of the Black Canyon 15' Quadrangle, Mohave County, Arizona, and Clark County, Nevada: United States Geological Survey Quadrangle Map 1394.

Anderson, R.E., Zoback, M.L., and Thompson, G.A., 1983, Implications of selected subsurface data on the structural formation of some basins in the northern Basin and Range province, Nevada and Utah: Geological Society of America Bulletin, v. 94, p. 1055-1072.

Axelrod, D.I., 1957, Late Tertiary floras and the Sierra Nevadan Uplift: Geological Society of America Bulletin, v. 68, p. 19-46.

Axelrod, D.I., 1962, Post-Pliocene uplift of the Sierra Nevada, California: Geological Society of America Bulletin, v. 73, p. 183-198.

Axen, G.J., 1988, The geometry of planar domino-style normal faults above a dipping basal detachment: Journal of Structural Geology, v. 10, p. 405-411.

Axen, G.J., Taylor, W.J., and Bartley, J.M., 1993, Space-time patterns and tectonic controls of Tertiary extension and magmatism in the Great Basin of the western United States: Geological Society of America Bulletin, v. 105, p. 56-76.

Ballance, P.F., 1984, Sheet-flow-dominated gravel fans of the non-marine middle Cenozoic Simmler Formation, central California: Sedimentary Geology, v. 38, p. 337-359

Bally, A.W., 1982, Musings over sedimentary basin evolution: Royal Society of London Philosophical Transactions, v. A305, p. 325-337.

Bally, A.W., and Snelson, S., 1980, Realms of subsidence: Bulletin of Canadian Petroleum Geology, v. 20, p. 9-75.

Barr, D., 1987, Structural/stratigraphic models for extensional basins of half graben type: Journal of Structural Geology, v. 9, p. 491-500.

Bartley, J.M., Axen, G.J., Taylor, W.J., and Fryxell, J.E., 1988, Tertiary tectonics of a transect through eastern Nevada near 38 degrees North latitude, in Weide, D.L., and Faber, M.L., eds., This extended land, geological journeys in the southern Basin and Range, Geological Society of America, Cordilleran Section, Field Trip Guidebook, p. 1-20.

Bartley, J.M., Fletcher, J.M., and Glazner, A.F., 1990, Tertiary extension and contraction of lower plate rocks in the central Mojave metamorphic core complex, southern California: Tectonics, v. 9, p. 521-534.

Bartley, J.M. and Gleason, G., 1992, Tertiary normal faults superimposed on Mesozoic thrusts, Quinn Canyon and Grant Ranges, Nye County, Nevada: in Wernicke, B.P., ed., Basin and Range extensional tectonics near the latitude of Las Vegas, Nevada: Geological Society of America Memoir 176, p. 195-212.

Bartley, J.M., Taylor, W.J., and Lux, D.R., 1992, Blue Ribbon volcanic rift in southeastern Nevada and its effects on Basin and Range fault segmentation: Geological Society of America Abstracts with Programs, v. 24, p. 2.

Beratan, K.K., Blom, R.G., Nielson, J.E., and Crippen, R.E., 1990, Use of Landsat Thematic Mapper Images in regional correlation of syntectonic strata, Colorado River extensional corridor, California and Arizona: Journal of Geophysical Research, v. 95, no. B1, p. 615-624.

Beratan, K.K., 1991, Miocene synextensional sedimentation patterns, Whipple Mountains, southeastern California: Implications for the geometry of the Whipple Mountains detachment system: Journal of Geophysical Research, v. 96, no. B7, p. 12,425-12,442.

Best, M.G., and Christiansen, E.H., 1991, Limited extension during peak Tertiary volcanism, Great Basin, Nevada and Utah: Journal of Geophysical Research, v. 96, no. B7, p. 13,509-13,528.

Blair, T.C., 1987, Tectonic and hydrologic controls on cyclic alluvial-fan, fluvial, and lacustrine rift-basin sedimentation, Jurassic-lowermost Cretaceous Todos Santos Formation, Chiapas, Mexico: Journal of Sedimentary Petrology, v. 57, p. 845-862.

Blair, T.C. and Bilodeau, W.L., 1988, Development of tectonic cyclothems in rift, pull-apart, and foreland basins: Sedimentary response to episodic tectonism: Geology, v. 16, p. 517-520.

Bortz, L.C., and Murray, D.K., 1979, Eagle Springs oil field, Nye County, Nevada: in Newman, G.H. and Goode, H.D., eds., Basin and Range symposium and Great Basin field conference; Rocky Mountain Association of Geologists and Utah Geological Association, p. 441-453.

Bosworth, W., 1985, Geometry of propagating rifts: Nature, v. 316, p. 625-627.

Buck, R.W., 1988, Flexural rotation of normal faults: Tectonics, v. 7, p. 959-973.

Bull, W.B., 1972, Recognition of alluvial fan deposits in the stratigraphic record: in Rigby, J.K.and Hamblin, W.K., eds., Recognition of ancient sedimentary environments, Society of Economic Paleontologists and Mineralogists Special Publication No. 16, p. 63-83.

Bull, W.B., 1984, Tectonic geomorphology: Journal of Geological Education, v. 32, p. 310-324.

Burchfiel, B.C., 1966, Tin Mountain landslide, southeastern California, and the origin of megabreccia: Geological Society of America Bulletin, v. 77, p. 95-100.

Burchfiel, B.C. and Davis, G.A., 1975, Nature and controls of Cordilleran orogenesis, western United States: Extensions of an earlier synthesis <1971>: American Journal of Science, v. 275-A, p. 363-396.

Camilleri, P.A., 1989, Superposed compressional and extensional strain in lower Paleozoic rocks of the northwestern Grant Range, Nevada [M.S. Thesis] : Corvallis, Oregon State University, 84 p.

Camilleri, P.A., 1992, Extensional geometry of a part of the northwestern flank of the northern Grant Range, Nevada: Inferences on its evolution: The Mountain Geologist, v. 29, p. 75-84.

Campbell, C.S., 1989, Self-lubrication for long-runout landslides: The Journal of Geology, v. 97, p. 653-665.

Cavazza, W., 1989, Sedimentation pattern of a rift-filling unit, Tesuque Formation (Miocene), Espanola basin, Rio Grande rift, New Mexico: Journal of Sedimentary Petrology, v. 59, p. 287-296.

Cebull, S.E., 1970, Bedrock geology and orogenic succession in southern Grant Range, Nye County, Nevada: American Association of Petroleum Geologists Bulletin, v. 54, p. 1828-1842.

Cohen, A.S., Ferguson, D.S., Gram, P.H., Hubler, S.L., and Sims, K.M., 1986, The distribution of coarse-grained sediments in modern Lake Turkana, Kenya: Implications for clastic sedimentation models of rift lakes: Geological Society of London Special Publication No. 28, p. 177-186.

Collinson, J.D., and Thompson, D.B., 1988, Sedimentary Structures, Second Edition: Unwin Hyman, London, 208 p.

Coney, P.J., 1987, The regional tectonic setting and possible causes of Cenozoic extension in the North American Cordillera, in Coward, M.P., Dewey, J.F., and Hancock, P.L., eds., Continental Extensional Tectonics: Geological Society of America Special Publication No. 28, p. 177-186.

Cook, E.F., 1965, Stratigraphy of Tertiary volcanic rocks in eastern Nevada: Nevada Bureau of Mines, Report 11, 61 p.

Costa, J.E., 1984, Physical geomorphology of debris flows, in Costa, J.E. and Fleisher, P.J., eds., Developments and applications of geomorphology: Berlin, Springer-Verlag, p. 268-317.

Costa, J.E, 1988, Rheologic, geomorphic, and sedimentologic differentiation of water floods, hyperconcentrated flows, and debris flows, in, Baker, V.R., Kochel, R.C., and Patton, P.C., eds., Flood geomorphology: John Wiley and Sons, New York, p. 113-122.

Davis, W.M., 1938, Sheetfloods and streamfloods: Geological Society of America Bulletin, v. 49, p. 1337-1416.

Davis, G.A., and Lister, G.S., 1988, Detachment faulting in continental extension; Perspectives from the southwestern U.S. Cordillera, in Clark, S.P., Jr., Burchfiel, B.C., and Suppe, J., eds., Processes in continental lithospheric deformation: Geological Society of America Special Paper 218, p. 133-159.

Dean, W.E., and Fouch, T.D., 1983, Lacustrine environment, in Scholle, P.A., Bebout, D.G., and Moore, C.H., eds., Carbonate depositional environments: American Association of Petroleum Geologists Memoir 33, p. 98-130.

DeCelles, P.G.,Gray, M.B., Ridgway, K.D., Cole, R.B., Pivnik, D.A.,Pequera, N., and Srivastava, P., 1991, Controls of synorogenic alluvial-fan architecture, Beartooth Conglomerate (Paleocene), Wyoming and Montana: Sedimentology, v. 38, p. 567-590.

DeCelles, P.G., Langford, R.P., and Schwartz, R.K., 1983, Two methods of paleocurrent determination from trough cross-stratification: Journal of Sedimentary Petrology, v. 53, p. 629-642.

Dickinson, W.R., 1970, Interpreting detrital modes of graywacke and arkose: Journal of Sedimentary Petrology, v. 40, p. 695-707.

Dickinson, W.R., Harbaugh, D.W., Saller, A.H., Heller, P. L., and Snyder, W.S., 1983, Detrital modes of upper Paleozoic sandstones derived from Antler orogen in Nevada: implications for nature of Antler orogeny: American Journal of Science, v. 283, p. 481-509.

Dickinson, W.R., and Suczek, C.A., 1979, Plate tectonics and sandstone compositions: American Association of Petroleum Geologists Bulletin, v. 63, p. 2164-2182.

Dickinson, W.R., 1991, Tectonic setting of faulted Tertiary strata associated with the Catalina core complex in southern Arizona: Geological Society of America Special Paper 264, 120 p.

DiGuiseppi, E.M., and Bartley, J.M., 1991, Stratigraphic effects of change from internal to external drainage in an extending basin, southeastern Nevada: Geological Society of America Bulletin, v. 103, p. 48-55.

Drewes, H., 1977, Geologic map and sections of the Rincon Valley Quadrangle, Pima County, Arizona: United States Geological Survey Miscellaneous Geologic Investigations Map I-997.

Duebendorfer, E.M. and Wallin, E.T., 1991, Basin development and syntectonic sedimentation associated with kinematically coupled strike-slip and detachment faulting: Geology, v. 19, p. 87-90.

Effimoff, I. and Pinezich, A.R., 1981, Tertiary structural development of selected valleys based on seismic data: Basin and Range province, northeastern Nevada: Royal Society of London, Philosophical Transactions, ser. A, v. 300, p. 435-442.

Effimoff, I. and Pinezich, A.R., 1986, Tertiary structural development of selected basins: Basin and Range province, northeastern Nevada: Geological Society of America Special Paper 208, p. 31-42.

Elliot, D.H., and Wells, N.A., 1982, Mesozoic alluvial fans of the South Orkney Islands, in, Craddock, C., ed., Antarctic geoscience, Madison, Wisconsin: University of Wisconsin Press, p. 235-244.

Enos, P., 1977, Flow regimes in debris flows: Sedimentology, v. 24, p. 133-142.

Fahnestock, R.K., and Bradley, W.C., 1973, Knik and Matanuska Rivers, Alaska: a contrast in braiding, in Morisawa, M., ed., Fluvial geomorphology: Proceedings of the 4th Annual Geomorphology Symposium, State University of New York, Binghamton, New York, p. 220-250.

Faulds, J.E., Geissman, J.W., and Mawer, C.K., 1992, Structural development of a major extensional accommodation zone in the Basin and Range Province, northwestern Arizona and southern Nevada: Implications for kinematic models of continental extension, in Wernicke, B.P., ed., Basin and Range extensional tectonics near the latitude of Las Vegas, Nevada: Geological Society of America Memoir 176, p. 37-76.

Fisher, R.V., 1971, Features of coarse-grained, high-concentration fluids and their deposits: Journal of Sedimentary Petrology, v. 41, p. 916-927.

Folk, R.L., 1980, Petrology of Sedimentary Rocks: Hemphill Publishing Company, Austin, Texas, 182 p.

Foster, N.H., 1979, Geomorphic exploitation used in the discovery of Trap Springs oil field, Nye County, Nevada, in Newman, G.H. and Goode, H.D., eds., Basin and Range Symposium and Great Basin field conference; Rocky Mountain Association of Geologists and Utah Geological Association, p. 469-476.

Fouch, T.D., and Dean, W.E., 1982, Lacustrine and associated clastic depositional environments, in Scholle, P.A., and Spearing, D., eds., Sandstone depositional environments, American Association of Petroleum Geologists Memoir 31, p. 87-114.

Frost, E.G., 1981, Structural style of detachment faulting in the Whipple Mountains, California and Buckskin Mountains, Arizona, in Stone, C. and Jenney, J.P., eds., Arizona Geological Society Digest 13: Tuscon, Arizona Geological Society, p. 25-29.

Frostick, L.E., and Reid, I., 1987, Tectonic control of desert sediments in rift basins ancient and modern: Geological Society of London Special Publication No. 35, p. 53-68.

Fryxell, J. E., 1984, Structural development of the west-central Grant Range, Nye County, Nevada [Ph.D. dissertation]: Chapel Hill, University of North Carolina, 139 p.

Fryxell, J.E., 1988, Geologic map and description of stratigraphy and structure of the west-central Grant Range, Nye County, Nevada: Geological Society of America Map and Chart Series MCH064, 16 p.

Fryxell, J.E., 1991, Tertiary tectonic denudation of an igneous and metamorphic complex, west-central Grant Range, Nye County, Nevada: Geology and ore deposits of the Great Basin symposium, Geological Society of Nevada, p. 87-92.

Galay, V.J., and Neill, C.R., 1967, Discussion of "Nomenclature for bed forms in alluvial channels": American Society of Civil Engineers Proceedings, Journal of the Hydraulics Division, v. 93, p. 130-133.

Galloway, W.E., and. Hobday, D.K., 1983, Terrigenous Clastic Depositional Systems: Springer-Verlag, New York, 423 p.

Gans, P.B., Mahood, G.A., and Schermer, E., 1989, Synextensional magmatism in the Basin and Range Province: a case study from the eastern Great Basin: Geological Society of America Special Paper 233, 53 p.

Gibbs, A.D., 1983, Balanced cross-section constructions from seismic sections in areas of extensional tectonics: Journal of Structural Geology, v. 3, p. 152-160.

Gibbs, A.D., 1984, Structural evolution of extensional basin margins: Journal of the Geological Society, London, v. 141, p. 609-620.

Gibbs, A.D., 1987, Development of extension and mixed-mode sedimentary basins: in Coward, M.P., Dewey, J.F., and Hancock, P.L., eds., Continental extensional tectonics: Geological Society of London Special Publication No. 28, p. 19-33.

Gibbs, A.D., 1990, Linked fault families in basin formation: Journal of Structural Geology, v. 12, p. 795-803.

Glazner, A.F., and Bartley, J.M., 1984, Timing and tectonic setting of Tertiary low-angle normal faulting and associated magmatism in the southwestern United States: Tectonics, v. 3, p. 385-396.

Gleason, G.C., 1988, The structural geology of the east flank of the southern Grant Range, Nye County, Nevada [M.S. thesis] : Salt Lake City, University of Utah, 114 p.

Gloppen, T.G., and Steel, R.G., 1981, The deposits, internal structure and geometry in six alluvial fan-fan delta bodies (Devonian-Norway) -- a study in the significance of bedding sequence in conglomerates: in Ethridge, F.G. and Flores, R.M., eds., Recent and ancient non-marine depositional environments: Models for Exploration, Society of Economic Paleontologists and Mineralogists Special Publication 31, p. 49-69

Golia, R.T., and Stewart, J.H., 1984, Depositional environments and paleogeography of the upper Miocene Wassuk Group, west-central Nevada: Sedimentary Geology, v. 38, p. 159-180.

Gordon, I. and Heller, P.L., 1993, Evaluating major controls on basinal stratigraphy, Pine Valley, Nevada: Implications for syntectonic deposition: Geological Society of America Bulletin, v. 105, p. 47-55.

Graham, S.A., Tolson, R.B., DeCelles, P.G., Ingersoll, R.V., Bargar, E., Caldwell, M., Cavazza, W., Edwards, D.P., Follo, M.F., Handschy, J.R., Lemke, L., Moxon, I., Rice, R., Smith, G.A., and White, J., 1986, Provenance modelling as a technique for analyzing source terrane evolution and controls on foreland sedimentation, in Allen, P., and Homewood, P., eds., Foreland basins, International Association of Sedimentologists Special Publication 8, p. 141-152.

Graham, J., 1988, Collection and analysis of field data, in Tucker, M., ed., Techniques in Sedimentology: Blackwell Scientific Publications, Palo Alto, California, p. 5-62.

Grier, S.P., 1983, Tertiary history and geologic history of the Sacramento Pass area, Nevada, in Nash, W.P. and Gurgel, K.D., eds., Geologic excursions in the overthrust belt and metamorphic core complexes of the intermountain region: Utah Geological and Mineral Survey Special Studies 59, p. 139-144.

Grier, S.P., 1984, Alluvial fan and lacustrine carbonate deposits in the Snake Range: A study of Tertiary sedimentation and associated tectonism [M.S. thesis] : Stanford, California, Stanford University, 61 p.

Guy, B.T., Dickinson, W.T., Rudra, R.P. and Wall, G.J., 1990, Hydraulics of sediment-laden sheetflow and the influence of simulated rainfall: Earth Surface Processes and Landforms, v. 15, p. 101-118.

Hadley, J.B., 1964, Landslides and related phenomena accompanying the Hebgen Lake earthquake of August 17, 1959: United States Geological Survey Professional Paper 435, p. 107-138.

Hamilton, W., 1988, Extensional faulting in the Death Valley region: Geological Society of America Abstracts with Programs, v. 20, p. 165-166.

Hampton, M.A., 1975, Competence of fine-grained debris flows: Journal of Sedimentary Petrology, v. 45, p. 834-844.

Harrison, S. and Fritz, W.J., 1982, Depositional features of March 1982 Mount St. Helens sediment flows: Nature, v. 299, p. 720-722.

Harrison, J.V. and Falcon, N.L., 1937, An ancient landslip at Saidmarreh in southwestern Iran: Geographical Journal, v. 89, p. 42-47

Hein, F.J., and Walker, R.G., 1977, Bar evolution and development of stratification in the gravelly, braided, Kicking Horse River, British Columbia: Canadian Journal of Earth Sciences, v. 14, p. 562-570.

Hendrix, E.H., and Ingersoll, R.V., 1987, Tectonics and sedimentation of the upper Oligiocene/ lower Miocene Vasquez Formation, Soledad basin, southern California: Geological Society of America Bulletin, v. 98, p. 647-663.

Heward, A.P., 1978, Alluvial fan and lacustrine sediments from the Stephanian A and B (La Magdalena, Cinera-Matallana and Sabero) coalfields, northern Spain: Sedimentology, v. 25, p. 451-488.

Hewitt, K., 1988, Catastrophic landslide deposits in the Karakoram Himalayas: Science, v. 242, p. 64-67.

Hogg, S.E., 1982, Sheetfloods, sheetwash, sheetflow, or ...?: Earth Science Reviews, v. 18, p. 59-76.

Hooke, R.L., 1967, Processes on arid-region alluvial fans: Journal of Geology, v.75, p. 438-460.

Hsu. K.J., 1975, Catastrophic debris streams (sturzstroms) generated by rockfalls: Geological Society of America Bulletin, v. 86, p. 129-140.

Hubert, J.F., and Hyde, M.G., 1982, Sheet-flow deposits of graded beds and mudstones on an alluvial sandflat-playa system: Upper Triassic Blomidon redbeds, St. Mary's Bay, Nova Scotia: Sedimentology, v. 29, p. 457-474.

Hyde, J.H., and Huttrer, G.W., 1970, Geology of the central Grant Range, Nevada: American Association of Petroleum Geologists Bulletin, v. 54, p. 503-521.

Illies, J.H., 1981, Mechanisms of graben formation: Tectonophysics, v. 73, p. 249-266.

Ingersoll, R.V., Bullard, T.F., Ford, R.L., Grimm, J.P., Pickle, J.D., and Sares, S.W., 1984, The effect of grain size on detrital modes: A test of the Gazzi-Dickinson point-counting method: Journal of Sedimentary Petrology, v. 54, p. 103-116.

Jackson, J.A., Gagnepain, J., Houseman, G., King, G., Papadimitriou, P., Soufleris, C., and Virieux, J., 1982, Seismicity, normal faulting, and the geomorphical evolution of the Gulf of Corinth, (Greece): the Corinth earthquakes of February and March, 1981: Earth and Planetary Science Letters, v. 57, pp. 377-397

Jackson, J.A., and McKenzie, D., 1983, The geometrical evolution of normal fault systems: Journal of Structural Geology, v. 5, pp. 471-482.

Jackson, J.A., 1987, Active normal faulting and crustal extension: Geological Society of London Special Publication No. 28, p. 3-18.

Jahns, R.H., and Engel, A.E.J., 1950, Chaotic breccias in southern California: tectonic or sedimentary? (abs.): Geological Society of America Bulletin, v.61, p. 1474.

Johnson, B., 1978, Blackhawk landslide, California, U.S.A., in, Voight, B., ed., Rockslides and Avalanches, 1: Elsevier Scientific Publishing, New York, p. 481-504.

Karcz, I., 1968, Fluvitile obstacle marks from the Wadis of the Negev (southern Israel): Journal of Sedimentary Petrology, v. 38, p. 1000-1012.

Kerr, D.R., 1984, Early Neogene continental sedimentation in the Vallecito-Fish Creek Mountains, western Salton Trough, California: Sedimentary Geology, v. 38, p. 217-246.

Krieger, M.H., 1977, Large landslides, composed of megabreccia, interbedded in Miocene basin deposits, southeastern Arizona: United States Geological Survey Professional Paper 1008, 25 p.

Larson, V., and Steel, R.J., 1978, The sedimentary history of a debris-flow dominated Devonian alluvial fan -- a study of texural inversion: Sedimentology, v. 25, p. 37-59.

Laznicka, P., 1988, Breccias and coarse fragmentites, Developments in Economic Geology 25: Elsevier Scientific Publishing 831 p.

Leeder, M.R. and Gawthorpe, R.L., 1987, Sedimentary models for extensional tilt-block/ half graben basins: in Coward, M.P., Dewey, J.F., and Hancock, P.L., eds., Continental extensional tectonics: Geological Society of London Special Publication No. 28, p. 139-152.

Li, Y., Geissman, J.W., Nur, A., Ron, H., and Huang, Q., 1990, Paleomagnetic evidence for counterclockwise block rotation in the north Nevada rift region: Geology, v. 18, pp. 79-82.

Lister, G.S. and Davis, G. A., 1989, The origin of metamorphic core complexes and detachment faults formed during Tertiary continental extension in the northern Colorado River region, USA: Journal of Structural Geology, v. 11, p. 65-94.

Longwell, C.R., 1951, Megabreccia developed downslope from large faults: American Journal of Science, v. 249, p. 343-355.

Lowe, D.R., 1976, Grain flow and grain flow deposits: Journal of Sedimentary Petrology, v. 46, p. 188-199.

Lowe, D. R., 1982, Sediment gravity flows: II. Depositional models with special reference to the deposits of high-density turbidity currents: Journal of Sedimentary Petrology, v. 52, p. 279-297.

Lumsden, W.W., 1964, Geology of the southern White Pine Range and northern Horse Range, Nye and White Pine Counties, Nevada [Ph.D. dissertation] : Los Angeles, University of California at Los Angeles.

Lund, K., Nash, J.T., Beard, L.S., Blank, H.R., and Tuftin, S.E., 1987, Mineral resources of the Blue Eagle Wilderness Study Area, Nye County, Nevada: U.S. Geological Survey Bulletin 1731-D, 19 p.

Lund, K., Beard, L.S., Blank, H.R., Hofstra, A.H., and Hamilton, M.M., 1988, Mineral resources of the Riordans Well Wilderness Study Area, Nye County, Nevada: U.S. Geological Survey Bulletin 1731-H, 16 p.

Mack, G.H., and Rasmussen, K.A., 1984, Alluvial-fan sedimentation of the Cutler Formation (Permo-Pennsylvanian) near Gateway, Colorado: Geological Society of America Bulletin, v. 95, p. 109-116.

Mack, G.H., and Seager, W.R., 1990, Tectonic control on facies distribution of the Camp Rice and Palomas Formations (Pliocene - Pleistocene) in the southern Rio Grande rift: Geological Society of America Bulletin, v. 102, p. 45-53.

Marangunic, C. and Bull, W.B., 1968, The landslide on Sherman Glacier, in The Great Alaska earthquake of 1964, part A, hydrology: National Academy of Sciences Publication 1603, p. 383-394.

Mastalerz, K., 1990, Diurnally and seasonally controlled sedimentation on a glaciolacustrin foreset slope: An example from the Pleistocene of eastern Poland, in Colella, A. and Prior, D.B., eds., Coarse-grained deltas: International Association of Sedimentologists Special Publication No. 10, p. 297-310.

McGee, W.J., 1897, Sheetflood erosion: Geological Society of America Bulletin, v. 8, p. 87-112.

McGowen, J.H., and Garner, L.E., 1970, Physiographic features and stratification types of coarse-grained point bars: modern and ancient examples: Sedimentology, v. 14, p. 77-111.

McManus, J., 1988, Grain size determination and interpretation, in Tucker, M., ed., Techniques in Sedimentology: Blackwell Scientific Publications, Palo Alto, California, p. 63-85.

Melosh, 1987, The mechanics of large rock avalanches: Geological Society of America Reviews in Engineering Geology, v. 12, p. 41-49.

Miall, A.D., 1977, A review of the braided river depositional environment: Earth Science Reviews, v. 13, p. 1-62.

Miall, A.D., 1985, Architectural-element analysis: A new method of facies analysis applied to fluvial deposits: Earth Science Reviews, v. 22, p. 261-308.

Middleton, L.T., and Trujillo, A.P., 1984, Sedimentology and depositional setting of the Upper Proterozoic Scanlan Conglomerate, central Arizona, in Koster, E.H. and Steel, R.J., eds., Sedimentology of gravels and conglomerates: Canadian Society of Petroleum Geologists Memoir 10, p. 189-201.

Miller, J.M.G., and John, B.E., 1988, Detached strata in a Tertiary low-angle normal fault terrane, southeastern California: A sedimentary record of unroofing, breaching, and continued slip: Geology, v. 16, p. 645-648.

Moores, E.M., 1963, Geology of the Currant area, Nye County, Nevada [Ph.D. dissertation] : Princeton, New Jersey, Princeton University, 122 p.

Moores, E.M., 1968, Mio-Pliocene sediments, gravity-slides, and their tectonic significance, east-central Nevada: Journal of Geology, v. 76, p. 88-98.

Moores, E.M., Scott, R.B., and Lumsden, W.W., 1968, Tertiary tectonics of the White Pine-Grant-Horse Range region, east-central Nevada, and some regional implications: Geological Society of America Bulletin, v. 79, p. 1703-1726.

Murray, M.E., 1985, Geology of the east-central Quinn Canyon Range, Nye County, Nevada, [M.S. thesis]: Chapel Hill, University of North Carolina, 107 pgs.

Naylor, M.A., 1980, The origin of inverse grading in muddy debris flow deposits -- a review: Journal of Sedimentary Petrology, v. 50, p. 1111-1116.

Nielson, J.E., and Beratan, K.K., 1990, Tertiary basin development and tectonic implications, Whipple detachment system, Colorado River extensional corridor, California and Arizona: Journal of Geophysical Research, v. 95, no.B1, p. 599-614.

Nilsen, T.H., 1982, Alluvial fan deposits, in Scholle, P.A. and Spearing, D., eds., Sandstone depositional environments: American Association of Petroleum Geologists Memoir 31, p. 86.

Noble, L.F., 1941, Structural features of the Virgin Spring area, Death Valley, California: Geological Society of America Bulletin, v. 52, p. 941-1000.

Norton, W.H., 1917, A classification of breccias: Journal of Geology, v. 25, p. 160-194.

Odom, I.E., Doe, T.W., and Dott, R.H., Jr., 1976, Nature of feldspar-grain size relations in some quartz-rich sandstones: Journal of Sedimentary Petrology, v. 46, p. 862-870.

Perry, S.K. and Schamel, S., 1990, The role of low-angle normal faulting and isostatic response in the evolution of the Suez rift, Egypt: Tectonophysics, v. 174, p. 159-173.

Pettijohn, F.J., Potter, P.E., and Siever, R., 1987, Sand and Sandstone, Second Edition: Springer-Verlag, New York, 553 p.

Pierson, T.C.and Costa, J.E., A rheologic classification of subaerial sediment-water flows: Geological Society of America Reviews in Engineering Geology, v. 12, p. 1-12.

Plafker, G. and Erickson, G.E., 1978, Nevados Huascaran avalanches, Peru, in Voight, B., ed., Rockslides and Avalanches, 1: Elsevier Scientific Publishing, p. 277-314.

Quinlivan, W.D., Rogers, C.L., and Dodge, H.J., 1974, Geologic map of the Portuguese Mountain Quadrangle, Nye County, Nevada: U.S. Geological Survey Miscellaneous Field Investigations Map I-804.

Reading, H.G., 1982, Sedimentary basins and global tectonics: Proceedings of the Geological Society of London, v. 93, p. 321-350.

Regnier, J., 1960, Cenozoic geology in the vicinity of Carlin, Nevada: Geological Society of America Bulletin, v. 71, p. 1189-1210.

Reid, I., and Frostick, L.E., 1986, Slope processes, sediment derivation and landform evolution in a rift valley basin, northern Kenya: Geological Society of London Special Publication No. 25, p. 99-111.

Rehig, W.A., Shafiqullah, M., and Damon, P. E., 1980, Geochronology, geology, and listric normal faulting of the Vulture Mountains , Maricopa County, Arizona: Arizona Geological Society Digest, v. 12, p. 89-110.

Rodine, J.D., and Johnson, A.M., 1976, The ability of debris, heavily freighted with coarse materials to flow on gentle slopes: Sedimentology, v. 23, p. 213-234.

Rosendahl, B.R., Reynolds, D.J., Lorber, P.H., Burgess, C.F., McGill, J., Scott, D., Lambiase, J.J., and Derksen, S., 1986, Structural expression of rifting: Lessons from Lake Tanganyika, Africa: Geological Society of London Special Publication 25, p. 29-43.

Rust, B.R., 1978, Depostional models for braided alluvium, in Miall, A.D., ed., Fluvial sedimentology, Canadian Society of Petroleum Geologists Memoir 5, p. 605-626.

Schlische, R.W. and Olsen, P.E., 1990, Quantitative filling model for continental extensional basins with applications to early Mesozoic rifts of eastern North America: Journal of Geology, v. 98, p. 135-155.

Schmitt, J.G., Jones, D.A, and Goldstrand, P.M., 1991, Braided stream deposition and provenance of the Upper Cretaceous-Paleocene (?) Canaan Peak Formation, Sevier foreland basin, southwestern Utah, in Nations J.D. and Eaton, J.G., eds., Stratigraphy, depositional environments, and sedimentary tectonics of the western margin, Cretaceous Western Interior Seaway: Geological Society of America Special Paper 260, p. 27-45.

Schmitt, J.G., Brown, C.L., Cechovic, M., Dando, L., and Craig-Hunter, C., in press, Delivery of sediment from Mt. Everts to the Gardner River, northern Yellowstone National Park, Wyoming: National Park Service Report to Congress.

Sclater, J.G., and Celerier, B., 1987, Extensional models for the formation of sedimentary basins and continental margins: Norsk Geologisk Tidsskrift, v. 67, p. 256-267.

Scott, R.B., 1965, The Tertiary geology and ignimbrite petrology of the Grant Range, east-central Nevada [Ph.D. dissertation] : Houston, Rice University, 116 p.

Sharp, R.P., 1939, The Miocene Humboldt Formation in northeastern Nevada: Journal of Geology, v. 47, p. 133-160.

Shreve, R.L., 1968, The Blackhawk landslide: Geological Society of America Special Paper 108, 47 p.

Shultz, A.W., 1984, Subaerial debris-flow deposition in the upper Paleozoic Cutler Formation, western Colorado: Journal of Sedimentary Petrology, v. 54, p. 759-772.

Smith, G.A., 1986, Coarse-grained nonmarine volcaniclastic sediment: Terminology and depositional process: Geological Society of America Bulletin, v. 97, p. 1-10.

Smith, W.L., 1960, History of oil exploration in Railroad Valley, Nye County, Nevada, in Guidebook to the geology of east-central Nevada: Intermountain Association of Petroleum Geologists-Eastern Nevada Geological Society, p. 233-236.

Snoke, A.W., and Lush, A.P., 1984, Polyphase Mesozoic - Cenozoic deformational history of the northern Ruby Mountains - East Humboldt Range, in Lintz, J., Jr., eds., Western Geological Excursions, Geological Society of America 1984 Field Guidebook, v. 4, p. 232-303.

Spencer, J. E., 1984, Role of tectonic denudation in warping and uplift of low-angle normal faults: Geology, v. 12, p. 95-98.

Stanley, K.O., 1976, Sandstone petrofacies in the Cenozoic high Plains sequence, eastern Wyoming and Nebraska: Geological Society of America Bulletin, v. 87, p. 297-309.

Stewart, J.H., 1978, Basin and Range structure in western North America: A review, in Smith, R.B. and Eaton, G.P., eds., Cenozoic tectonics and regional geophysics of the Western Cordillera: Geological Society of America Memoir 152, p. 1-31.

Stewart, J.H., and Diamond, D.S., 1990, Changing patterns of extensional tectonics; overprinting of the basin of the Middle and Upper Esmeralda Formation in western Nevada by younger structural basins, in Wernicke, B.P., ed., Basin and Range extensional tectonics near the latitude of Las Vegas, Nevada: Geological Society of America Memoir 176, p. 447-475.

Surdam, R.C., and Wolfbauer, C.A., 1975, Green River Formation, Wyoming: A playa-lake complex: Geological Society of America Bulletin, v. 86, p. 335-345.

Surdam, R.C., and Eugster, H.P., 1976, Mineral reactions in the sedimentary deposits of the Lake Magadi region, Kenya: Geological Society of America Bulletin, v. 87, p. 1739-1752.

Taylor, W.J., Bartley, J.M., Lux, D.R., and Axen, G.J., 1989, Timing of Tertiary extension in the Railroad Valley - Pioche transect, Nevada: constraints from $^{40}Ar/^{39}Ar$ ages of volcanic rocks: Journal of Geophysical Research, v. 94, p. 7757-7774.

Tircelin, J.J., 1986, The Pliocene Hadar Formation, Afar depression of Ethiopia: Geological Society of London Special Publication No. 25, p. 221-240.

Todd, S.P., 1989, Stream-driven, high-density gravelly traction carpets: possible deposits in the Trabeg Conglomerate Formation, SW Ireland and some theoretical considerations of their origin: Sedimentology, 1989, v. 36, p. 513-530.

Twiss R.J. and Moores, E.M., 1992, Structural Geology: W.H. Freeman and Company, New York, 532 p.

Van Houten, F.B., 1956, Reconnaissance of Cenozoic sedimentary rocks of Nevada: American Association of Petroleum Geologists Bulletin, v. 40, p. 2801-2825.

Vendeville, B. and P.R. Cobbold, 1988, How normal faulting and sedimentation interact to produce listric fault profiles and stratigraphic wedges: Journal of Structural Geology, v. 10, p. 649-659.

Vreeland, J.H., and Berrong, B.H., 1979, Seismic exploration in Railroad Valley, Nevada, in Newman, G.H. and Goode, H.D., eds., Basin and Range symposium and Great Basin field conference: Rocky Mountain Association of Geologists and Utah Geological Association, p. 557-572.

Walker, R.G., 1978, Deep-water sandstone facies and ancient submarine fans: Models for exploration for stratigraphic traps: American Association of Petroleum Geologists Bulletin, v. 62, p. 932-966.

Watson, R.A. and Wright, H.E., 1969, The Saidmarreh landslide, Iran: United States Contributions to Quaternary Research, Geological Society of America Special Paper 123, p. 115-139.

Waresback, D.B., and Turbeville, B.N., 1990, Evolution of a Plio-Pleistocene volcanogenic-alluvial fan: The Puye Formation, Jemez Mountains, New Mexico: Geological Society of America Bulletin, v. 102, p. 298-314.

Wernicke, B., 1981, Low-angle normal faults in the Basin and Range province: Nappe tectonics in an extending orogen: Nature, v. 291, p. 645-648.

Wernicke, B., 1985, Uniform-sense normal simple shear of the continental lithosphere: Canadian Journal of Earth Sciences, v. 22, p. 108-125.

Wernicke, B. and Burchfiel, B.C., 1982, Modes of extensional tectonism: Journal of Structural Geology, v. 4, p. 105-115.

Wernicke, B., and Axen, G.J., 1988, On the role of isostacy in the evolution of normal fault systems: Geology, v. 16, p. 848-851.

Williamson, P.G., and Savage, R.J.G., 1986, Early rift sedimentation in the Turkana basin, northwestern Kenya: Geological Society of London Special Publication No. 25, p. 267-283.

Whipple, K.X., and Dunne, T., 1992, The influence of debris-flow rheology on fan morphology, Owens Valley, California: Geological Society of America Bulletin, v. 104, p. 887-900.

Wire, J.C., 1959, Geology of the Currant Creek area, Nevada [M.A. Thesis] : Los Angeles, University of California, 154 p.

Woodford, A.O. and Harriss, T.F., 1928, Geology of Blackhawk Canyon, San Bernadino mountains, California: Bulletin of the University of California Department of Geological Sciences, v. 17, p. 265-291.

Yarnold, J.C., and Lombard, J.P., 1989, A facies model for large rock-avalanche deposits formed in dry climates, in Colburn, I.P., Abbott, P.L., and Minch, J., eds., Conglomerates in basin analysis: Society of Economic Paleontologists and Mineralogists, Pacific Section Symposium, v. 62, p. 9-31.

Young, S.W., 1976, Petrographic textures of detrital polycrystalline quartz as an aid to interpreting crystalline source rocks: Journal of Sedimentary Petrology, v. 46, p. 603.

Zoback, M.L., Anderson, R.E., and Thompson, G.A., 1981, Cainozoic evolution of the state of stress and style of tectonism of the Basin and Range province of the western United States: Royal Society of London Special Publication, p. 189-216.

APPENDIX

COMPOSITION DATA

Table 2. Clast count data summarizing the eight different types of clasts recognized in Member 1 of the Horse Camp Formation.

LOCATION	TOTAL	Trv	Tbs	Tsc	Twb	Tnr	Ts	CO3	Qtzt
A3	508	0	0	0	508	0	0	0	0
A5	537	152	0	0	385	0	0	0	0
A6	298	105	0	0	180	0	0	13	0
B3	260	74	0	0	186	0	0	0	0
B5	269	124	0	0	133	0	0	12	0
B6	252	86	0	0	162	0	0	4	0
B15	253	220	0	0	33	0	0	0	0
C1	266	63	0	0	198	0	0	5	0
C2	252	85	0	0	165	0	0	2	0
C4	263	84	0	0	175	0	0	4	0
D1	230	8	0	0	190	0	0	25	7
D2	291	32	0	0	103	0	0	144	12
F2	253	23	0	0	230	0	0	0	0
F3	262	47	0	0	215	0	0	0	0
F4	276	22	0	0	134	0	0	111	9
G2	330	102	2	43	143	0	0	26	14
G3	258	56	0	0	179	0	0	23	0
G3a	272	134	17	12	80	0	0	29	0
G4	280	43	16	14	68	0	0	117	22
G5	268	68	0	11	98	0	0	77	14
G6	255	78	0	0	147	0	0	27	3
H1	241	52	0	0	189	0	0	0	0
H2	264	56	0	0	208	0	0	0	0
H3	255	16	0	7	164	0	0	68	0
H4	258	36	4	7	116	0	0	92	3
H5	277	58	0	0	111	0	0	92	16
I1	250	25	0	8	217	0	0	0	0
I2	253	29	0	2	210	0	0	12	0
I3	251	32	0	2	202	4	1	10	0
I4	260	35	0	0	218	0	0	7	0
I5	276	19	0	16	207	3	5	26	0
I6	280	27	0	0	222	0	0	26	5

Table 3. Tabulation of the relative percentages of the eight different types of clasts of Member 1.

SAMPLE	TOTAL	%Trv	%Tbs	%Tsc	%Twb	%Tnr	%Ts	%TTV	%CO_3	%Qtzt	%TPz
A3	508	0	0	0	100	0	0	100	0	0	0
A5	537	28.3	0	0	71.7	0	0	100	0	0	0
A6	298	35.2	0	0	60.4	0	0	95.6	4.4	0	4.4
B3	260	28.5	0	0	71.5	0	0	100	0	0	0
B5	269	46.1	0	0	49.4	0	0	95.5	4.5	0	4.5
B6	252	34.1	0	0	64.3	0	0	98.4	1.6	0	1.6
B15	253	87	0	0	13	0	0	100	0	0	0
C1	266	23.7	0	0	74.4	0	0	98.1	1.9	0	1.9
C2	252	33.7	0	0	65.5	0	0	99.2	0.8	0	0.8
C4	263	31.9	0	0	66.5	0	0	98.5	1.5	0	1.5
D1	230	3.5	0	0	82.6	0	0	86.1	10.9	3	13.9
D2	291	11	0	0	35.4	0	0	46.4	49.5	4.1	53.6
F2	253	9.1	0	0	90.9	0	0	100	0	0	0
F3	262	17.9	0	0	82.1	0	0	100	0	0	0
F4	276	8	0	0	48.6	0	0	56.5	40.2	3.3	43.5
G2	330	30.9	0.6	13	43.3	0	0	87.9	7.9	4.2	12.1
G3	258	21.7	0	0	69.4	0	0	91.1	8.9	0	8.9
G3a	272	49.3	6.3	4.4	29.4	0	0	89.3	10.7	0	10.7
G4	280	15.4	5.7	5	24.3	0	0	50.4	41.8	7.9	49.6
G5	268	25.4	0	4.1	36.6	0	0	66	28.7	5.2	34
G6	255	30.6	0	0	57.6	0	0	88.2	10.6	1.2	11.8
H1	241	21.6	0	0	78.4	0	0	100	0	0	0
H2	264	21.2	0	0	78.8	0	0	100	0	0	0
H3	255	6.3	0	2.7	64.3	0	0	73.3	26.7	0	26.7
H4	258	14	1.6	2.7	45	0	0	63.2	35.7	1.2	36.8
H5	277	20.9	0	0	40.1	0	0	61	33.2	5.8	39
I1	250	10	0	3.2	86.8	0	0	100	0	0	0
I2	253	11.5	0	0.8	83	0	0	95.3	4.7	0	4.7
I3	251	12.7	0	0.8	80.5	1.6	0.4	96	4	0	4
I4	260	13.5	0	0	83.8	0	0	97.3	2.7	0	2.7
I5	276	6.9	0	5.8	75	1.1	1.8	90.6	9.4	0	9.4
I6	280	9.6	0	0	79.3	0	0	88.9	9.3	1.8	11.1

Table 4. Point count data summarizing the amount each type of framework grain recognized in the sandstones of the northern portion of Member 1.

SAMPLE	SIZE	TOTAL	Q	Qm	Qp	F	Lt	L	Ls	Lv
A1	m-vc	264	40	38	2	71	155	153	0	153
A3	f-c	273	32	28	4	60	185	181	0	181
A4	f-c	250	40	35	5	100	115	110	0	110
A5	m-g	265	42	41	1	47	177	176	5	171
A6	m-vc	293	43	37	6	26	230	224	2	222
A8	m-g	258	73	68	5	70	120	115	2	113
A10	m-g	299	32	30	2	61	208	206	0	206
A12	f-c	270	46	42	4	28	200	196	5	191
B1a	m-vc	265	47	47	0	67	151	151	0	151
B1b	f-vc	265	10	10	0	64	191	191	0	191
B3	m-g	253	36	32	4	32	189	185	0	185
B5	f-vc	288	46	45	1	44	199	198	0	198
B6	f-g	298	32	31	1	44	223	222	0	222
B8	f-vc	277	34	33	1	48	196	195	0	195
B15a	m-c	316	78	74	4	188	54	50	2	48
B15b	m-vc	289	51	45	6	102	142	136	1	135
B15c	f-c	251	4	3	1	80	168	167	3	164
B15d	vf-m	258	13	10	3	72	176	173	2	171
B15e	m-p	258	11	11	0	51	196	196	8	188
C1	vf-vc	262	24	23	1	67	172	171	1	170
C2	f-vc	270	23	21	2	51	198	196	2	194
C3a	f-vc	276	24	24	0	27	225	225	0	225
C3b	f-g	234	23	22	1	48	164	163	0	163
C4a	f-g	263	51	50	1	57	156	155	3	152
C4b	f-g	271	46	43	3	38	190	187	3	184
C5a	f-m	266	42	36	6	23	207	201	7	194
E1a	f-m	262	45	43	2	63	156	154	11	143
E1b	m-g	336	45	45	0	87	204	204	2	202
E2b	f-c	302	38	37	1	58	207	206	2	204
E4a	f-m	272	21	21	0	186	65	65	7	58
F1	m-c	275	35	34	1	60	181	180	7	173
F2	m-g	278	45	43	2	79	156	154	1	153
F4	m-g	273	46	46	0	59	168	168	0	168
F4a	f-c	269	34	32	2	52	185	183	0	183
F4b	f-c	265	24	22	2	52	191	189	0	189
F5	f-c	262	50	50	0	82	130	130	1	129
F6a	f-c	291	42	40	2	66	185	183	7	176
F6b	m-c	273	84	75	9	114	84	75	2	73
F6c1	f-vc	290	13	12	1	39	239	238	0	238
F6c2	f-c	290	38	23	15	65	202	187	2	185
F6c3	f-vc	258	39	36	3	26	196	193	2	191

Table 5. Tabulation of the relative percentages of the framework grains that were identified from sandstones in the northern portion of Member 1.

SAMPLE	TOTAL	%Q	%F	%L	%Qm	%F	%Lt	%Qp	%Ls	%Lv
A1	264	15.2	26.9	58	14.4	26.9	58.7	1.29	0	98.7
A3	273	11.7	22	66.3	10.3	22	67.8	2.16	0	97.8
A4	250	16	40	44	14	40	46	4.35	0	95.7
A5	265	15.8	17.7	66.4	15.5	17.7	66.8	0.56	2.82	96.6
A6	293	14.7	8.87	76.5	12.6	8.87	78.5	2.61	0.87	96.5
A8	258	28.3	27.1	44.6	26.4	27.1	46.5	4.17	1.67	94.2
A10	299	10.7	20.4	68.9	10	20.4	69.6	0.96	0	99
A12	270	17	10.4	72.6	15.6	10.4	74.1	2	2.5	95.5
B1a	265	17.7	25.3	57	17.7	25.3	57	0	0	100
B1b	265	3.77	24.2	72.1	3.77	24.2	72.1	0	0	10
B3	253	14.2	12.6	73.1	12.6	12.6	74.7	2.12	0	97.9
B5	288	16	15.3	68.8	15.6	15.3	69.1	0.5	0	99.5
B6	298	10.7	14.8	74.5	10.4	14.8	74.8	0.45	0	99.6
B8	277	12.3	17.3	70.4	11.9	17.3	70.8	0.51	0	99.5
B15a	316	24.7	59.5	15.8	23.4	59.5	17.1	7.41	3.7	88.9
B15b	289	17.6	35.3	47.1	15.6	35.3	49.1	4.23	0.7	95.1
B15c	251	1.59	31.9	66.5	1.2	31.9	66.9	0.6	1.79	97.6
B15d	258	5.04	27.9	67.1	3.88	27.9	68.2	1.7	1.14	97.2
B15e	258	4.26	19.8	76	4.26	19.8	76	0	4.08	95.9
C1	262	9.16	25.6	65.3	8.78	25.6	65.6	0.58	0.58	98.8
C2	270	8.52	18.9	72.6	7.78	18.9	73.3	1.01	1.01	98
C3a	276	8.7	9.78	81.5	8.7	9.78	81.5	0	0	100
C3b	234	9.83	20.5	69.7	9.4	20.5	70.1	0.61	0	99.4
C4a	263	19.4	21.7	58.9	19	21.7	59.3	0.64	1.92	97.4
C4b	271	17	14	69	15.9	14	70.1	1.58	1.58	96.8
C5a	266	15.8	8.65	75.6	13.5	8.65	77.8	2.9	3.38	93.7
E1a	262	17.2	24	58.8	16.4	24	59.5	1.28	7.05	91.7
E1b	336	13.4	25.9	60.7	13.4	25.9	60.7	0	0.98	99
E2b	302	12.6	19.2	68.2	12.3	19.2	68.5	0.48	0.97	98.6
E4a	272	7.72	68.4	23.9	7.72	68.4	23.9	0	10.8	89.2
F1	275	12.7	21.8	65.5	12.4	21.8	65.8	0.55	3.87	95.6
F2	278	16.2	28.4	55.4	15.5	28.4	56.1	1.28	0.64	98.1
F4	273	16.8	21.6	61.5	16.8	21.6	61.5	0	0	100
F4a	269	12.6	19.3	68	11.9	19.3	68.8	1.08	0	98.9
F4b	265	9.06	19.6	71.3	8.3	19.6	72.1	1.05	0	99
F5	262	19.1	31.3	49.6	19.1	31.3	49.6	0	0.77	99.2
F6a	291	14.4	22.7	62.9	13.7	22.7	63.6	1.08	3.78	95.1
F6b	273	30.8	41.8	27.5	27.5	41.8	30.8	10.7	2.38	86.9
F6c1	290	4.48	13.4	82.1	4.14	13.4	82.4	0.42	0	99.6
F6c2	290	13.1	22.4	64.5	7.93	22.4	69.7	7.43	0.99	91.6
F6c3	258	15.1	10.1	74.8	14	10.1	76	1.53	1.02	97.4

Plate 1. Location and description of the nine measured stratigraphic sections of Member 1 of the Horse Camp Formation.

Plate 2. General distribution of alluvial fan, sandflat and lacustrine facies assemblages of Member 1 of the Horse Camp FormationSee legend on Plate 2 for symbols.

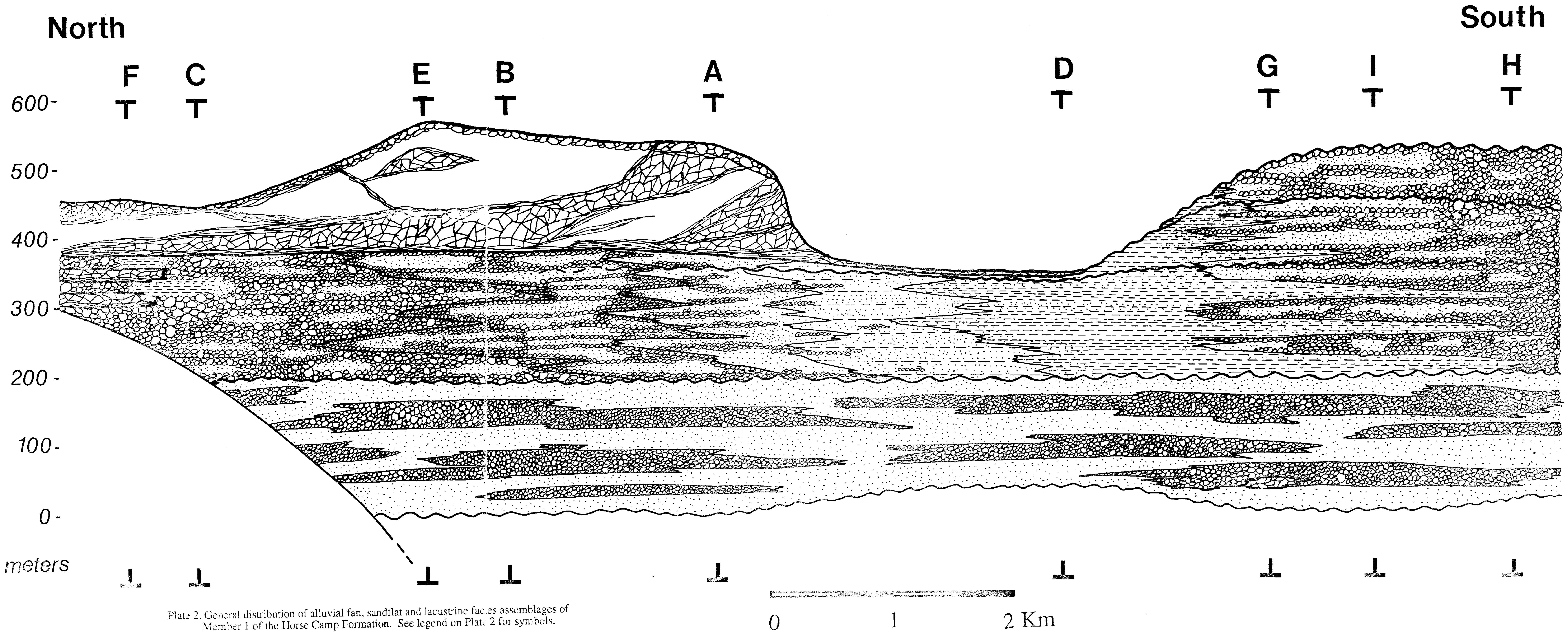

Plate 2. General distribution of alluvial fan, sandflat and lacustrine facies assemblages of Member 1 of the Horse Camp Formation. See legend on Plate 2 for symbols.

MEASURED STRATIGRAPHIC SECTIONS OF MEMBER 1 OF THE NEOGENE HORSE CAMP FORMATION, EAST-CENTRAL NEVADA

Plate 1. Location and description of the nine measured stratigraphic sections of Member 1 of the Horse Camp Formation.